MicroRNA-103 and 107 Target RAD51 and RAD51D to Regulate Homologous Recombination and Enhance Cellular Sensitivity to DNA Damaging Agents

Jen-Wei Huang

A dissertation

submitted in partial fulfillment of the

requirements for the degree of

Doctor of Philosophy

University of Washington

2013

Reading Committee:

Toshiyasu Taniguchi, Chair

Matthew Fero

Amanda Paulovich

Program Authorized to Offer Degree:

Molecular and Cellular Biology

University of Washington

Abstract

MicroRNA-103 and 107 Target RAD51 and RAD51D to Regulate Homologous Recombination and Enhance Cellular Sensitivity to DNA Damaging Agents

Jen-Wei Huang

Chair of the Supervisory Committee:
Affiliate Associate Professor Toshiyasu Taniguchi
Department of Pathology

Homologous recombination mediates the error-free repair of DNA double-strand breaks. RAD51 is a protein that is essential for homologous recombination and its recruitment to DNA double-strand breaks is mediated by several factors including the products of the breast and ovarian cancer susceptibility genes, such as BRCA1 and BRCA2, and the RAD51 paralogs, such as RAD51D. Deregulation of these factors leads to genomic instability and cellular sensitivity to ionizing radiation, DNA interstrand cross-linking agents, poly(ADP-ribose) polymerase (PARP) inhibitors and other DNA damaging agents. The regulation of homologous recombination by microRNAs, which are non-coding RNAs that post-transcriptionally downregulate gene expression, is not well characterized.

To systematically identify microRNAs with the potential to regulate homologous recombination, we performed overexpression screens of human microRNA libraries using the efficiency of ionizing radiation-induced RAD51 foci formation as a readout. Three microRNAs

(miR-103, miR-107 and miR-221) consistently reduced ionizing radiation-induced RAD51 foci formation in screens performed in both HeLa and U2OS cells. Accordingly, these microRNAs potently impaired homologous recombination repair efficiency. Furthermore, miR-103 and miR-107 enhanced cellular sensitivity to various DNA damaging agents, including cisplatin and a PARP inhibitor (AZD2281/olaparib), *in vitro* and *in vivo*. Importantly, we identified RAD51 and RAD51D as direct targets of miR-103 and miR-107 and demonstrated that their repression was critical for miR-103/107-mediated inhibition of RAD51 foci formation as well as chemosensitivity to DNA damaging agents. Altogether, we identified novel microRNA players in the regulation of homologous recombination and chemoresistance to DNA damaging agents. MiR-103, miR-107 and other hits from our screens provide a more complete picture of the regulatory crosstalk that exists between microRNA and DNA repair pathways to maintain genomic stability. Furthermore, these microRNAs may potentially be useful as prognostic indicators of chemotherapy response or as therapeutic agents for the chemosensitization of tumors.

TABLE OF CONTENTS

LIST OF FIGURES

Figure Number and Title **Page**

LIST OF TABLES

Table Number and Title **Page**

ACKNOWLEDGEMENTS

First and foremost, I would like to thank my advisor, Toshiyasu Taniguchi, for taking a chance on a first-year graduate student who was on his fourth rotation. His dedication to the study of DNA repair and the rigor with which he approaches the scientific process has been edifying and inspirational to me over the past six years. The freedom I was given to explore all aspects of my project has set me on the path to becoming an independent scientist. I cannot imagine receiving training of a higher quality from anyone else.

I would also like to thank Drs. Matthew Fero, David Kimelman, Raymond Monnat and Amanda Paulovich for taking the time to be on my committee. Their feedback, advice and encouragement over the years have been invaluable. I would especially like to thank Matthew Fero and Amanda Paulovich for reading this dissertation and providing helpful suggestions.

Lastly, I would like to thank all current and past members of the Taniguchi lab for the integral roles that they played in my training. I have had the privilege of working with and learning from many talented post-docs, graduate students and technicians: Drs. Maria Castella, Ronald Cheung, Kiran Dhillon and Wataru Sakai; Antonio Abeyta and Philamer Calses; and Emily Villegas. I am deeply indebted to Drs. Celine Jacquemont and Yemin Wang, whose technical expertise, advice and opinions provided me the tools and the perspective I needed to complete my dissertation.

DEDICATION

To my parents, Ming-Hsien Huang and Yun-Jin Wu.

CHAPTER ONE

Introduction

The maintenance of genomic stability is critical for organismal viability. This is a particularly daunting task given the approximately 100,000 lesions that occur daily within the genomes of mammalian cells [1]. The sources of DNA damage arise from both endogenous and exogenous sources. The reactive oxygen species (ROS) generated from metabolic processes can damage bases or create strand breaks [1, 2]. Abasic nucleotides can arise from spontaneous hydrolysis [1, 2]. Exogenous agents such as radiation (e.g. ultraviolet, ionizing radiation (IR)), chemicals and other xenobiotics can also induce base damage or strand breaks [1]. These various lesions interfere with critical cellular processes such as DNA replication and transcription and their immediate sensing and repair is therefore crucial for survival. In metazoans, genomic stability can result in inactivating or activating mutations in tumor suppressors or oncogenes, respectively, which may lead to cellular transformation and cancer [3].

The importance of genomic stability to viability is evidenced by the multitude of cancer susceptibility syndromes caused by defective alleles of factors that mediate DNA repair [3]. For example, hereditary non-polyposis colon carcinoma (HNPCC) is caused by mutated alleles of genes involved in the mismatch repair pathway [3]. Hypersensitivity to ultraviolet radiation and UV-induced tumor formation in Xenoderma pigmentosum patients is caused by mutations in the eight genes whose products coordinate nucleotide excision repair [3].

Arguably the most toxic lesions that can occur in the genome are DNA double-strand breaks (DSBs). These – if unrepaired or misrepaired – can lead to the loss of whole chromosome arms or gross chromosomal rearrangements. Sources of DSBs include replication fork stalling

and collapse or exposure to certain DNA damaging agents, including ionizing radiation, radiomimetics, DNA interstrand crosslinking agents and topoisomerase poisons [1]. The tolerance of DSBs in eukaryotes is low and if unrepaired, a single DSB break can lead to cell cycle arrest [4] or cell death [5].

The repair of DSBs is handled by two major pathways: non-homologous end-joining (NHEJ) and homologous recombination (HR) [1]. NHEJ occurs throughout the cell cycle and requires minimal processing of DNA ends [6]. It is considered an error-prone process since the broken ends are ligated without the use of a template [6]. Repair by HR is generally restricted to S/G2 phases of the cell cycle and requires extensive processing of the DNA break ends [7]. HR is considered an error-free process due to the use of homologous sequences (e.g. sister chromatid or chromosome) as the template for the restoration of information [7]. The significance of error-free repair by HR to genomic stability is evidenced by cancer susceptibility syndromes such as Fanconi anemia and familial breast/ovarian cancer, which are caused by the inheritance of defective alleles of BRCA1, FANCD1/BRCA2, XRCC2, FANCO/RAD51C, RAD51D, FANCN/PALB2 and others [3, 8-11].

Homologous Recombination

DNA DSB repair by HR uses regions of homology as the templates for error-free repair [7]. The current model of HR-mediated DSB repair was first proposed by Szostak and colleagues [12]. The critical initiating event of this model is the expansion of a DSB by nucleolytic processing of the broken strands to generate 3'-tailed ends, a process termed resection (Figure 1.1A). One of these tailed-ends is then used to probe for regions of homology, ideally on a sister chromatid. Once found, the 3'-tailed end invades the double-stranded (ds)DNA to form a heteroduplex with the complementary strand and then serves as the primer for DNA synthesis.

After synthesis, the extended 3'-tailed end can then be displaced from the heteroduplex and anneal with the second 3'-tailed end (Figure 1.1B). Subsequent gap-filling synthesis and ligation restores the DNA duplex. This is one potential outcome of HR, termed synthesis-dependent strand annealing (SDSA), and does not result in crossover products (reciprocal exchange of information between homologous sequences) [13]. Alternatively, the strand of the duplex displaced by invasion and initial round of synthesis (the D-loop) can anneal with the second 3'-tailed end (second-end capture) (Figure 1.1C). A second round of synthesis can then be initiated following the formation of this secondary heteroduplex. The resulting intermediate consists of the two DNA duplexes physically linked through two Holliday junctions (HJs). Resolution or dissolution of the double HJs by endonucleolytic cleavage events restores the linear duplexes. During HJ resolution, cleavage of the inner strands at both HJs (Figure 1.1C, blue arrows) or cleavage of the outer strands at both HJs (Figure 1.1C, green arrows) result in non-crossover products. If cleavage occurs at the inner strands of one HJ and the outer strands at the other, crossover products are generated (Figure 1.1C, blue and green arrows). During HJ dissolution, the double HJs can converge by branch migration to form a hemicatenane, which can then be dissolved in a single cleavage event (Figure 1.1D). The outcome of HJ dissolution is non-crossover products. The molecular factors that regulate HR in higher eukaryotes are outlined in the following section.

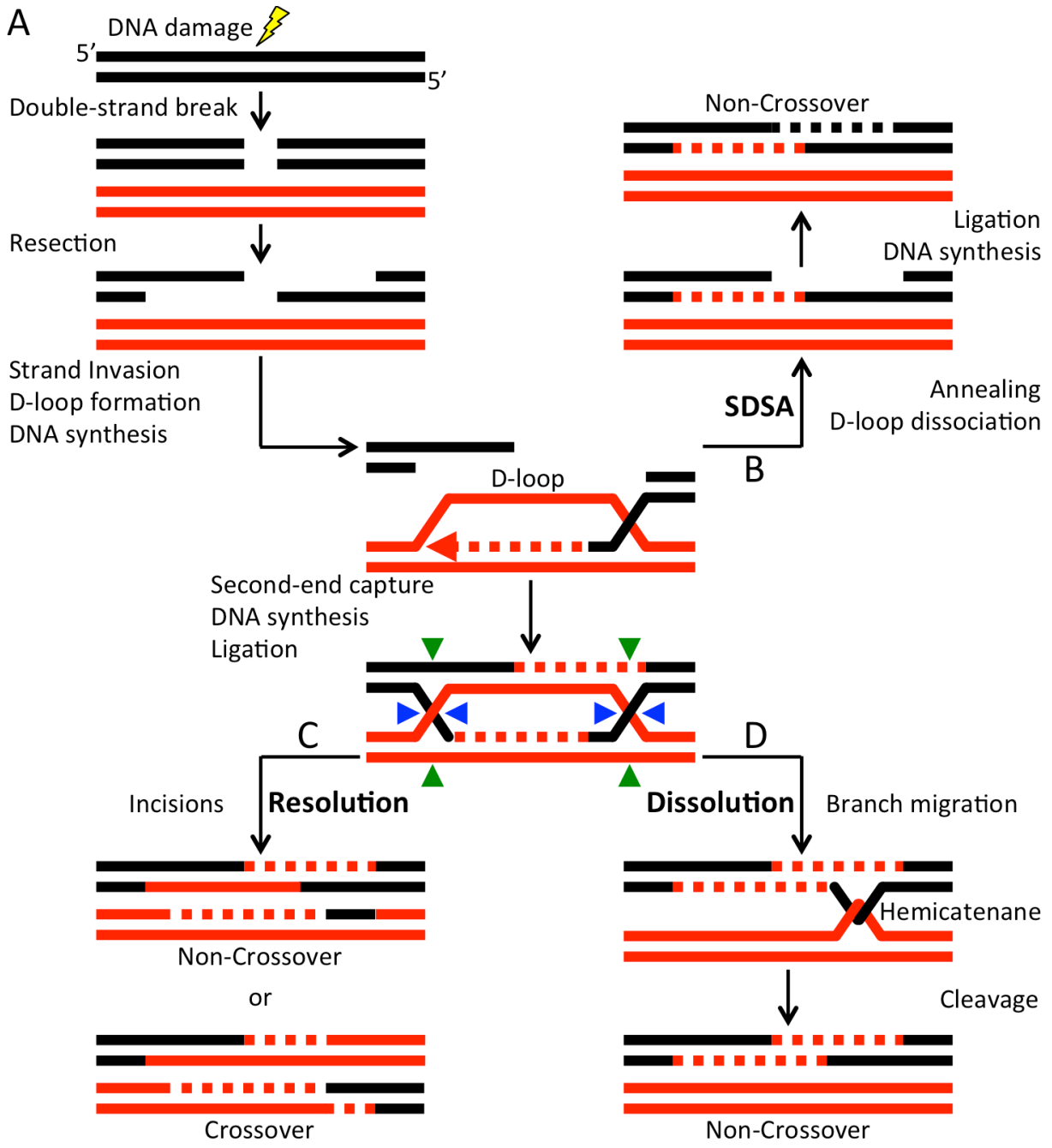

Figure 1.1. The homologous recombination pathway.
A. 5'-end resection at a DNA double-strand break results in 3'-tailed ends. One of the resected ends invades a DNA duplex to pair with homologous sequences, forming a D-loop, and serves as a primer for DNA synthesis. **B.** Synthesis-dependent strand annealing (SDSA): Displacement of strand and annealing to the second 3'-tailed end results in repair with non-crossover products. **C-D.** Capture of second resected end by the D-loop and subsequent synthesis and ligation results in double Holliday junctions (HJs). Resolution by symmetric incisions (same-colored arrowheads) at both HJs result in non-crossover while asymmetric incisions (different-colored arrowheads) result in crossover (**C**). Branch migration of double HJs result in a hemicatenane and its dissolution by cleavage results in non-crossover (**D**). Adapted from (7).

Molecular Regulation of Homologous Recombination

When a DNA DSB occurs, the MRN (MRE11/RAD50/NBS1) complex localizes to the broken ends and promotes the autophosphorylation and subsequent activation of the PI3K-like kinase, ATM [14, 15]. Activated ATM then initiates the DNA damage response by phosphorylating up to 700 downstream targets [16]. Its major early targets include the effector kinase, CHK2, which initiates cell cycle checkpoint signaling, and the histone variant, H2AX [16]. Phosphorylated H2AX (γH2AX) is recognized by MDC1, which then recruits more ATM molecules to the site of DNA damage, thereby amplifying ATM signaling [17, 18]. MDC1 also serves as a platform for the subsequent recruitment of multiple members of the ubiquitin conjugation machinery, such as RNF8 [19-22] and RNF168 [23, 24]. These factors modify histones proximal to the DNA DSB, which promotes DNA end processing and facilitates the recruitment of downstream factors required for HR such as BRCA1, BRCA2 and PALB2 [25].

In addition to promoting DNA damage response signaling, the MRN complex also plays a role in the initial processing of the DNA double-strand break. MRE11 has exonuclease activity, though of the opposite polarity for generating 3'-tailed ends (it degrades 3'→5') [26]. However, MRE11 also has single-stranded (ss)DNA endonuclease activity that is enhanced by its interaction with CtIP (Sae2 in yeast), an interacting protein of the CtBP transcriptional repressor [26]. By nicking DNA internally followed by successive removal of the oligonucleotides that are generated, resection in the 5'→3' direction effectively occurs. The phosphorylation of CtIP at several sites by cyclin-dependent kinases (CDKs) promotes its interaction with the MRN complex, which allows for its subsequent phosphorylation by ATM/ATR to regulate resection [27-29]. CDK-dependent phosphorylation of CtIP is thus a simple and elegant mechanism by

which eukaryotic cells couple resection of DSBs (and commitment to HR pathway) to cell cycle entry, where sister chromatids become available for use as templates [30].

CtIP-MRE11-mediated endonuclease activity is the initial step of resection that results in a few hundreds of nucleotides of resection (estimated from yeast) [31]. The CtIP-MRN complex also recruits EXO1 [32] and BLM/DNA2 nuclease-containing complexes to DNA ends, which have redundant roles in more processive 5'→3' degradation of DNA ends [33, 34]. The result of resection is extensive 3'-tailed ends that have been estimated to be several kilobases in length at IR-induced DSBs [35]. These 3'-tailed ends are then coated with RAD51 molecules and the resulting RAD51 nucleoprotein filament drives the search for homology and subsequent strand invasion [35]. However, prior to RAD51 loading, the 3'-tailed ends are bound by the ssDNA-binding heterotrimer, replication protein A (RPA) [36]. The coating of RPA on the 3'-tailed ends stimulates HR through several mechanisms. One function of RPA binding is to remove secondary structure from the 3'-tailed end to allow efficient RAD51 nucleoprotein filament formation [37, 38]. Another is the protection and stabilization of the ssDNA from degradation [39]. Lastly, RPA-coated ssDNA promotes further checkpoint signaling by recruiting another P13K-like kinase, ATR, through interaction with its binding partner, ATRIP [40]. Full activation of ATR also requires the recruitment of TOPBP1, which is recruited to the ssDNA-dsDNA junction of the 3'-tailed ends by the RAD9-RAD1-HUS1 ("9-1-1") complex [41]. An effector kinase of ATR, CHK1, then phosphorylates RAD51 at T309, which is required for the localization of RAD51 to chromatin [42].

Due to the higher affinity of RPA for ssDNA, RAD51 loading onto RPA-coated ssDNA requires auxiliary factors [43]. These factors form a functional class of proteins known as the RAD51 mediators and include some of the breast cancer susceptibility gene products (BRCA1,

BRCA2 and PALB2) and the RAD51 paralogs [7] (discussed in the next section). These proteins interact with RAD51, promote the displacement of RPA and/or its assembly onto 3'-tailed ends, and stabilize the RAD51 nucleoprotein filament so that it can perform homology search and strand invasion efficiently [7].

Once a region of homology has been found on the sister chromatid, the RAD51 nucleoprotein filament invades and forms a heteroduplex with the complementary strand. Disruption of the heteroduplex is avoided in part by the coating of the D-loop by RPA, which prevents reannealing to its complementary strand [44]. After stable heteroduplex formation, the RAD51 filament is disassembled in part by RAD54, a SWI/SNF class of chromatin remodeler, which allows for DNA synthesis [45]. Recent evidence points to the translesion synthesis polymerase, Pol η, in the extension and subsequent sequence restoration of the 3'-tailed end across the DNA break [46]. The replicative polymerase, Pol δ, also has a role in recombination-associated DNA synthesis [47].

The molecular factors that resolve or dissolve the double HJs that form during HR in higher eukaryotes have recently been identified. HJ resolution in higher eukaryotes involves the activities of two endonucleases: GEN1 [48] and SLX1 [49]. A scaffolding protein, SLX4, coordinates SLX1 in addition to two other nucleases, XPF and MUS81 [49]. In the alternative pathway, the BLM-TOPOIIIa-RMI1/2 complex coordinates the dissolution of the double HJs [50]. The helicase activity of BLM promotes the convergence of the double HJs by branch migration to form the hemicatenane, which is then cleaved by the topoisomerase, Topo-IIIa, thereby disentangling the two strands [50].

The RAD51 Recombinase

The recombinase function of RAD51 is highly conserved in all three domains of life (archaeal RadA, prokaryotic RecA, and eukaryotic RAD51) [51-54]. In the human genome, there are seven members of the RecA/RAD51 family: RAD51, DMC1, RAD51B, RAD51C, RAD51D, XRCC2 and XRCC3 [55]. While DMC1 exclusively mediates recombination in meiosis, the other RAD51 family members participate in both mitotic and meiotic recombination.

RAD51 is an essential gene in higher eukaryotes. Inactivation of RAD51 in mice results in embryonic lethality with no RAD51 -/- embryos found beyond the morula/blastocyst stage (100 hours post-coitum) in one study [56] and 7.5 days post-coitum in another [57]. Combining RAD51 inactivation with p53 mutation does not rescue embryonic lethality, though embryonic development progresses further to at least 9.5 days post-coitum [57]. Furthermore, RAD51 -/- blastocysts do not proliferate in culture, exhibit sensitivity to γ-radiation, and have reduced DNA content due to chromosomal loss [57]. Consistent with the mammalian studies, inactivation of RAD51 from chicken DT40 lymphoblasts causes extensive chromosomal breakage followed by cellular disintegration within the span of a single cell cycle [58]. The importance of RAD51 to viability at the cellular and organismal level in higher eukaryotes has been suggested to reflect the critical role of recombination in maintaining larger and more complex genomes [57].

Biochemical Function of RAD51

The protein architecture of human RAD51 consists of two domains joined by a linker region [59]. The N-terminal domain is a module of 5 short helices containing a positively charged cluster of lysine residues that mediates interaction with DNA [60]. The C-terminal domain of RAD51 contains the highly conserved ATPase core, which consists of Walker A-type

and B-type motifs that bind and hydrolyze ATP [59]. Additionally, there are two highly conserved loops (L1 and L2) within the ATPase domain that also mediate interaction with DNA [61].

Purified RAD51 can form right-handed helical filaments on DNA at a stoichiometric ratio of 1 RAD51 monomer to every 3 nucleotides or 3 base pairs [62]. The structural basis for RAD51 polymerization is physical interaction between the linker region of one RAD51 monomer and the ATPase domain of the adjacent monomer [59]. Importantly, the formation of the RAD51 nucleoprotein filament unwinds and extends the ssDNA within the filament by 50-60% [62]. This stretching of the DNA disrupts secondary structure and is believed to aid in homology search [62, 63].

RAD51 nucleoprotein filaments can interact with dsDNA *in vitro* thereby mimicking the ternary complex that forms during homology search [63]. Moreover, RAD51 coated ssDNA can promote strand invasion *in vitro* [63]. In one version of a strand-exchange assay, pre-coating RAD51 on circular ssDNA can promote base-pairing with and subsequent transfer of a strand of complementary sequence from a linearized DNA duplex [63]. These assays have demonstrated that the preferred DNA substrate of RAD51 for strand invasion is tailed DNA [64]. Additionally, the polarity of this pairing is 3' to 5' relative to the RAD51-coated ssDNA, suggesting that homology search may be initiated from closer to the ssDNA-dsDNA junction of tailed ends [37, 65]. Lastly, the formation of a RAD51 nucleofilament competent for strand invasion *in vitro* requires ATP-binding [66]. This homologous pairing mediated by RAD51 nucleofilaments however does not require the hydrolysis of ATP as RAD51 carrying the K133R mutation of the Walker A-type motif, which abrogates ATP hydrolysis but not binding, can still perform efficient strand invasion *in vitro* [66]. Furthermore, RAD51 nucleofilaments form [62] and strand

invasion occurs [63] in the presence of non-hydrolyzable ATP analogs. The hydrolysis of ATP is required for RAD51 filament disassembly and dissociation from DNA [66], which allows for DNA synthesis at the heteroduplex. Consistent with the importance of ATP binding and hydrolysis to its function, the expression of RAD51 ATPase-mutants in cells is cytotoxic, with increased levels of spontaneous and DNA-damage induced chromosomal aberrations, reduced HR repair efficiency and cellular sensitivity to DNA damaging agents [67, 68].

One of the central questions surrounding RAD51 function is the mechanism by which RAD51-ssDNA filaments perform homology search. Detailed structural studies of this process have not been reported so the exact mechanism of homology search and heteroduplex formation is unclear. However, it is currently hypothesized that the RAD51 nucleoprotein filament samples nearby duplexes by random collision until complementary sequence is found [69]. Interaction with the N-terminal (DNA binding) domains of the RAD51 monomers in the filament potentially destabilizes the duplexes, which allows for bases within the double helix to be revealed [60].

Recent structural analyses of a crystallized RecA-ssDNA filament revealed that rather than uniform unwinding and extension of the ssDNA, the RecA filament mainly extended the DNA backbone in between triplets of nucleotides [70]. The intercalation of the L1 loop of each RAD51 monomer in between triplets of nucleotides may extend ssDNA in a similar manner in human RAD51 as it does with prokaryotic RecA [71]. Within each triplet, B-form DNA is maintained suggesting a structural mechanism for pairing stringency conveyed by limiting the heteroduplex interactions during homology search to Watson-Crick base-pairing [70].

In support of this model, *in vitro* strand-exchange assays demonstrate that sampling occurs most efficiently at A-T rich regions of duplex, which can more easily flip-out of the double-helix and potentially form Watson-Crick base-pairing with the ssDNA of the

nucleoprotein filament [72]. Additionally, studies with RecA filaments *in vitro* suggest that multiple points of interaction between a nucleoprotein filament and the duplex DNA are required for efficient and stable heteroduplex formation [73].

RAD51 Foci Formation

After damaging cells with DNA DSB-inducing agents (e.g. IR, mitomycin C, methyl methanesulfonate, etc.), punctate subnuclear RAD51 foci can be detected and visualized immunocytochemically [35, 74]. These DNA damage-induced RAD51 foci co-localize with BrdU foci in non-denaturing conditions, which suggests the loading of RAD51 on ssDNA. Thus, these RAD51 foci are believed to represent RAD51 nucleoprotein filament formation *in vivo* [35]. The estimated length of the ssDNA at foci is several kilobases [35], indicating filaments of potentially thousands of RAD51 monomers in length are present at foci. However, it is unclear whether the RAD51 detectable in a focus are nucleoprotein filaments from a single break site or indicate an accumulation of nucleoprotein filaments from multiple break sites [35]. Furthermore, particularly bright and large foci may represent excessively long RAD51 nucleoprotein filaments (~100 kilobases of ssDNA) that form when homology search is still ongoing or has failed [35].

Despite some uncertainty in what RAD51 foci actually represent, their formation in response to DNA damage is an apparent indicator of RAD51 loading proficiency as both process are contingent on several key upstream events in the HR pathway. Factors that promote DNA damage response signaling (e.g. ATM/ATR, RNF8) or resection (e.g. CtIP) or phosphorylate key sites on RAD51 (e.g. PLK1 and CK2) or directly mediate RAD51 loading on resected 3'-tailed ends (e.g. BRCA2, RAD51 paralogs) are all required for the efficient formation of DNA damage-induced RAD51 foci (summarized in Table 1.1). Therefore, RAD51 foci can be used to monitor the overall integrity of the HR pathway upstream of RAD51 loading.

Table 1.1. Summary of factors that regulate the formation of DNA damage-induced RAD51 foci.

	Gene Name	Function in HR	Ref.
RAD51 Mediators	RAD51B	*RAD51 mediator*	[75, 76]
	RAD51C	*RAD51 mediator*	[76]
	RAD51D	*RAD51 mediator*	[76]
	XRCC2	*RAD51 mediator*	[76, 77]
	XRCC3	*RAD51 mediator*	[76, 78]
	BRCA2	*RAD51 mediator*	[79]
	PALB2	*RAD51 mediator*	[80]
	RAD52	*RAD51 mediator*	[81]
RAD51/RAD51 Mediator-Interacting Proteins	BRCA1	*PALB2/BRCA2 interactor*	[82]
	RAD18	*RAD51/RAD51 paralog interactor, Ub ligase*	[83]
	PP1α	*BRCA1 interactor*	[84]
	FLNA	*BRCA1 and BRCA2 interactor*	[85]
	MCPH1	*BRCA2 interactor*	[86]
	DSS1	*BRCA2 interactor*	[87]
	BCCIP	*BRCA2 interactor*	[88]
	APRIN	*BRCA2 interactor*	[89]
	MRG15	*PALB2 interactor*	[90]
	RAD54	*RAD51 interactor*	[91]
	MCM8	*RAD51 interactor*	[92]
	MCM9	*RAD51 interactor*	[92]
	SWI5	*RAD51 interactor*	[93]
	MEI5	*RAD51 interactor*	[93]
	GEMIN2	*RAD51 interactor*	[94]
	MDC1	*RAD51 interactor*	[95]
	Cyclin D1	*RAD51 interactor*	[96]
	EVL	*RAD51/RAD51 paralog interactor*	[97]
	hSWS1	*RAD51/RAD51 paralog interactor*	[98]
	SWSAP1	*RAD51/RAD51 paralog interactor*	[98]
RAD51/RAD51 Mediator Expression	CUX1	*Transcription of ATR, BRCA1, CHEK1*	[99]
	LAMINA/C	*Transcription of RAD51*	[100]
	E2F1	*RAD51 protein expression*	[101]
	PTEN	*Transcription of RAD51*	[102]
	FOXM1	*Transcription of RAD51, BRCA2*	[103]
	CBP	*Transcription of RAD51*	[104]
	p300	*Transcription of RAD51*	[104]
	Jab1	*Transcription of RAD51*	[105]
	PML	*RAD51 protein stability*	[106]
	HSP90	*RAD51 and BRCA1 protein stability*	[107]
	SMAD3	*RAD51 protein stability*	[108]
	SMAD4	*Transcription of RAD51 & BRCA1, RAD51 protein stability*	[108, 109]
	RBMX	*Post-transcription/Splicing of BRCA2*	[110]

	Gene Name	Function in HR	Ref.
Resection	CtIP	*BRCA1 interactor*	[111]
	MRE11	*MRN complex member, nuclease*	[111]
	BLM	*Helicase, RAD51 interactor*	[111]
	EXO1	*Nuclease*	[111]
	DNA2	*Nuclease*	[112]
Kinases	ATM	*DDR signaling*	[113]
	ATR	*DDR signaling*	[114]
	CHK1	*Phosphorylates RAD51*	[42]
	PLK1	*Phosphorylates RAD51*	[115]
	CK2	*Phosphorylates RAD51*	[115]
	CDK1	*BRCA1 phosphorylation*	[116]
	CDK2	*CtIP phosphorylation*	[117]
Ubiquitin-mediated signaling	RNF8	*Ubiquitinates H2A/H2AX*	[118]
	BRE1A/B (RNF20/RNF40)	*Ubiquitinates H2B*	[119, 120]
	p97	*Interacts with RNF8-dependent Ub K48 linkages*	[121]
	NPL4	*Recruits p97*	[121]
	Ubc13	*E2 with RNF8*	[122]
	USP14	*Proteasome-associated, de-ubiquitination*	[87]
	USP11	*BRCA2 interactor, de-ubiquitination*	[123, 124]
	RNF4	*RPA turnover at resected ends, proteasome recruitment*	[125]
	Proteasome	*Protein degradation, de-ubiquitination?*	[87]
	POH1	*Proteasome subunit, de-ubiquitination*	[126]
ATM/ATR signaling	PP4C/PP4R2	*RPA dephosphorylation*	[127]
	MMS22L	*RPA interactor, MCM interactor*	[128, 129]
	TONSL	*RPA interactor, MCM interactor*	[128, 129]
	RPA	*ATR signaling*	[130]
	RFWD3	*ATR signaling, RPA interactor*	[131]
	HCLK2	*ATR signaling*	[132]
	INTS3	*ATM signaling*	[133]
	hSSB1	*ATM signaling*	[133]
	PTIP	*ATM/ATR signaling*	[134]
Chromatin Modifier/Remodeler	SNF2h	*Chromatin remodeler*	[120]
	p400	*Chromatin remodeler, RAD51 interactor*	[135]
	KIF4A	*Chromatin modifier*	[136]
	TIP48	*Chromatin modifier*	[137]
	TIP49	*Chromatin modifier*	[137]
	TIP60	*Chromatin modifier*	[138]
	TRRAP	*Chromatin modifier*	[138]
	HP1α	*Chromatin interacting protein*	[139]
	p150/CAF-1	*Chromatin interacting protein*	[139]

Regulation of RAD51 Loading by Mediators

The main mediator of RAD51 filament formation in higher eukaryotes is the gene product of the breast cancer susceptibility gene, BRCA2 [7]. BRCA2 is a 3418-aa long protein with multiple motifs that interact with both RAD51 and DNA [140]. The BRCA2 protein contains eight BRC repeats, six of which can interact with RAD51 monomers. The stoichiometric ratio of purified BRCA2-RAD51 complexes is 1:6, suggesting that each motif can bind a RAD51 monomer contemporaneously [140]. Purified BRCA2 can efficiently load RAD51 onto RPA-coated ssDNA and promote strand invasion in vitro [140]. Furthermore, BRCA2 can downregulate ATP hydrolysis activity of RAD51, thereby stabilizing RAD51 nucleoprotein filaments [140, 141]. BRCA2 contains two DNA-binding domains: three-oligosaccharide-binding (OB) domains and a tower domain [142]. The three OB-folds and the tower domain have affinity to ssDNA and dsDNA, respectively, targeting the BRCA2-RAD51 complex to resected DNA [142].

The localization of BRCA2 to DNA damage sites also depends on two other breast cancer susceptibility gene products, BRCA1 and PALB2 (Partner And Localizer of BRCA2) [80]. BRCA1 localizes to DNA DSBs through several mechanisms and recruits BRCA2-RAD51 complexes through PALB2, which directly bridges BRCA1 and BRCA2 [80]. PALB2 can interact with and stabilize RAD51 filaments and stimulate strand invasion in vitro, suggesting a mediator function [143].

RAD52 is the critical mediator of RAD51 filament formation and HR in lower eukaryotes [7]. The importance of RAD52 to RAD51-mediated HR in higher eukaryotes has been unclear. While RAD52 stimulates RAD51-mediated strand invasion in vitro [144], mouse ES cells lacking RAD52 exhibit only mild HR defects as determined by gene targeting

efficiencies [145]. Furthermore, in contrast to RAD51 null mice, RAD52 null mice are viable with no overt phenotype [145]. Thus, it is believed that BRCA2 is the functional analog of RAD52 in higher eukaryotes and compensates for RAD52 loss in mediating HR [145]. Consistently, synthetic lethality is seen between BRCA2 and RAD52 [81]. Furthermore, the importance of RAD52 to RAD51 foci formation and cellular resistance to DNA damaging agents also becomes clear in the absence of BRCA1, PALB2 or the RAD51 paralogs [146, 147].

Regulation of RAD51 Expression

The expression of RAD51 is ubiquitous across cell types with enrichment in germ cells, presumably to support meiotic recombination [52, 53]. RAD51 expression is transcriptionally coupled to cell cycle progression with little to no expression in G0/G1 and peak expression in S-phase [148]. This is another regulatory mechanism of restricting the HR pathway to the S/G2 phase of the cell cycle. Several transcriptional factors are currently known to regulate RAD51 expression including STAT5 [149], E2F1[149], SMAD4 [109], FOXM1 [103] and the p300/CBP histone acetyltransferase complex [104]. Transcriptional repressors of RAD51 include the p53 tumor suppressor [150] and the p130/E2F4 complexes [151]. Post-translational stability of RAD51 is regulated by caspases [152], the molecular chaperone, HSP90 [107], and PML [106]. Importantly, many of these factors have been implicated in the regulation of HR through controlling RAD51 expression and foci formation (Table 1.1).

RAD51 in Disease

Mutations in several factors that regulate RAD51-mediated HR, including RAD51 mediators such as BRCA2 and RAD51C, confer breast and ovarian cancer susceptibility [8, 9, 153]. While cancer susceptibility of RAD51 heterozygous mice has not been reported, xenografted cells overexpressing a dominant negative allele of RAD51 exhibit increased

tumorigenicity in mice [154]. Additionally, RAD51 protein and mRNA expression is decreased in some cancers [155, 156]. These findings indicate that RAD51 itself may be a tumor suppressor in cancer. However, disease-associated alleles of RAD51 are rare, indicating the intolerability of RAD51 to genetic defect. A rare missense mutation (R150Q) was identified in two unrelated breast cancer patients, which was not seen in controls [157]. This mutation decreases ssDNA and dsDNA binding ability, suggesting the mutation compromises function [158]. Another mutation, the G135C single-nucleotide polymorphism in the 5'UTR of RAD51, potentially confers intermediate breast cancer risk in BRCA1/2 carriers, but this remains controversial [159]. The SNP reduces the abundance of an alternatively-spliced isoform of RAD51, potentially affecting protein expression [160]. While compromising mutations in RAD51 are rare, other mechanisms of RAD51 dysregulation in cancer may exist.

Interestingly, inherited mutations in RAD51 appear to be causal in an autosomal-dominantly inherited neurological condition, congential mirror movements (CMM) [161]. Patients with CMM have malformed motor neuron networks, which leads to voluntary movements on one side of the body mirrored by involuntary movements on the other [162]. Two unrelated European families with CMM carry different truncating alleles of RAD51 suggesting RAD51 haploinsufficiency is causal [161]. It is unclear how RAD51 dysfunction causes this disease. Does defective RAD51-mediated HR cause CMM? Or is an HR-independent function of RAD51 responsible for proper development of the motor neuron network? Of particular note is the recently reported interaction between RAD51 and GEMIN2 to regulate HR [94]. GEMIN2 interacts with SMN (Survival of Motor Neurons), which is the disease-causing gene of spinal muscular atrophy (SMA) [163].

The RAD51 Paralogs

The discovery of RAD51 in humans [53] prompted the search for RAD51 paralogs, as two such paralogs, RAD55 and RAD57, were known in yeast. Five paralogs were identified in the human genome (RAD51B, RAD51C, RAD51D, XRCC2 and XRCC3) [164-168] and are believed to have arisen from gene duplication [55, 169, 170]. These paralogs share 20-30% sequence identity between each other and with RAD51 [169]. Preliminary biochemical characterization of the paralogs demonstrated properties that were similar to those found for RAD51. Namely, the RAD51 paralogs could bind to both single and double-stranded DNA, and exhibited DNA-stimulated ATP hydrolysis activity [171-175]. Other than XRCC2, the paralogs also share similar domain architecture with RAD51 such that they contain an N-terminal domain and a C-terminal ATPase-containing domain joined by a flexible linker [169]. Interestingly, the linker region, which in RAD51 contains the polymerization motif, mediates interactions between the RAD51 paralogs [169] to form the following heterodimers: RAD51C-XRCC3 (CX3) [172, 175], RAD51B-RAD51C (BC) [43, 174] and RAD51D-XRCC2 (DX2) [171, 173]. The latter two complexes have also been shown to form a stable quaternary (BCDX2) complex [176].

Like RAD51, the RAD51 paralogs are essential for embryonic development and cannot be rescued by co-inactivation of p53 [177-180]. However, unlike RAD51-null cells, cells lacking the RAD51 paralogs and p53 can proliferate in culture albeit with decreased viability [76, 178, 179, 181, 182]. This suggests that RAD51 performs a critical function (i.e. recombination) that cannot be compensated for by any of the RAD51 paralogs. On the other hand, chemosensitivity of cells lacking any of the paralogs can be partially complemented by RAD51 overexpression [76].

The RAD51 paralogs are RAD51 mediators [170]. In support of this, purified BC heterodimers enhance RAD51-mediated strand exchange *in vitro* in the presence of RPA [43]. Furthermore, inactivating mutations in these paralogs in either mammalian or chicken cells compromise DNA damage-induced RAD51 foci formation [75-78], HR repair efficiency [183], chromosomal stability and cellular resistance to ionizing radiation or DNA interstrand-crosslinking agents [76]. While BCDX2 and CX3 complexes share overlapping functions in RAD51 loading, they are functionally distinct with respect to chemosensitivity and chromosomal breakage as simultaneously inactivating RAD51D and XRCC3 (intercomplex) results in more severe phenotypes than the co-inactivation of RAD51D and RAD51B (intracomplex) [184]. Furthermore, RAD51C has an additional role upstream of RAD51 loading in the nuclear import of RAD51 in response to DNA damage [185].

As mediators of RAD51 loading, the paralogs also localize to the site of DNA damage. RAD51C and XRCC3 both form foci in response to irradiation with faster kinetics than RAD51 [186, 187]. Additionally, while foci formation has not been reported for RAD51B, RAD51D or XRCC2, these proteins accumulate at an enzyme-induced DNA DSB as determined by chromatin immunoprecipitation [188]. The factors required for the localization of the RAD51 paralogs to DNA DSBs have not been extensively investigated, but RAD51C foci formation is dependent on RAD18, ATM, NBS1 and RPA but not BRCA2 [186].

The RAD51 paralogs play late roles in HR as well. The BCDX2 complex has affinities for Y-branched DNA, which mimics stalled replication forks, and HJs *in vitro* [189, 190]. Additionally, RAD51D interacts with the BLM helicase, and stimulates BLM-mediated dissolution of synthetic HJs *in vitro* [191]. The CX3 complex is required for branch migration and HJ resolution [192]. While the CX3 heterodimer does not have nuclease activity, it

associates with HJ resolvase activity *in vivo* [192]. Recent evidence suggests a functional link between XRCC3 and the GEN1 resolvase [193]. However, physical interaction between CX3 and GEN1 has not been detected [48]. The exact mechanisms by which the RAD51 paralogs contribute to HJ resolution and dissolution are not yet clear. Lastly, the CX3 heterodimer has additional roles in checkpoint signaling in response to DNA damage. Upon irradiation, RAD51C is required for efficient CHK2 phosphorylation [186].

MicroRNAs

MicroRNAs are 21-24 nucleotide-long, non-coding RNAs that downregulate gene expression post-transcriptionally [194, 195]. The first microRNA, lin-4, was discovered in *C. elegans* and was found to negatively regulate lin-14 protein expression suggesting the presence of an endogenous RNAi pathway [196, 197]. MicroRNAs were then found to be a common mechanism of gene regulation in all multicellular eukaryotes with the identification of a second *C. elegans* microRNA, let-7, and its homologues in other protostomes as well as deuterostomes [198, 199]. Currently, there are over 1500 microRNA genes that have been identified in the human genome [200]. These microRNAs are predicted to regulate ~60% of the protein-coding transcriptome [201], suggesting a role for microRNAs in the regulation of the majority of biological processes. Furthermore, the deregulation of microRNA expression can promote the progression of diseases such as cancer [202].

MicroRNA Biogenesis

MicroRNA genes are located in both intragenic (intronic) and intergenic loci throughout vertebrate genomes in roughly equal proportion [200]. MicroRNAs are transcribed by RNA polymerase II or III within larger transcripts called primary (pri)-microRNAs (Figure 1.2A) [195]. Specifically, the microRNA is situated within one of the two strands that form the stems

of a stem-loop or hairpin secondary structures within the pri-microRNA transcript. The stem region of these structures are recognized and cleaved ~11 base-pairs from the base by the Microprocessor complex, which consists of the double-stranded RNA binding protein, DGCR8, and a RNase III, Drosha (Figure 1.2B) [195].

The ~70 nucleotide excised stem-loop, or precursor microRNA (pre-microRNA), is subsequently translocated to the cytosol by the GTP-binding nuclear export protein, Exportin-5 [203], for further processing (Figure 1.2C). There, cleavage of the terminal loops of pre-microRNAs by another RNAse III, Dicer, and its dsRNA-binding partner, TARBP2 (TRBP), releases the mature microRNA duplex (Figure 1.2D) [204]. The mature microRNA is then incorporated into the RNase H-containing component of RISC (RNA-induced silencing complex), Argonaute (Ago) [205], while the other strand of the duplex is subsequently degraded (Figure 1.2E) [195]. Selection of the strand that is preferentially loaded into Ago depends on the thermodynamic properties at each end of the microRNA duplex. Generally, the strand that has its 5'-end at the more thermodynamically unstable (less stable base-pairing interactions) end is incorporated into RISC [195].

While the biogenesis of the majority of microRNAs is dependent on processing by the Microprocessor and Dicer complexes [195], the maturation of a subset of microRNAs can bypass either Drosha/DGCR8 or DICER/TARBP2 processing. "Mirtrons" are pre-microRNAs situated within small introns (50-200bp) that are released by splicing [206, 207]. Additionally, a single microRNA, miR-451, in the human genome does not require processing by Dicer [208, 209].

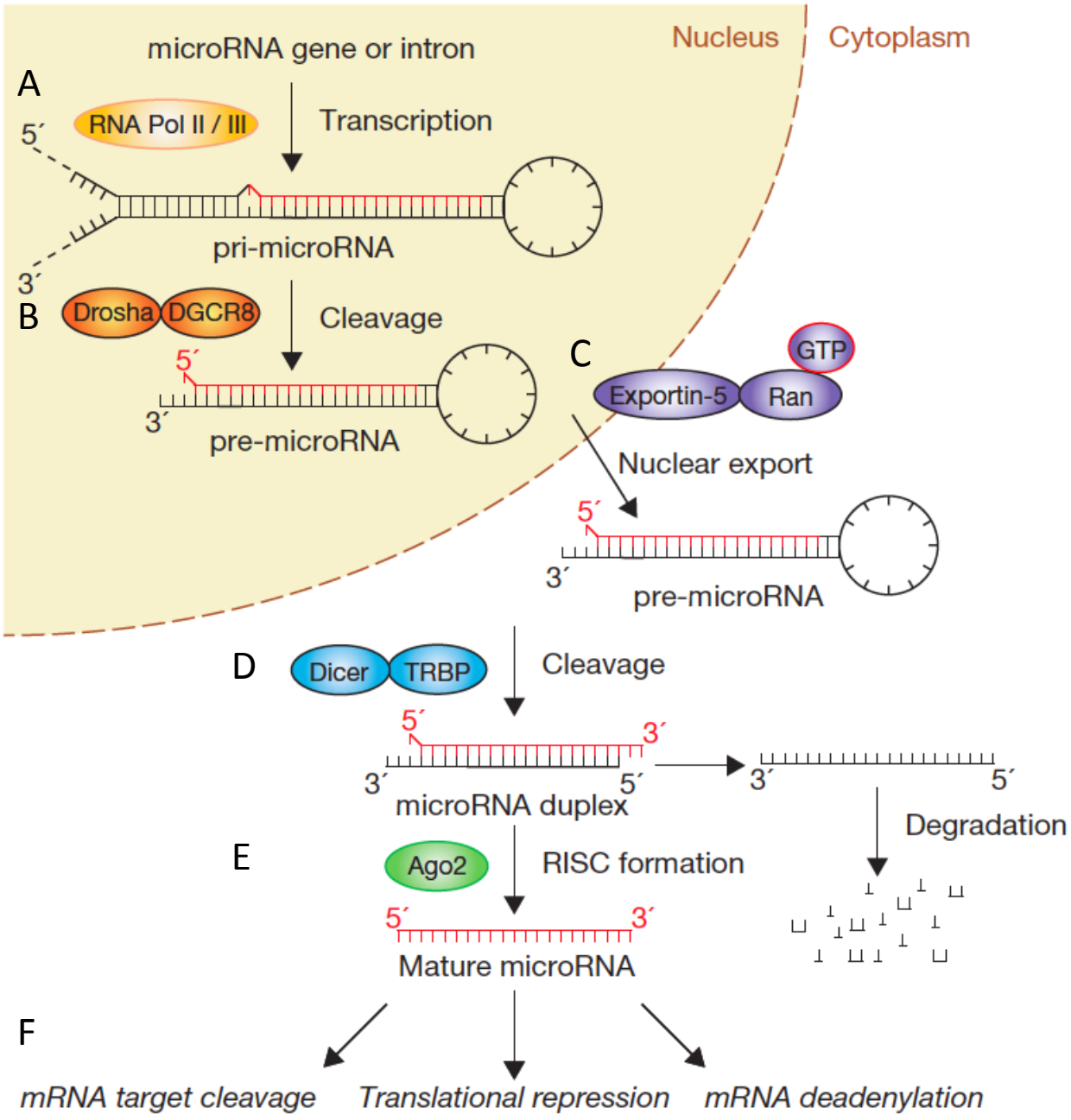

Figure 1.2. The microRNA biogenesis pathway.
A. The intronic or intergenic microRNA (red strand) is expressed within a larger pri-microRNA transcript by RNA polymerase II or III and forms a stem-loop structure. **B.** The double-stranded RNA stem is recognized and cleaved at the base by the Drosha/DGCR8 (Microprocessor) complex, which releases the pre-microRNA. **C-D.** The pre-microRNA is exported from the nucleus by Exportin-5 (**C**) where it is further processed by the Dicer/TRBP complex (**D**). **E.** The mature microRNA is then incorporated into Ago and directs the RISC complex to target mRNAs while the passenger strand (black) is degraded. **F.** The target mRNA is cleaved or translationally repressed and/or deadenylated depending on the degree of complementarity with the microRNA. Adapted from (195).

Mechanism of MicroRNA-mediated Silencing

MicroRNAs negatively regulate gene expression by mediating interaction between RISC and target mRNAs (Figure 1.2F). The basis of this interaction is perfect Watson-Crick base-pairing between the "seed" sequence of the microRNA (nucleotide positions 2-7 from the 5'-end) and the complementary site, which is generally located in the 3'UTR of the target transcript [210]. Consistent with the importance of binding to the seed region, the most common sequence motif identified in the transcripts of the most significantly downregulated mRNAs (by microarray) or proteins (by mass-spectrometry) in microRNA overexpression studies is the seed sequence complement [211, 212]. Additionally, several studies have demonstrated the importance of the 5'-end of microRNAs and/or 3'-end of microRNA binding sites in microRNA-mediated gene regulation by mutagenesis [213, 214]. There are additional sequence determinants in addition to seed complementation as well as exceptions to the "seed" rule that are further discussed in the next section.

The consequences of microRNA-mediated association of RISC with a messenger RNA are translational repression and mRNA destabilization [195]. Both of these processes are promoted primarily by the Ago-binding protein, GW182 (TNRC6A-C in mammals) [215, 216]. While the N-terminal glycine-tryptophan (GW) repeat-containing domain is responsible for interaction with Ago [217-219], both the N- and C-terminal domains of GW182 interact with the DCP1-DCP2 mRNA-decapping complex and the CCR4-NOT and PAN2-PAN3 mRNA-deadenylase complexes [215, 220-224]. The recruitment of these complexes to target mRNAs promotes the removal of 5'-caps and poly-adenylated tails from the ends of transcripts thereby exposing coding sequences to the exoribonucleolytic activities of Xrn1 and the exosome, which mediate 5'→3' and 3'→5' degradation, respectively [225].

In addition to promoting deadenylation, the CCR4-NOT complex also represses cap-dependent translation [226]. The tethering of CNOT1, the scaffolding component of the CCR4-NOT complex [220], to luciferase reporter transcripts lacking a poly-adenylated tail can promote translational repression in GW182-depleted cells [221]. This translational repression, as judged by reduction in luciferase activity, is observed without concomitant decreases in transcript levels [221]. These findings indicate that translational repression is primarily a consequence of CCR4-NOT complex recruitment to target mRNAs by GW182 and that it is independent of mRNA destabilization. More recently, CNOT7/CAF-1, one of the catalytic subunits of the CCR4-NOT deadenylase complex, was found to interact with the translation initiation factor, eIF4A2, to disrupt 5'-cap-dependent translation [227]. Thus, microRNAs regulate gene expression by mediating the recruitment of Ago/GW182/CCR4-NOT components of RISC, which couple translational repression and transcript destabilization, to targeted mRNAs.

Additional mechanisms of microRNA-mediated translational repression have been described. The MID domain within Ago2 shares homology with the 5'-cap-binding domain of the eIF4E initiation factor [228]. The microRNA-mediated association of Ago with target transcripts may prevent translation initiation by competing for binding of the 5'-cap [228]. Another potential mechanism of translational repression is the recruitment of eIF6, which is a protein factor that prevents formation of 80s ribosomes, to target transcripts by RISC [229]. Lastly, GW182 also interact with poly-A binding protein (PABP), which is required for mRNA circularization and formation of polysomes [224]. The disruption of PABP association with the 5'-cap by RISC renders translation less efficient [230].

An additional mechanism of microRNA-mediated mRNA destabilization has also been described in animals. In a small-interfering (si)RNA-like mechanism, perfect or near-perfect

complementarity between the target mRNA and the entire microRNA induces cleavage of the target mRNA by Ago2, which is the only one of the four mammalian Argonaute members that has endoribonuclease activity *in vivo* [231]. However, very few examples of siRNA-like targeting by microRNAs are known in animals due to imperfect complementarity typically observed between microRNAs and their mRNA targets [232, 233].

Identification of MicroRNA Targets

Critical to elucidating the physiological role of microRNAs is the accurate identification of their targets. Given the importance of seed-sequence interactions, the major target prediction algorithms (miRanda, TargetScan & PicTar) use the presence of seed complementary sites in the 3'UTR as the most basic criterion for the identification of putative targets [210, 234-236]. Additionally, Grimson and colleagues reported five other features of microRNA binding sites that improve the accuracy of microRNA target prediction by TargetScan [237]. Generalized from empirical data, these additional parameters include distance of the microRNA site from the center of the 3'UTR and its local AU content. Despite these considerations, the false-positive rate of the *in silico* approach remains in the range of 40-70% [210, 211].

The false-negative rate of target prediction algorithms is also high [210]. While perfect seed-sequence complementation may constitute the majority of microRNA-mRNA interactions, there are noted exceptions to the "seed" rule. For example, some targets mRNAs contain mismatches, deletions or G:U wobbles in the seed binding region yet are still sensitive to microRNA-mediated repression [238]. These mismatches are compensated for in part by more extensive complementation to the 3'-end of the microRNA [237]. However, these 3'-compensatory sites are estimated to constitute less than 10% of microRNA:mRNA interactions [210, 237]. Additionally, there are sites in which extensive pairing occurs between an ~11-mer

region of the middle of the microRNA and the target mRNA binding site. These "centered-paired" microRNA targets are subject to both siRNA-like cleavage and the conventional translational repression and mRNA destabilization [239]. Similar to the 3'-compensatory sites, this type of targeting interaction is also thought to be relatively rare [239]. Lastly, another non-canonical interaction are seed-binding sites that include single-nucleotide bulges, which represent at least 15% of microRNA-mRNA interactions detected in the brain tissue of P13 mice [240]. Collectively, these various non-canonical target interactions account for a significant proportion of microRNA:mRNA interactions [241] yet target prediction algorithms, such as TargetScan [236], do not comprehensively predict these types of interactions from the transcriptome.

Expression profiling approaches have been used to empirically identify potential targets of microRNAs. In particular, several studies have used a quantitative proteomic approach (stable isotope labeling by amino acids in culture (SILAC)) to determine changes in protein expression in response to microRNA overexpression or inhibition [211, 212]. While analyses of protein expression changes are most directly relevant to function, these proteomic approaches are limited by the fraction of the proteome that can be detected by mass spectrometry. For example, SILAC studies from Baek and colleagues [211] and Selbach and colleagues [212] were able to identify 1500-5000 unique proteins in HeLa cells yet this covers no more than half of the estimated proteome of HeLa [242].

While kinetic studies have demonstrated that translational repression precedes mRNA destabilization [243-245], changes in mRNA expression can largely account for changes in protein expression in steady state conditions [211, 212, 246]. Thus, transcriptome profiling is useful in the identification of potential microRNA targets although distinguishing between

primary and secondary effects on gene expression may present a challenge [212, 213]. More recent approaches have enriched for microRNA-mRNA interactions by deep-sequencing RNAs that co-immunoprecipitate with Ago proteins (HITS-CLIP and PAR-CLIP) [247, 248]. A distinct advantage of these approaches is the identification of Ago-associated microRNAs and mRNAs as well as the location of the binding sites within the bound transcripts [247, 248]. Additionally, these particular approaches have further clarified aspects of microRNA-mediated regulation of gene expression. For example, Hafner and colleagues demonstrated that Ago-binding sites are evenly distributed between both coding regions and 3'UTRs in HEK293 cells by using PAR-CLIP [248]. Putative microRNA binding sites outside of the 3'UTR are entirely missed by TargetScan and other prediction algorithms.

Regulation of Endogenous Targets by MicroRNAs

When microRNAs were inhibited by antisense oligonucleotides [212] or by genetic deletion [211], the observed upregulation of mRNAs or proteins that contained at least a binding site for the inhibited microRNA in their transcripts (i.e. putative endogenous targets) was very modest. These studies revealed that microRNAs rarely regulate endogenous targets significantly (50-80% repression) but more commonly make only a mild contribution (~30-50% repression) to gene expression [210-212]. These studies support a potential role for microRNAs as fine-tuners of protein output rather than switches for the majority of endogenous targets [210]. Alternatively, depending on expression levels of the endogenous targets and their respective thresholds for either activation or suppression, modest regulation by the microRNA may elicit a switch-like response [210]. Another possibility is that modest regulation of several components of a biological pathway may collectively have a significant impact on pathway functionality. Examples include miR-24 and miR-15/16 family, each of which regulates several targets

involved in the cell cycle progression [249, 250]. Lastly, it has also been proposed that the majority of endogenous targets of a given microRNA may be "pseudo-targets" in that their individual interactions with the microRNA are phenotypically inconsequential due to haplosufficiency [251]. However, through their collective occupancy of the microRNA, pseudo-targets may indirectly regulate the activity of "authentic" endogenous targets, whose functions are more sensitive to changes in expression [251].

MicroRNAs and DNA Repair

MicroRNAs have recently been implicated in the regulation of factors that mediate DNA repair [252, 253]. The DNA repair pathways that can be targeted by microRNAs include nucleotide excision repair, mismatch repair and translesion synthesis [252, 253]. Several factors involved in the repair of DSBs, such as ATM [254] and H2AX [255], are also targeted. Furthermore, components of the HR pathway in particular are also subject to microRNA-mediated regulation. These include BRCA1, which can be targeted by miR-24 [249] and miR-146a/146b-5p [256], and BRCA2, which can be targeted by the c-Myc-regulated miR-1245 [257]. Additionally, the hypoxia-inducible miR-210 and miR-373 directly regulate RAD52 expression [258] and two members of the oncogenic miR-183/96/182 cluster regulate RAD51 [259] and BRCA1 [260].

Both ATM and BRCA1 have been implicated in the regulation of microRNA expression, which demonstrates another level of cross-talk between microRNAs and DNA repair pathways [261, 262]. ATM-dependent phosphorylation of the KHSRP splicing regulatory protein, which interacts with the terminal-loops of both pri-microRNAs and pre-microRNAs to enhance their processing [263], modulates the expression of a subset of microRNAs in response to DNA damage [262]. It remains unclear how regulating the expression of these microRNAs contributes

to the cellular response to DNA damage, although it was noted that some of the microRNAs, like miR-16, have known roles in the regulation of cell cycle and apoptosis [262].

Interestingly, BRCA1 has been shown to be a novel component of the Microprocessor complex and promotes the processing of a subset of pri-microRNAs [261]. In addition to interaction with components of the Microprocessor such as Drosha, BRCA1 may also directly interact with pri-microRNAs [261]. It is unclear whether BRCA1 is required for modulating the expression of microRNAs in response to DNA damage.

Lastly, components of the microRNA biogenesis machinery has been implicated in the regulation of DNA damage response and HR. Specifically, Drosha and Dicer promote efficient DNA damage response signaling at early timepoints, as judged by diminished IR-induced foci formation of MDC1 and 53BP1 when Drosha or Dicer expression is knocked down [264]. Surprisingly, it was found that the generation of small RNAs at DSBs by these RNase III enzymes was required for the DNA damage response [264]. Furthermore, a role for canonical microRNA-mediated silencing in this aspect of the DNA damage response was ruled out because GW182 depletion had no effect on IR-induced 53BP1 or MDC1 foci formation [264]. Consistent with these findings, Wei and colleagues have shown that components of the microRNA biogenesis pathway, such as Dicer and Ago2, are required for efficient HR in both plants and human cells [265]. Deep-sequencing of plant and animal cells also revealed the generation of small RNAs at DSBs [265]. Therefore, a role for the microRNA biogenesis machinery in the DNA damage response may be evolutionarily conserved.

Aims of Dissertation

The overall aims of my dissertation were to characterize novel microRNA regulators of HR. From the results of human microRNA library-screenings conducted by the Taniguchi lab, I

focused on characterizing three microRNAs (miR-103, miR-107 and miR-221) that were putative negative regulators of HR. I demonstrated that these microRNAs can inhibit DNA damage-induced RAD51 foci formation and HR-mediated repair efficiency and that miR-103/107 in particular can enhance chemosensitivity to DNA damaging agents *in vitro* and *in vivo*. These findings are presented in Chapter Two. The identification of direct targets of miR-103/107 that are relevant for their regulation of HR and chemoresistance are presented in Chapter Three. Potential physiological contexts in which miR-103/107 might regulate HR and chemoresistance are explored in Chapter Four. The major conclusions and future directions of my dissertation are presented in Chapter Five.

CHAPTER TWO

Identification and characterization of microRNAs that regulate homologous recombination

Abstract

Homologous recombination mediates error-free repair of DNA double-strand breaks. RAD51 is a protein critical for homologous recombination and its recruitment to double-strand breaks is regulated by many factors including the RAD51 paralogs and breast/ovarian cancer susceptibility gene products such as BRCA1 and BRCA2. Deregulation of these factors leads to impaired homologous recombination, genomic instability, and cellular sensitivity to cisplatin and poly(ADP-ribose) polymerase (PARP) inhibitors. MicroRNAs are short, non-coding RNAs that negatively regulate gene expression post-transcriptionally. The role of microRNAs in the regulation of homologous recombination is not well characterized. To address this, we screened a human microRNA library and identified three microRNAs (miR-103, miR-107 and miR-221) that reduced RAD51 foci formation in response to ionizing radiation in HeLa and U2OS cells without altering cell cycle distribution. Consistent with the inhibition of RAD51 foci formation, miR-103 and miR-107 reduced HR repair efficiency and sensitized cells to various DNA damaging agents, including cisplatin and a PARP inhibitor. While miR-221 also reduced HR-mediated repair efficiency, it did not modulate cellular resistance to cisplatin. Our findings suggest a potential role for these cancer-associated microRNAs in promoting genomic instability and chemosensitivity in cancer.

Introduction

Homologous recombination (HR) is an error-free pathway of DNA double-strand break (DSB) repair. DSBs occur in the genome following exposure to exogenous DNA damaging agents such as ionizing radiation (IR) or from endogenous cellular events such as replication fork stalling and collapse [50]. The RAD51 recombinase is essential for HR and is recruited to sites of DNA damage to mediate repair; this recruitment can be visualized immunocytochemically as the appearance of distinct nuclear foci [74]. The loading of RAD51 at sites of DNA damage requires many factors including the breast and ovarian cancer susceptibility proteins (BRCA1, BRCA2/FANCD1, and PALB2/FANCN) and the RAD51 paralogs (RAD51B, RAD51C/FANCO, RAD51D, XRCC2 and XRCC3) [55, 183]. Defects in the regulation of HR are associated with genomic instability and mutations in some genes involved in HR, such as BRCA1, BRCA2, PALB2, RAD51C and RAD51D lead to cancer susceptibility [3, 8, 9, 11]. On the other hand, HR defects render cancer cells hypersensitive to DNA damaging chemotherapeutic agents such as interstrand DNA crosslinking agents and inhibitors of poly(ADP-ribose) polymerases (PARP) and topoisomerases [266]. Thus, identifying and understanding novel modes of regulating HR in cancer is critical for understanding the pathobiology cancer as well as in shaping the course for more effective treatment.

MicroRNAs are short non-coding RNAs that negatively regulate gene expression post-transcriptionally [194, 195]. MicroRNAs are excised from longer transcripts by endoribonucleolytic processing and incorporated into the Argonaute protein of RNA-induced silencing complexes (RISC). MicroRNAs then mediate interaction between RISC and messenger RNAs by base-pairing with complementary sites generally in the 3'-UTR of target transcripts. MicroRNA-mediated silencing results from translational repression and mRNA destabilization

[246]. There are over 1500 microRNAs in the human genome and are estimated to collectively regulate at least 60% of protein-coding transcripts [201] and thus, the majority of biological processes. Furthermore, aberrantly expressed microRNAs can initiate or drive the progression of diseases such as cancer [267].

Some microRNAs have been implicated in the regulation of factors required for DNA DSB repair [252, 253]. For example, the N-Myc regulated miR-421 targets the DNA DSB-responsive kinase, ATM, and can confer cellular radiosensitivity [254]. MiR-24 and the breast cancer-associated microRNAs miR-182 and miR-146a/b-5p can regulate BRCA1 [249, 256, 260] while a c-Myc-regulated microRNA, miR-1245, can target BRCA2 [257]. MiR-24 can also regulate the DSB-associated histone variant, H2AX, as does miR-138 [255, 268]. Additionally, we recently reported that miR-96 directly targets RAD51 [259]. To systematically identify microRNAs that regulate HR, we developed a cell-based screen to identify microRNAs whose overexpression altered RAD51 nuclear foci formation following irradiation with IR. In this study, we present our screen and the characterization of the three hits from this screen: miR-103, miR-107 and miR-221. We found that these microRNAs inhibit DNA damage-induced RAD51 foci formation, impair HR, and confer cellular sensitivity to DNA damaging agents *in vitro* and *in vivo*.

Results

Identification of microRNAs that regulate HR

Initially, we devised a screen using IR-induced RAD51 foci formation as a readout to systematically identify microRNAs that potentially regulate HR. A library of 394 human microRNA mimics (Dharmacon) was effectively overexpressed in HeLa cells by transfection.

Transfected cells were then irradiated with IR (15 Gy), fixed 8 hours later and immunostained for RAD51 foci. After acquiring images and manually scoring the percentage of RAD51-foci positive cells (cells with 5 or more nuclear foci), we identified 45 microRNAs whose overexpression reduced the percentage of RAD51-foci positive cells relative to the negative control (data not shown). Twenty of these microRNAs were then validated independently of the screen as negative regulators of IR-induced RAD51 foci formation in HeLa cells (Figure 2.1A).

HR and RAD51 loading are coupled to cell cycle progression [27]. In order to determine whether the reduction of IR-induced RAD51 foci formation may be due to changes in cell cycle progression, we examined the cell cycle profiles of HeLa cells overexpressing the 20 validated microRNAs. Using identical conditions as the screen (15 Gy IR, fixation 8 hours post-IR), we found that 10 of these microRNAs altered cell cycle progression as judged by significant increases in the percentage of G1-phase cells (Figure 2.1B). We subsequently excluded these 10 microRNAs from further analysis.

Using an updated microRNA library containing 810 human microRNA mimics (Dharmacon v10.1), we conducted another screen in U2OS cells. The updated microRNA library was overexpressed in U2OS cells by transfection and the transfected cells irradiated (10 Gy), fixed 6 hours post-IR and immunostained for RAD51 (Figure 2.2A). Images were then acquired by automated microscopy and the percentage of RAD51 foci-positive cells (10 or more nuclear foci) was determined by automated foci quantitation. From this U2OS-based screen, fifty-two microRNAs were found to significantly inhibit IR-induced RAD51 foci formation (Z-score < -2), including miR-96 [259], while only one microRNA (miR-372) increased (Z-score > 2) foci formation (Figure 2.2B, Table 2.1).

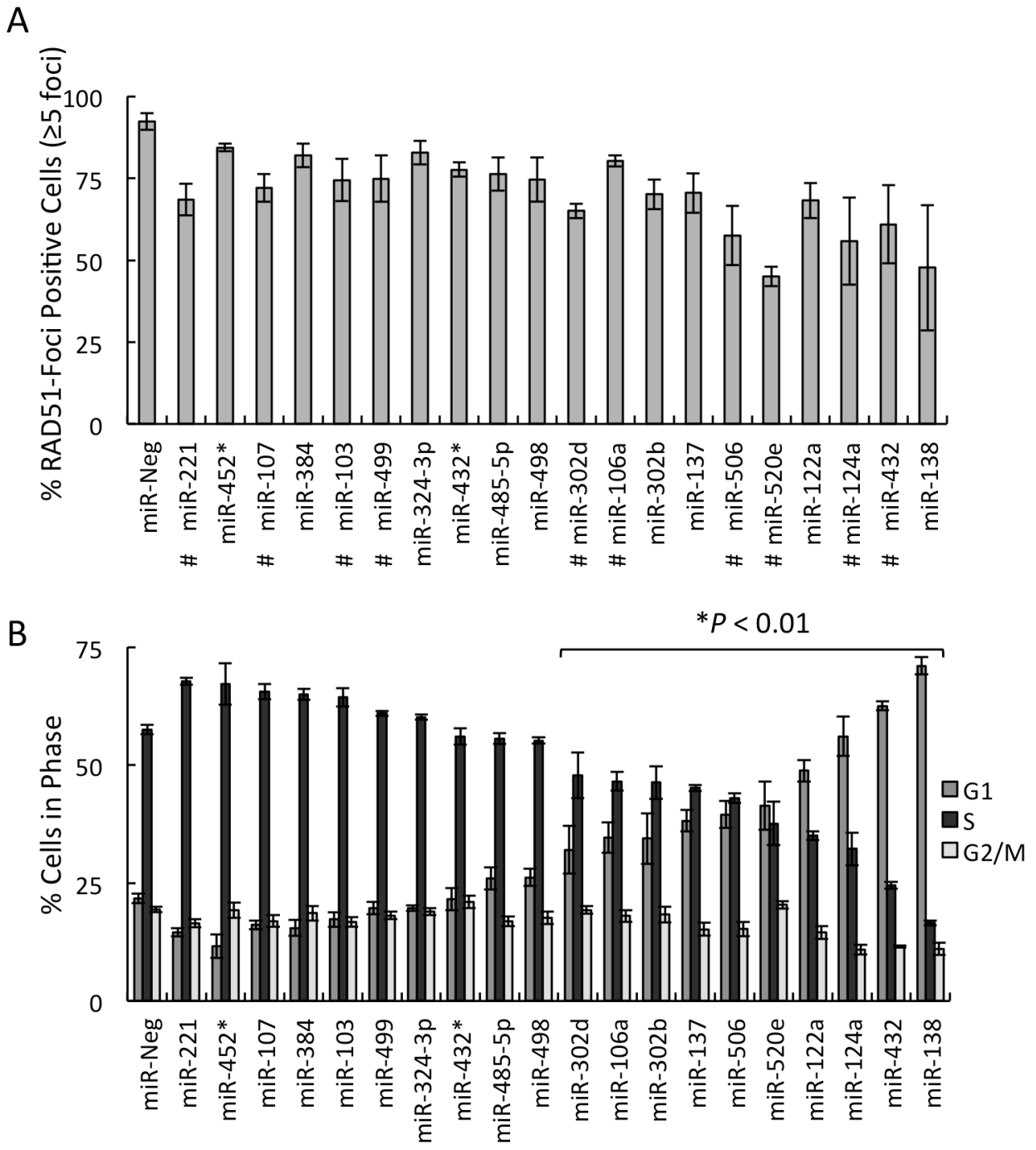

Figure 2.1. Identification of microRNAs that regulate IR-induced RAD51 foci formation in HeLa. **A.** HeLa cells transfected with indicated microRNAs (100 nM) were irradiated (15 Gy) 48 hours later, fixed 8 hours post-IR, and immunostained for RAD51. Nuclei were counterstained with DAPI. Cells that contained at least 5 RAD51 nuclear foci were scored as positive (n=3, +/-SEM). MicroRNAs that are predicted by TargetScan (236) to target the 3'UTR of RAD51 are indicated by "#". **B.** HeLa cells transfected with indicated microRNAs (100 nM) were irradiated (15 Gy) 48 hours later, pulse-labeled with BrdU for 15 minutes (8 hours post-IR), then fixed and stained for flow cytometry (n=3, +/-SEM) (Student's t-test: *$P < 0.01$).

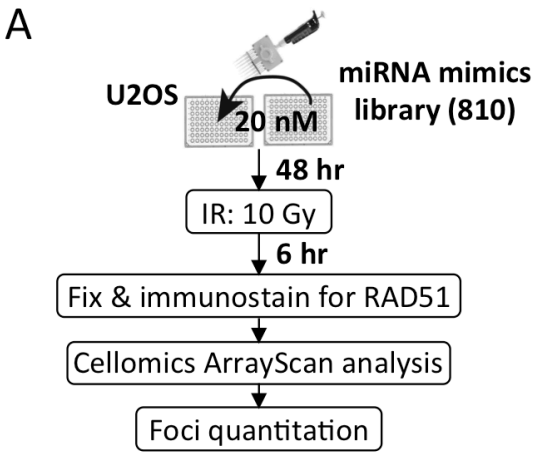

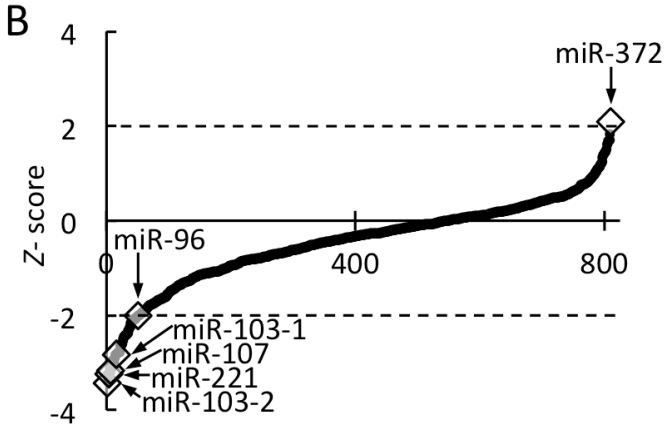

	Z-score	% RAD51 foci-positive cells	No. of RAD51 foci/cell	RAD51 intensity/cell
miR-Neg	-	67.05	29.19	189.44
miR-103-1	-2.83	36.97	13.80	91.79
miR-103-2	-3.44	40.21	15.05	90.22
miR-107	-3.16	41.71	15.09	106.46
siRAD51 #1	-5.23	1.51	3.04	52.47

C

miR-103 5'-AGCAGCAUUGUACAGGGCUAUGA*-3'
miR-107 5'-AGCAGCAUUGUACAGGGCUAUCA-3'

Figure 2.2. Identification of microRNAs that regulate IR-induced RAD51 foci formation in U2OS. **A.** Screening strategy for the identification of microRNAs that regulate IR-induced RAD51 foci formation in U2OS cells. **B.** The mean Z-scores of each microRNA from the screen are ranked (n=3). A table of Cellomics analyses for miR-103, miR-107 and a positive control, siRAD51, is presented. **C.** Mature sequence of miR-103 and miR-107 differ at a single nucleotide (*) and their respective seed regions are underlined.

Table 2.1. Summary of library screening to identify microRNAs that regulate IR-induced RAD51 foci formation.

The mean Z-scores of three independent experiments are ranked in ascending order. 'SD' is standard deviation. For the 52 microRNAs that significantly reduced the percentage of RAD51 foci-positive cells (mean Z-score < -2) (presented on this page), "#" indicates those microRNAs that are predicted to target the RAD51 3'UTR by TargetScan (236).

	Mature Sanger ID	Precursor Accession	Z-score	SD
#	hsa-miR-103	MI0000108	-3.4406	1.0962
	hsa-miR-182*	MI0000272	-3.4001	1.3546
#	hsa-miR-124a	MI0000444	-3.3158	0.6427
#	hsa-miR-221	MI0000298	-3.2462	0.9355
	hsa-miR-181c*	MI0000271	-3.2174	0.4847
#	hsa-miR-124a	MI0000443	-3.1742	0.3150
#	hsa-miR-107	MI0000114	-3.1644	0.2324
#	hsa-miR-124a	MI0000445	-3.1166	0.5546
	hsa-miR-15a	MI0000069	-3.0940	0.2331
	hsa-miR-15b	MI0000438	-3.0592	0.8551
	hsa-miR-497	MI0003138	-3.0118	0.5243
	hsa-miR-16	MI0000070	-2.9859	0.4059
	hsa-miR-593*	MI0003605	-2.9112	0.9978
#	hsa-miR-494	MI0003134	-2.8425	0.8179
	hsa-miR-34b*	MI0000742	-2.8353	0.5061
#	hsa-miR-103	MI0000109	-2.8262	0.6109
	hsa-miR-556-3p	MI0003562	-2.8013	0.3966
	hsa-miR-15a*	MI0000069	-2.7885	2.2032
	hsa-miR-17-3p	MI0000071	-2.7873	0.3436
#	hsa-miR-506	MI0003193	-2.7826	0.3959
	hsa-miR-424	MI0001446	-2.7768	1.6335
	hsa-miR-16	MI0000115	-2.6433	0.2763
	hsa-miR-148b*	MI0000811	-2.6417	0.2654
	hsa-miR-214*	MI0000290	-2.6300	0.8250
	hsa-miR-195	MI0000489	-2.6042	0.7020
	hsa-miR-223*	MI0000300	-2.5394	0.1109

	Mature Sanger ID	Precursor Accession	Z-score (mean)	SD
	hsa-miR-219-1-3p	MI0000296	-2.4926	0.7441
	hsa-miR-9*	MI0000467	-2.4400	0.6693
	hsa-miR-221*	MI0000298	-2.4376	0.5244
#	hsa-miR-655	MI0003677	-2.4302	0.5918
	hsa-miR-541	MI0005539	-2.4174	1.3746
#	hsa-miR-526b	MI0003150	-2.4103	1.7767
	hsa-miR-488*	MI0003123	-2.4015	0.3765
#	hsa-miR-222	MI0000299	-2.3763	0.8289
	hsa-miR-671-3p	MI0003760	-2.3253	1.0955
	hsa-miR-499-3p	MI0003183	-2.3006	0.0408
	hsa-miR-610	MI0003623	-2.2541	2.7964
	hsa-miR-520d*	MI0003164	-2.2380	0.3975
	hsa-miR-27b*	MI0000440	-2.1656	0.5913
	hsa-miR-32*	MI0000090	-2.1546	0.5203
	hsa-miR-628-5p	MI0003642	-2.1129	0.3263
	hsa-miR-124*	MI0000445	-2.1075	0.1575
	hsa-miR-147	MI0000262	-2.0913	1.4338
	hsa-miR-383	MI0000791	-2.0766	0.9602
	hsa-miR-183*	MI0000273	-2.0730	0.4348
	hsa-miR-143*	MI0000459	-2.0711	1.0609
	hsa-miR-183	MI0000273	-2.0579	0.2856
	hsa-miR-646	MI0003661	-2.0459	0.9443
	hsa-miR-137	MI0000454	-2.0192	0.7733
	hsa-miR-624	MI0003638	-2.0163	0.5438
#	hsa-miR-96	MI0000098	-2.0117	0.3159
	hsa-miR-532	MI0003205	-2.0016	0.6652

When the microRNA hits from the HeLa- and U2OS-based screens were compared, three microRNAs were found to be in common: miR-103, miR-107 and miR-221. We initially focused on miR-103 and miR-107 for further study based on the following considerations. These microRNAs are deregulated in cancer [269-274] and their overexpression in a subset of breast cancer is linked to tumor invasiveness [275]. Furthermore, miR-103/107 are upregulated after doxorubicin-induced DNA damage [276-279] or in response to hypoxic conditions [270]. This suggests that miR-103/107 may have fundamental roles in the regulation of HR in response to cellular stress or in cancer development.

MiR-103 and miR-107 inhibit DNA damage-induced RAD51 foci formation

MiR-103/107, a pair of paralogous microRNAs that differ at a single nucleotide and likely regulate overlapping targets due to seed region identity (Figure 2.2C), stood out as the most potent inhibitors of RAD51 foci formation (Figure 2.2B). We independently validated the inhibition of IR-induced RAD51 foci formation by miR-103/107 overexpression in U2OS cells and found the inhibition to be intermediate of BRCA2 and RAD51D depletion (Figure 2.3A) and similar to the effects seen in HeLa cells (Figure 2.3B). Additionally, we observed similar inhibition of IR-induced RAD51 foci formation by miR-103/107 in a third cell line, PEO1 C4-2 [280] (Figure 2.3C). Furthermore, RAD51 foci formation in response to a different DSB-inducing agent, cisplatin, was similarly inhibited by miR-103/107 (Figure 2.3D). These data indicate that miR-103/107 overexpression impairs DNA damage-induced RAD51 foci formation in a manner that is independent of cell-type or the DNA damaging agent used.

Next, we determined whether the reduction of DNA damage-induced RAD51 foci formation in U2OS and PEO1 C42 cells was due to changes in cell cycle progression. We

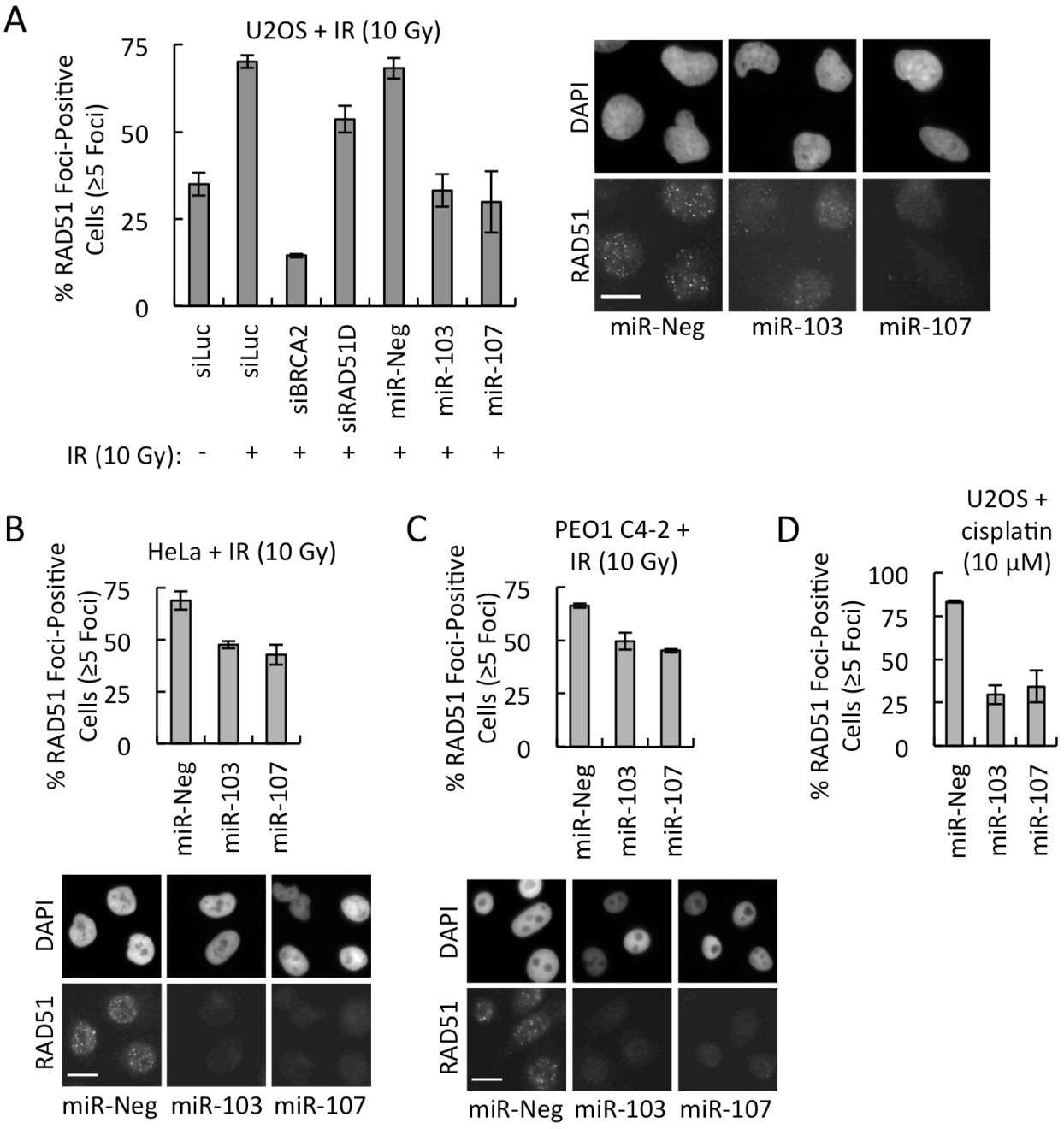

Figure 2.3. MiR-103/107 regulates DNA damage-induced RAD51 foci formation.
A-C. U2OS (**A**), HeLa (**B**) and PEO1 C4-2 cells (**C**) transfected with indicated microRNAs or siRNAs (10 nM) were irradiated (10 Gy) 48 hours later, fixed 6 hours post-IR, and immunostained for RAD51. Nuclei were counterstained with DAPI. Cells that contained at least 5 RAD51 nuclear foci were scored as positive (n=3, +/-SEM). Representative images are shown (scale bar = 20 μm). **D.** U2OS cells transfected with indicated microRNAs (10 nM) were treated with cisplatin (10 μM) 48 hours later, fixed after 24 hours of cisplatin treatment, and immunostained for RAD51. Nuclei were counterstained with DAPI. Cells that contained at least 5 RAD51 nuclear foci were scored as positive (n=3, +/-SEM).

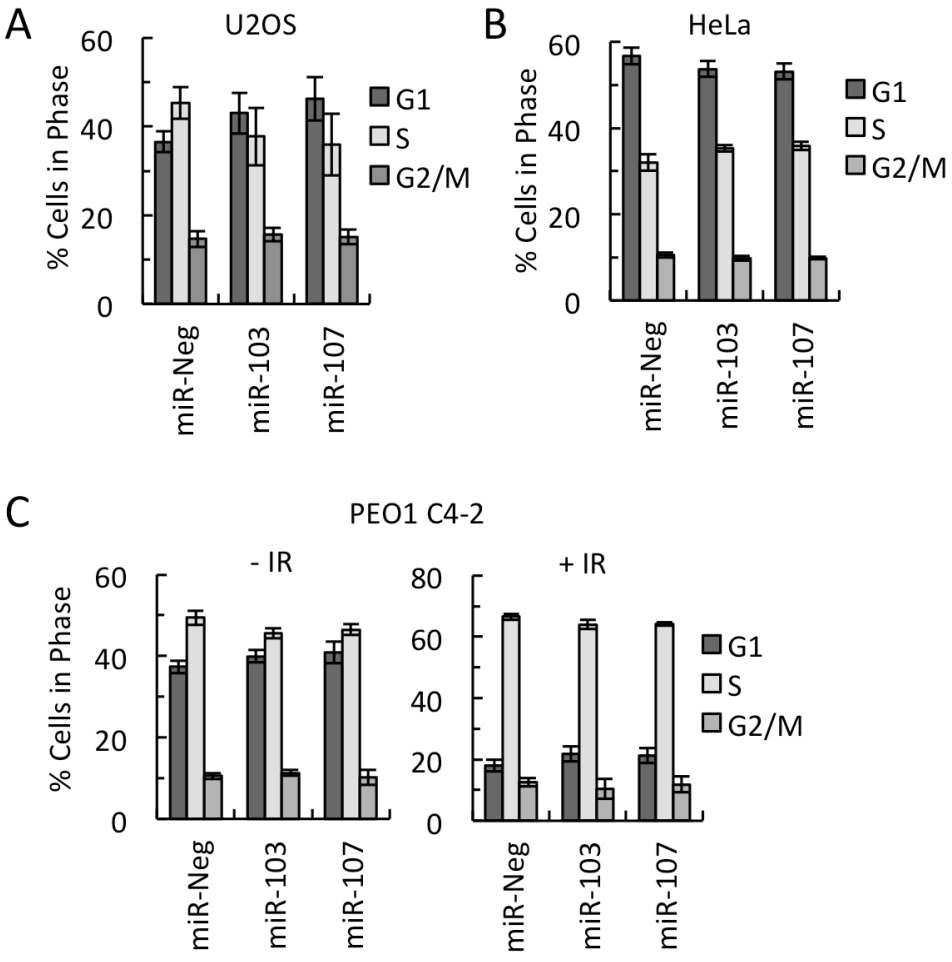

Figure 2.4. MiR-103/107 does not significantly alter cell cycle progression.
A-B. U2OS (**A**) and HeLa (**B**) were transfected with indicated microRNAs (10 nM), pulse-labeled with BrdU for 15 minutes 48 post-transfection, then fixed and stained for flow cytometry (n=3, +/-SEM). **C.** PEO1-C4-2 cells transfected with indicated microRNAs (10 nM) were irradiated (10 Gy) 48 hours after transfection ("+ IR"), pulse-labeled with BrdU for 15 minutes (6 hours post-IR), then fixed and stained for flow cytometry (n=3, +/-SEM).

performed cell cycle analyses and found that miR-103/107 overexpression did not significantly increase the percentage of cells in G1 in untreated HeLa, U2OS or PEO1 C4-2 cells or in PEO1 C4-2 cells that had been irradiated (Figure 2.4A-C). We therefore concluded that the reduction in DNA damage-induced RAD51 foci formation by miR-103/107 overexpression is due to a mechanism independent of cell cycle regulation.

MiR-103 and miR-107 impair HR and promote chemosensitivity to DNA damaging agents

The loading of RAD51 at sites of DSBs is essential for repair by HR. We therefore examined whether the efficiency of HR repair is impacted by the overexpression of miR-103/107 in the U2OS DR-GFP cell line [281] . This cell line carries a stably integrated copy of the DR-GFP direct-repeat reporter construct, which uses restoration of a GFP reading frame as an indicator of successful HR repair [282]. The overexpression of miR-103/107 or the depletion of BRCA2 was found to significantly reduce the percentage of GFP-positive cells following induction of a site-specific DSB by I-SceI (Figure 2.5A).

Proficient HR is required for cellular resistance to DNA damaging agents that induce DSBs in S-phase, including PARP inhibitors, interstrand DNA crosslinkers (e.g. cisplatin) and topoisomerase inhibitors (e.g. camptothecin and etoposide). Consistent with HR deficiency, miR-103/107 overexpression sensitized several cell lines to a PARP inhibitor, AZD2281, and cisplatin (Figure 2.5B and C and Figure 2.6A and B). Additionally, the overexpression of miR-103/107 sensitized U2OS and HeLa cells to camptothecin and etoposide (Fig. 2.7A and B) while PEO1 C4-2 cells did not exhibit sensitivity to these compounds. Consistent with defects in IR-induced RAD51 foci formation, miR-103/107 overexpression also sensitized cells to ionizing radiation (Figure 2.7C). Stable expression of miR-103/107 by lentiviral transduction of microRNA precursors (Figure 2.8A and B) enhanced chemosensitivity in multiple cell lines (Figure 2.8C-F).

In contrast, miR-103/107 overexpression did not sensitize cells to paclitaxel, a microtubule-stabilizing agent.

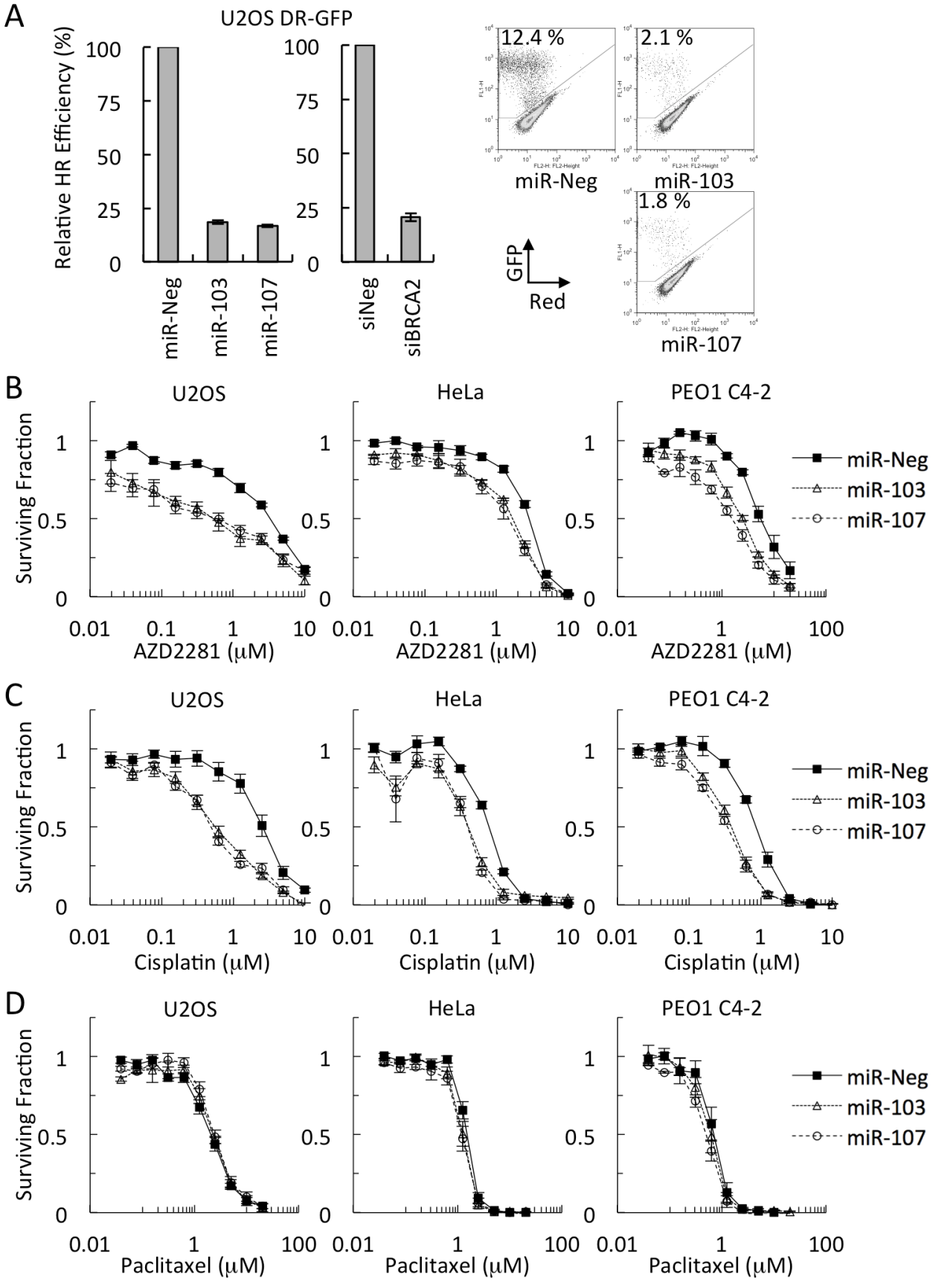
A
U2OS DR-GFP
Relative HR Efficiency (%)
100
75
50
25
0
miR-Neg
miR-103
miR-107
siNeg
siBRCA2
12.4 %
2.1 %
1.8 %
miR-Neg
miR-103
miR-107
GFP
Red
B
U2OS
HeLa
PEO1 C4-2
Surviving Fraction
AZD2281 (μM)
C
Cisplatin (μM)
D
Paclitaxel (μM)
miR-Neg
miR-103
miR-107

Figure 2.5. MiR-103 and miR-107 impair HR and promote chemosensitivity to DNA damaging agents.
A. U2OS DR-GFP cells initially transfected with indicated microRNAs (10 nM) were subsequently transfected with an I-SceI homing endonuclease-expression vector the next day and harvested 48 hours later for flow cytometry. U2OS DR-GFP cells depleted of BRCA2 (10 nM) were used as a positive control of impaired HR. Representative flow cytometry profiles with gated GFP-positive populations are shown (n=4, +/-SEM). HR repair efficiency is presented as a percentage of the miR-Neg- or siNeg-transfected controls. **B-D.** U2OS, HeLa and PEO1 C4-2 cells transfected with indicated microRNAs (10 nM) were reseeded 48 hours later to assay for cellular survival in response the PARP inhibitor, AZD2281 (**B**), cisplatin (**C**), and the microtubule stabilizing agent, paclitaxel (**D**). Cell survival was assayed by crystal violet staining and expressed as a fraction of the untreated control (n=3, +/-SEM).

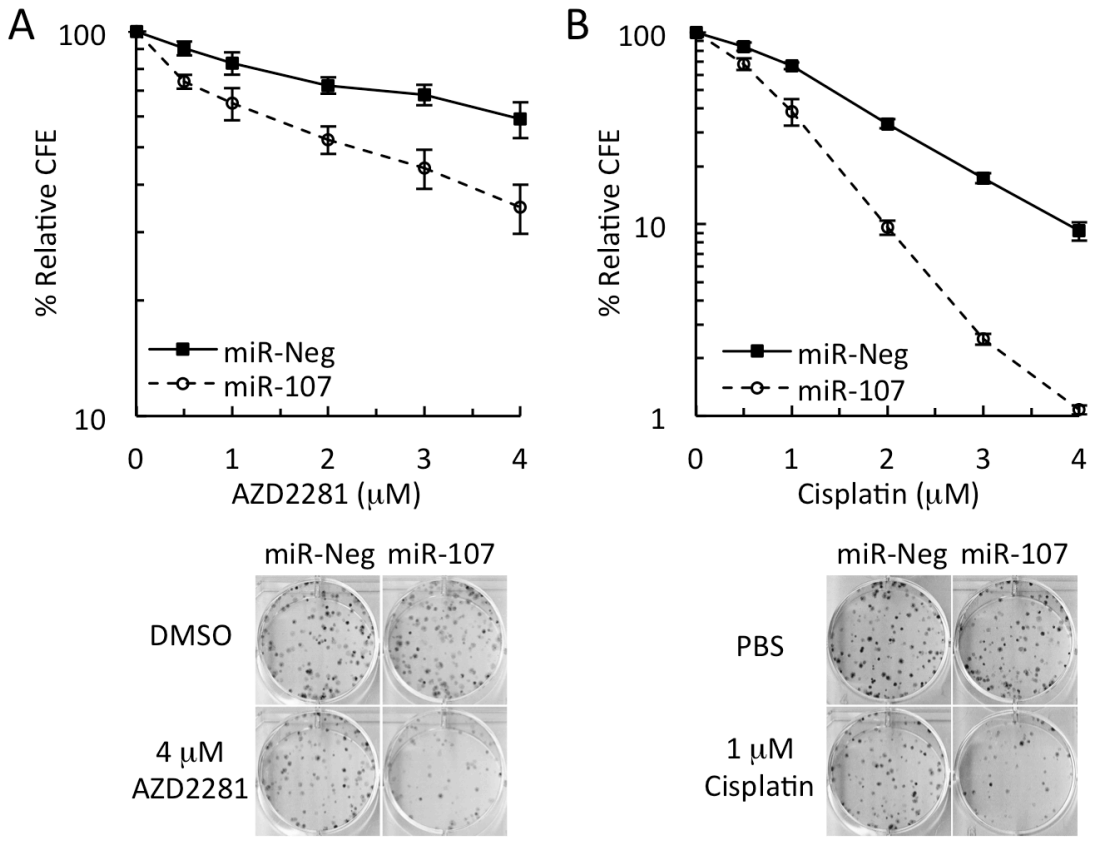

Figure 2.6. MiR-103/107 enhances cellular sensitivity to cisplatin and PARP inhibition.
A-B. Clonogenic assays of HeLa cells transfected with indicated microRNAs (10 nM) in response to AZD2281 (**A**) and cisplatin (**B**). Transfected HeLa cells were treated with indicated doses of cisplatin and AZD2281 for 24 hours, and then allowed to recover for 10 days. Colonies were stained with crystal violet and scored if they contained 50 or more cells. Colony formation efficiency (CFE) is expressed as a percentage of the PBS or DMSO treated control (n=3-4, +/-SEM). Representative images of clonogenic assays are shown.

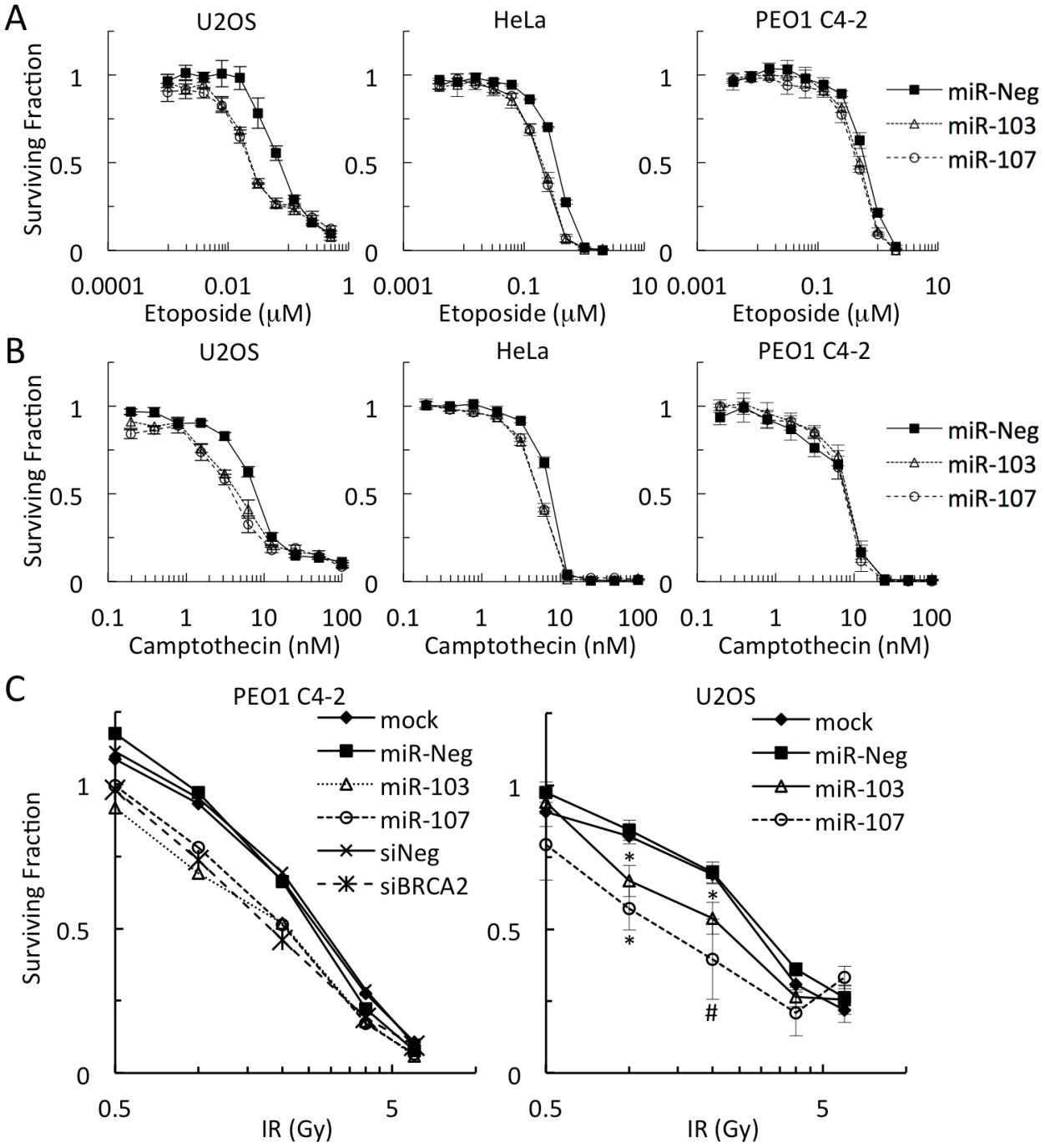

Figure 2.7. MiR-103/107 promotes cellular sensitivity to topoisomerase inhibitors and ionizing radiation.

A-B. U2OS, HeLa and PEO1 C4-2 cells transfected with indicated microRNAs (10 nM) were reseeded 48 hours later to assay for cellular survival in response to the topoisomerase inhibitor etoposide (**A**) or camptothecin (**B**). Cell survival was assayed by crystal violet staining and expressed as a fraction of the untreated control (n=3, +/-SEM). **C.** PEO1 C4-2 and U2OS cells transfected with indicated siRNAs or microRNAs (10 nM) were reseeded 48 hours later to assay for cellular survival in response to ionizing radiation. Cell survival was assayed by crystal violet staining and expressed as a fraction of the untreated control. Survival curves for PEO1 C4-2 cells are the averages of two independent experiments. Survival curves for U2OS cells are the average of three independent experiments (+/-SEM) (Student's t-test: *P < 0.05, n.s. = not significant).

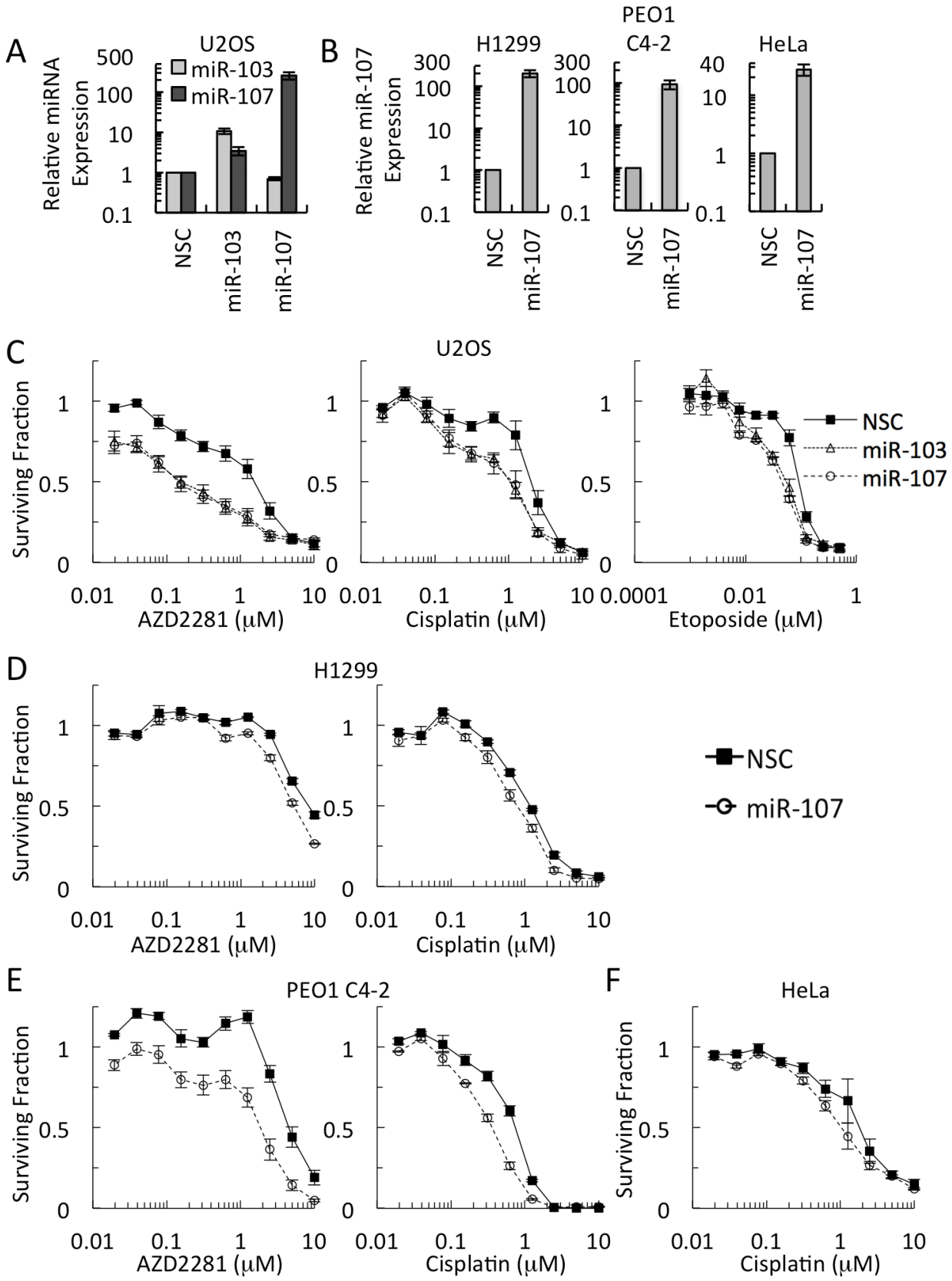
A
U2OS
miR-103
miR-107
Relative miRNA Expression
500
100
10
1
0.1
NSC
miR-103
miR-107
B
PEO1
H1299
C4-2
HeLa
Relative miR-107 Expression
300
100
10
1
0.1
40
10
1
0.1
NSC
miR-107
C
U2OS
Surviving Fraction
1
0.5
0
0.01
0.1
1
10
AZD2281 (μM)
Cisplatin (μM)
0.0001
Etoposide (μM)
NSC
miR-103
miR-107
D
H1299
NSC
miR-107
E
PEO1 C4-2
F
HeLa

Figure 2.8. Stable transduction of miR-103/107 precursors promotes chemosensitivity.
A. U2OS cells stably expressing a non-silencing control hairpin (NSC) or precursors of miR-103 or miR-107 were harvested for real-time PCR (n=3, +/-SEM). **B.** H1299, PEO1 C4-2 and HeLa cells stably expressing NSC or miR-107 precursor were harvested for real-time PCR (n=3, +/-SEM). **C.** Cell survival in U2OS cells stably expressing indicated precursors in response to cisplatin, AZD2281 and etoposide. Cell survival was assayed by crystal violet staining and expressed as a fraction of the untreated control (n=3-4, +/-SEM). **D-F.** Cell survival of NSC- or miR-107-transduced H1299 (**D**) and PEO1 C4-2 (**E**) cells in response to cisplatin and AZD2281 and NSC- or miR-107-transduced HeLa cells (**F**) in response to cisplatin. Cell survival was assayed by crystal violet staining and expressed as a fraction of the untreated control (n=3, +/-SEM).

(Figure 2.5D), suggesting that cellular sensitivity is specific to DNA damage and not due to general cytotoxicity.

In order to determine whether miR-103/107 mediate chemosensitivity only through the inhibition of HR, we assayed cell survival in miR-107-transfected PEO1 cells treated with AZD2281 or cisplatin (Figure 2.9A and B). PEO1 cells carry a hemizygous truncating mutation in BRCA2 and are HR-deficient [280]. The overexpression of miR-103/107 very mildly sensitized PEO1 cells to PARP inhibition and cisplatin (Figure 2.9A and B). The depletion of a translesion synthesis polymerase, REV1 [259], served as an HR-independent cisplatin sensitivity control (Figure 2.9B). These results suggest that miR-103/107 mainly target HR to mediate chemosensitivity to DNA damaging agents but additional HR-independent mechanisms of chemoresistance may also be targeted.

MiR-107 mediates chemosensitivity *in vivo*

The targeting of HR in tumors to enhance therapeutic response to DNA damaging agents has gained increasing interest [283]. To address the therapeutic potential of miR-103/107, we used a xenograft model of tumor growth to determine whether miR-107 overexpression can mediate chemosensitivity *in vivo*. After confirming *in vitro* chemosensitivity and target repression (Figure 2.10A and B), we implanted H1299 cells stably expressing miR-107 or a non-targeting control (NSC) into the flanks of immunodeficient mice. Upon tumor formation (18 days after implantation of cells), we began administering cisplatin (5 mg/kg/week) or PBS (vehicle) intraperitoneally and monitored tumor volume. Over the course of tumor outgrowth in the PBS-treated mice, we observed no significant difference in tumor growth between the control and miR-107-overexpressing tumors (Figure 2.10C). In contrast, miR-107 overexpression modestly reduced tumor growth relative to the control when combined with cisplatin treatment

(Figure 2.10C). A single miR-107-overexpressing tumor grew markedly faster (outlier) than the rest of the group (Figure 2.10D). If the outlier was removed, tumor growth was significantly reduced in the cisplatin-treated miR-107-overexpressing group relative to the NSC control group (not shown) ($P < 0.05$ for days 24-33, Student's t test). When examining the time tumors took to reach 10-fold their initial volumes, we found a 1.5-day difference between PBS-treated NSC and miR-107-overexpressing tumors that increased to a 6-day growth delay with cisplatin treatment. Similarly, this difference did not reach statistical significance because of the inclusion of the faster growing miR-107 tumor (Figure 2.10D and E). However, cisplatin delayed the growth of miR-107-overexpressing tumors by 8.5 days relative to PBS treatment while cisplatin delayed NSC tumor growth by only 4 days (Figure 2.10E). These results indicate that miR-107 mediates mild cisplatin sensitivity of H1299-xenografted tumors.

MiR-221 impairs HR but not chemoresistance to cisplatin

Lastly, we characterized the third microRNA commonly identified in our two screens, miR-221. Consistent with impaired RAD51 foci formation, the overexpression of miR-221 strongly reduced HR repair efficiency in U2OS DR-GFP cells (Figure 2.11A). The degree of HR deficiency was similar to the overexpression of miR-103 or miR-107 (Figure 2.11A). We then investigated whether the HR deficiency mediated by miR-221 would similarly lead to chemosensitivity to DNA damaging agents. The overexpression of miR-103 significantly compromised survival of PEO1 C4-2 cells in response to cisplatin as observed before (Figure 2.11B). Surprisingly, we found that miR-221 overexpression at two different concentrations of mimic transfection did not alter cell survival in response to cisplatin (Figure 2.11B).

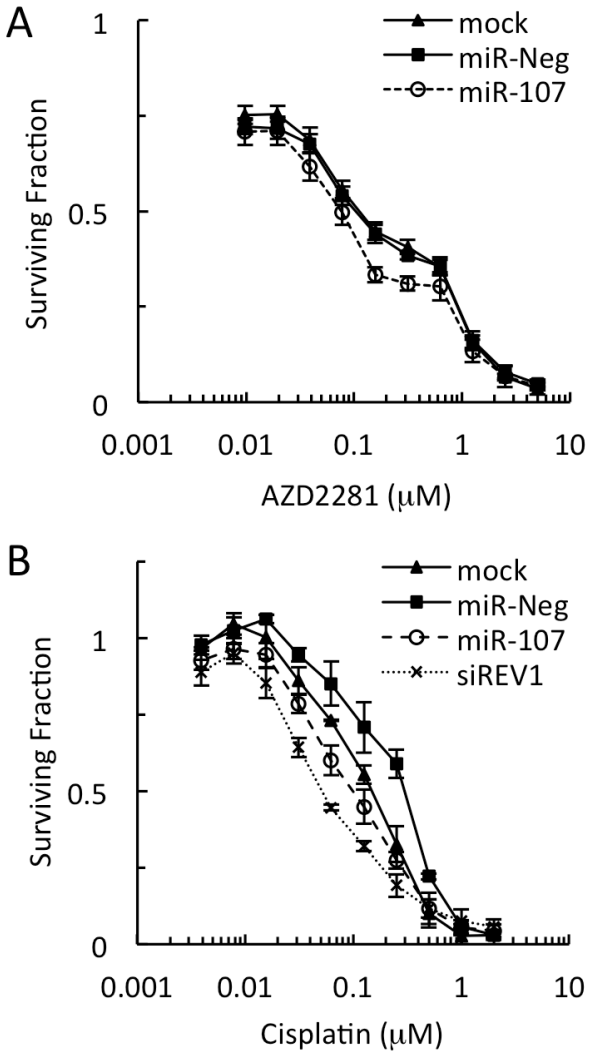

Figure 2.9. MiR-103/107 do not significantly chemosensitize BRCA2-deficient cells.
A-B. PEO1 cells transfected with indicated microRNAs or siRNAs (10 nM) were reseeded 48 hours later to assay for cell survival in response to AZD2281 (**A**) and cisplatin (**B**). Cell survival was assayed by crystal violet staining and expressed as a fraction of the untreated control (n=4, +/-SEM).

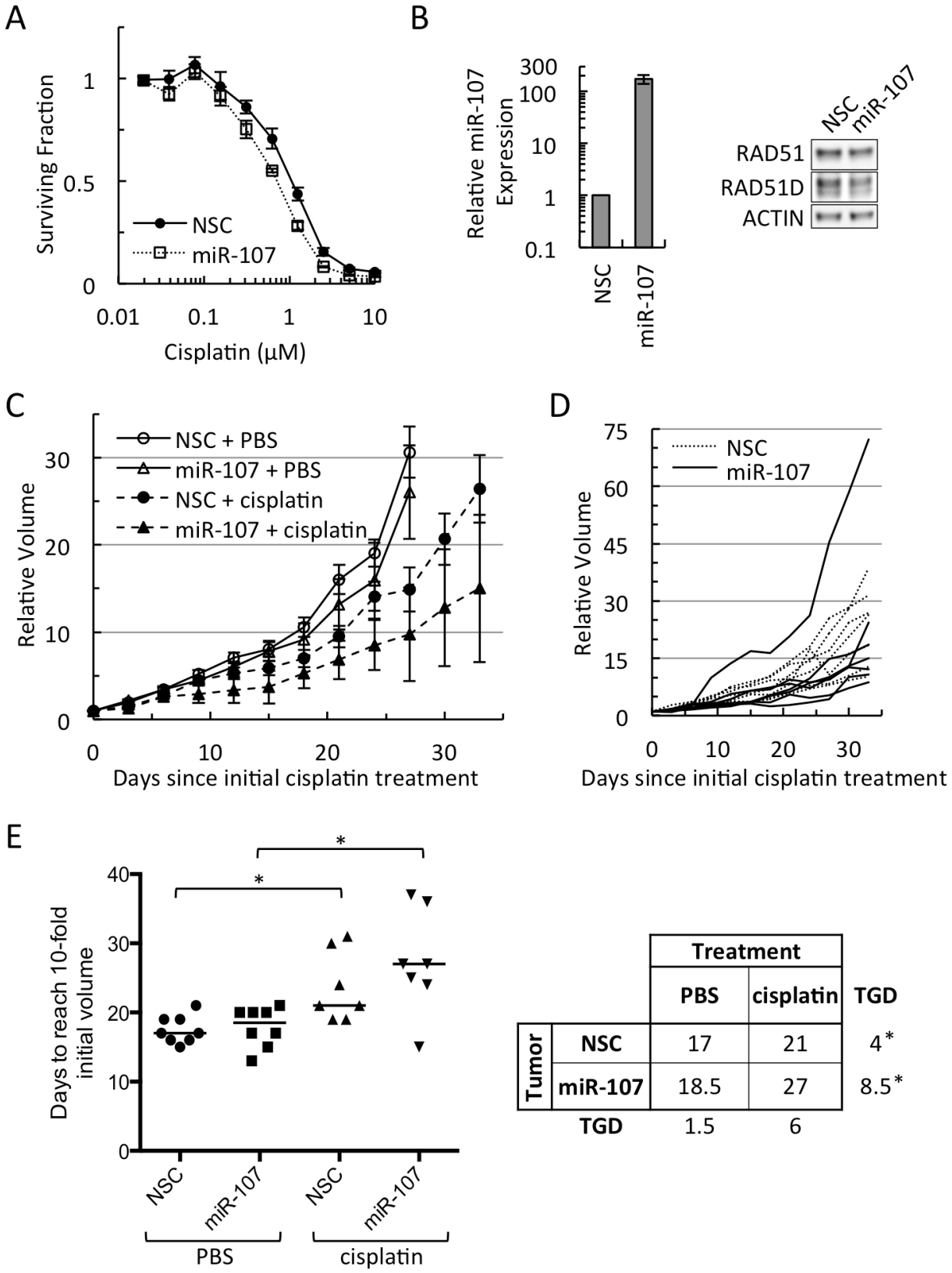

		Treatment		
		PBS	cisplatin	TGD
Tumor	NSC	17	21	4*
	miR-107	18.5	27	8.5*
	TGD	1.5	6	

Figure 2.10. MiR-107 enhances cisplatin sensitivity *in vivo*.
A-B. H1299 cells stably expressing NSC or miR-107 were (**A**) assessed for survival in response to cisplatin and (**B**) harvested for real-time PCR and Western blotting (n=3, +/-SEM). Cell survival is expressed as a fraction of the untreated control (n=3, +/-SEM). C. H1299 cells stably expressing NSC or miR-107 were subcutaneously injected into the flanks of NOD/SCID mice. Upon tumor formation, mice were treated weekly with cisplatin (5 mg/kg/week) or PBS by i.p. injection and tumor volumes determined every 3 days. The median tumor volume relative to the day PBS/cisplatin-treatment was initiated (day 0) for each group is plotted over time (n=7-8, +/-SEM). **D.** Relative tumor volumes of individual cisplatin-treated NSC and miR-107 tumors are plotted. Tumor volumes are normalized to the volume when cisplatin-treatment was initiated (day 0). **E.** The number of days for tumors to reach 10-fold their initial volume was determined. The median of each group is indicated by the horizontal line and is also presented in the table (TGD = tumor growth delay) (Student's t-test: $*P < 0.005$).

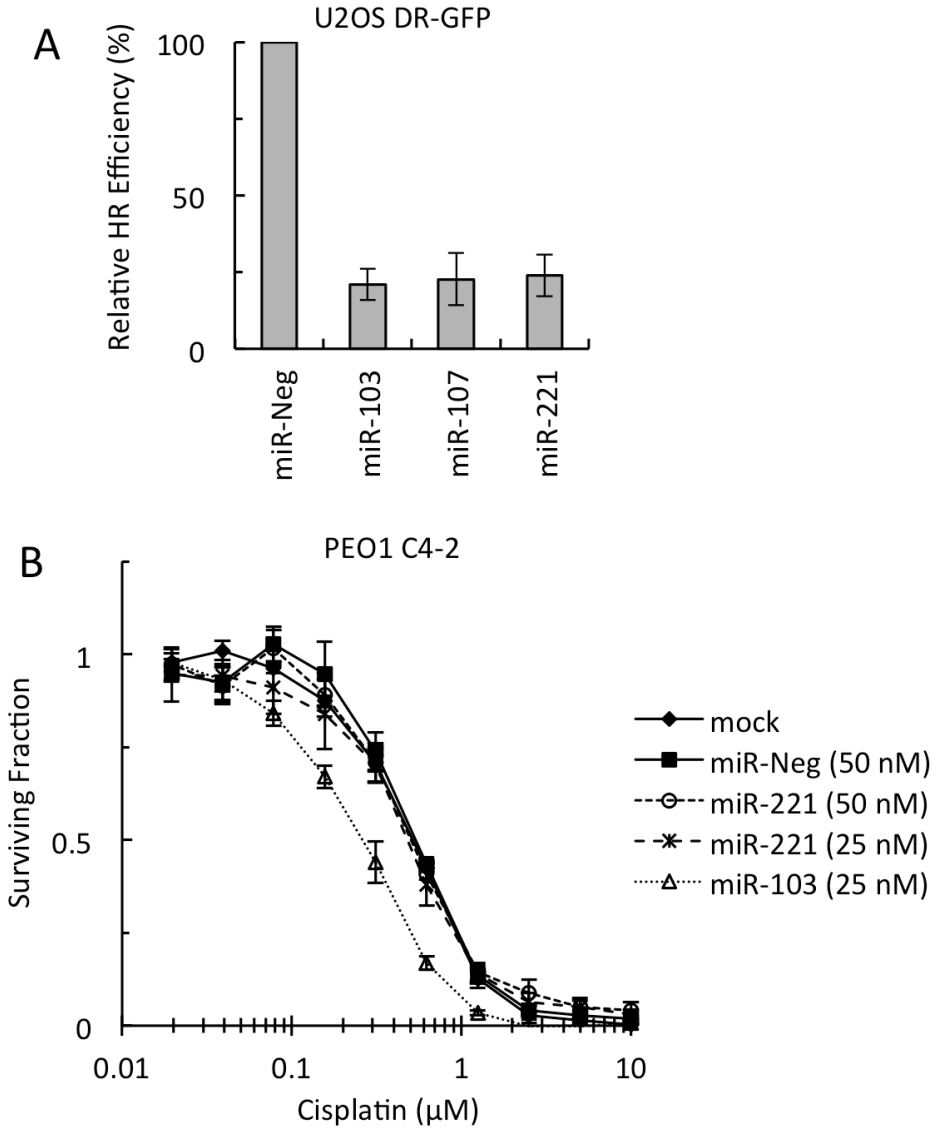

Figure 2.11. MiR-221 regulates HR but does not confer chemosensitivity to cisplatin.
A. U2OS DR-GFP cells initially transfected with indicated microRNAs (100 nM) were subsequently transfected with an I-SceI homing endonuclease-expression vector the next day and harvested 48 hours later for flow cytometry. HR repair efficiency is presented as a percentage of the miR-Neg transfected controls. **B.** PEO1 C4-2 cells transfected with microRNAs at indicated concentrations were reseeded 48 hours later to assay for cellular survival in response to cisplatin. Cell survival was assayed by crystal violet staining and expressed as a fraction of the untreated control (n=3, +/-SEM).

Discussion

In this study, we conducted unbiased screens of a human microRNA mimic library in two cell lines to systematically identify microRNAs that potentially regulate HR. We further characterized the three microRNAs (miR-103, miR-107 and miR-221) that were identified in both screens. We show that miR-103/107 overexpression can inhibit DNA damage-induced RAD51 foci formation, impair HR-mediated repair of DSBs, and confer radiosensitivity as well as chemosensitivity to DNA damaging agents *in vitro* and *in vivo*. A third microRNA, miR-221, was found to impair HR but did not impact chemosensitivity. To date, several microRNAs have been implicated in the regulation of factors that mediate repair of DNA DSBs [252, 253]. The identification of novel roles for miR-103, miR-107 and miR-221 in the regulation of HR raise the possibility that they contribute to genomic instability and chemosensitivity in the cancers in which their expression is deregulated [269-274, 284-286].

Interestingly, none of the microRNAs that have been reported to target HR factors were identified by our screens. For some of these microRNAs, this was not surprising. The targeting of RAD52 by miR-210 and miR-373 [258] is not expected to impact RAD51 foci formation as both HeLa and U2OS cells express wild-type BRCA2 [287]. Furthermore, miR-1245, which targets BRCA2 [257], was not present in either one of our microRNA mimic libraries. As for miR-24, miR-146a/5p and miR-182, it is unclear why their targeting of BRCA1 [249, 256, 260] did not reduce DNA damage induced-RAD51 foci formation in our screens. While RAD51 foci formation was not examined in their respective studies, the overexpression of both miR-145a/b-5p and miR-182 did reduce HR repair efficiency as assayed with the DR-GFP reporter [256, 260]. A possible explanation for the discrepancy in our studies is that the degree of BRCA1

depletion mediated by these microRNAs was not sufficient to impact RAD51 foci formation in our experimental system. This remains to be investigated.

The approach that we took to identify novel microRNA regulators of HR was limited by the coverage of our microRNA libraries. Currently, there are over 1500 microRNAs in the microRNA-ome [200] yet the largest library we screened contained 815 microRNAs. It is reasonable to predict that several microRNAs in the remaining half of the human microRNA-ome regulate HR, such as miR-1245 [257]. Further screening of these several hundred microRNAs may therefore yield more candidates and help provide a more complete picture of microRNA-mediated regulation of HR in human cells.

The physiological significance of microRNA-mediated regulation of DNA repair has remained elusive. One possibility that has been proposed is that these microRNAs suppress DNA repair in cellular states when DSB repair would be risky or not economical [255]. Consistent with this, both miR-24 and miR-182, which respectively repress H2AX and BRCA1 expression, are upregulated in differentiating leukemia cell lines [255, 260]. Intriguingly, miR-103 and miR-107 are upregulated during retinoic acid-induced differentiation of cultured neuroblastoma and leukemia cells, respectively [288, 289]. With additional targets in cell cycle regulation such as CDK6 [272, 278], cyclin E and CDK2 [290], miR-103/107 are well suited to couple the regulation of DNA repair and proliferation during cellular differentiation.

The dynamic expression of microRNAs in response to DNA damage may modulate cellular outcome through microRNA-mediated regulation of DNA repair [259]. Both miR-103 and miR-107 are upregulated in response to doxorubicin-induced cellular stress through p53-dependent transcriptional and post-transcriptional mechanisms [276-279]. Based on our results, this upregulation could potentially inhibit DNA repair and sensitize cells to DNA damage. While

it may be counterintuitive for a cell to suppress DNA repair in response to cellular stress, this suppression may serve to push a damaged cell towards apoptosis [255] or is a part of the apoptotic response [152]. Alternatively, restricting or limiting HR may prevent illegitimate recombination thereby promoting genomic stability and survival. Consistent with the suppression of DNA repair in response to DNA damage, the p53 tumor suppressor [291] transcriptionally represses RAD51 expression [150, 292] and potentially antagonizes RAD51, RPA and BRCA2 by physical interaction [293-295]. It is therefore an intriguing possibility that miR-103/107 are effectors of p53 signaling that act to post-transcriptionally regulate HR and ultimately play a role in determining cellular outcomes in response to genotoxic stress. This possibility is further explored in Chapter Four.

While miR-103/107 have not been reported to target any factors in the HR pathway (Table 1.1), some validated targets of miR-103/107 may play a role in chemosensitivity. MiR-103/107 have been reported to target Dicer and TARBP2, which are both components of the microRNA biogenesis pathway (Figures 1.2D) [275, 296]. More recently, both of these factors have been implicated in promoting chemoresistance to cisplatin, particularly when depleted in combination [297, 298]. Furthermore, Dicer has been implicated in both DNA damage response signaling [264] as well as HR [265] though the exact functional role in these pathways is unclear. Additionally, miR-103/107 have been reported to target the CLOCK transcription factor [299], which is a regulator of chemoresistance to cisplatin [300]. Therefore, the targeting of Dicer, TARBP2, CLOCK or other factors by miR-103/107 may play a role in miR-103/107-mediated regulation of HR and chemosensitivity.

The targeting of the HR pathway in tumors has garnered increasing interest because of the resultant hypersensitivity to agents that promote DNA double-strand break formation in S-

phase (e.g. cisplatin, olaparib/AZD2281) [283]. We examined the potential for miR-107-mediated chemosensitivity *in vivo* in a xenograft model of tumor formation and found a modest delay of tumor growth when miR-107 overexpression is combined with cisplatin treatment (Figure 2.10C and E). The overall effect did not appear to be striking in part because of the inclusion of the exceptionally faster-growing miR-107 tumor in our analysis (Figure 2.10A and C-E). Additionally, the *in vivo* sensitization may also reflect the mild cisplatin sensitivity seen *in vitro* with H1299 cells. The therapeutic utility of miR-103/107 in combination with cisplatin or other DNA damaging agents therefore remains unclear and requires further investigation. Interestingly, the use of miR-107 as a therapeutic agent in cancer treatment has already been proposed [301]. It is tempting to ask whether the combination of a DNA damaging agent with the nanoparticle delivery of miR-107 will chemosensitize tumors [301].

Our screen identified a novel role for miR-221 in the regulation HR. In the characterization of miR-221, we found that its overexpression inhibited IR-induced RAD51 foci formation and HR repair efficiency as expected. Surprisingly, this HR deficiency did not render cells sensitive to cisplatin. There may be several explanations for this. First, while we found that miR-221 inhibited IR-induced RAD51 foci formation in HeLa and U2OS cells, we did not determine whether this was also the case in PEO1 C4-2 cells. It is therefore possible that miR-221 does not regulate HR in PEO1 C4-2 cells as it does in the other two cell lines, potentially due to mutations at miR-221-binding sites of the HR-relevant targets. This will need to be further investigated. Another possibility is that in addition to targeting factor(s) that regulate HR, miR-221 may also target other factor(s) that suppress cellular sensitivity to DNA damaging agents caused by HR deficiency. Indeed, miR-221 has been reported to target the PTEN tumor suppressor [284], which promotes cell survival in response to both cisplatin [286] and radiation

[285]. This raises the possibility that the expected chemosensitivity of miR-221-overexpressing cells can be revealed by the ectopic expression of miR-221-resistant PTEN. This also needs to be further investigated.

MiR-221 upregulation in cancer is potentially an oncogenic event because of the targeting of p27 [302] and PTEN [284] tumor suppressors to promote proliferation and cell survival. Our study suggests another oncogenic role for miR-221 upregulation in the promotion of genomic instability. Possibly due to the simultaneous downregulation of HR and apoptosis, miR-221 overexpression did not render cells sensitive to DNA damaging agents and may therefore not be therapeutically useful as a chemosensitizing agent in combination therapy. The targeting of miR-221 itself in cancer however becomes more important in light of our findings.

In summary, we employed a high throughput screen to systematically identify microRNAs that regulate HR. From this screen, we identified the paralogous miR-103 and miR-107 and show that they are potent inhibitors of HR and chemoresistance to DNA damaging agents. These microRNAs as well as others from our screen add further complexity to the cellular regulation of DNA repair in eukaryotes. In Chapter Three, we elucidate the molecular mechanisms through which miR-103/107 regulate HR and cellular sensitivity to DNA damaging agents.

Materials & Methods

Cell lines

U2OS, HeLa, PEO1 and H1299 were purchased from the American Type Culture Collections. PEO1 C4-2 clones were described previously [280]. H1299 cells were cultured in RPMI-1640 supplemented with 10% FBS and 2 mM L-glutamine in a humidified 5% CO_2-

containing atmosphere at 37°C. All other cell lines were grown in DMEM with 10% FBS, 2 mM L-glutamine.

Plasmids, siRNAs, microRNA mimics and virus production

To obtain constructs expressing miR-103 and miR-107 precursors, miR-103-2 and miR-107 and their flanking sequences (150 bp on each end) were amplified by PCR and cloned between the XhoI and MluI sites of the pLemiR vector (Open Biosystems). Lentivirus was produced as previously described [268]. Transduced cells, except for U2OS, were selected in puromycin for 2-3 days (H1299: 5 μg/mL; PEO1 C4-2: 4 μg/mL; and HeLa: 2 μg/mL)

SiRNAs targeting BRCA2 [303], RAD51 (#1 target sequence: 5'-AACTAATCAGGTGGTAGCTCA-3'), RAD51D (target sequence: 5'-CTGGGTGGAAATAAGCTTATA-3') and REV1 (target sequence: 5'-ATCGGTGGAATCGGTTTGGAA -3') (Qiagen and Sigma) were transfected at 10nM using HiPerFect (Qiagen). Transfection of siRNAs or miRNA mimics (Dharmacon) was done at 10-100 nM using HiPerFect (Qiagen) or DharmaFECT 1 (Thermo Fisher). MiR-Neg2 mimic (Dharmacon) or a non-targeting siRNA [303] were used as negative controls.

Immunofluorescence microscopy

Transfected or transduced cells were grown on coverslips, irradiated with IR (10 Gy) using a JL Shepherd Mark I Cesium Irradiator (JL Shepherd & Associates), and then simultaneously fixed and permeabilized (2% paraformaldehyde and 0.5% Triton X-100 in PBS for 20-30 minutes) as described [268]. Cells were immunostained for RAD51 (Ab-1 (Calbiochem) or H-92 (Santa Cruz)). Images were acquired with a microscope (TE2000, Nikon) and analyzed using MetaVue (Universal Imaging) and ImageJ (National Institute of Health). At

least 100 cells per experimental point were scored for the presence of foci, and each experiment was repeated at least three times independently.

MicroRNA mimic library screening

HeLa cells were transfected (at 100 nM, DharmaFECT 1) with the Human miRIDIAN miRNA mimic library in 96-well cell culture plates. U2OS cells were transfected (at 20 nM, HiPerFect) with the Human miRIDIAN miRNA mimic library (v10.1) (Dharmacon) in glass-bottom 96-well plates (#655892, Greiner Bio-one). Two days post-transfection, cells were irradiated, simultaneously fixed and permeabilized, and immunostained for RAD51 as described above. Images were acquired with the Cellomics Arrayscan microscope (Thermo Scientific) and processed as described [268]. Using DAPI staining to define nuclei, the number of RAD51 foci-positive cells (at least 10 nuclear foci) was counted using the automated counter. The Z-score was calculated based on the formula $Z = (X-\mu nc)/\sigma$, where X was the individual sample score, μnc was the mean of negative controls in each plate and σ was the standard deviation of the whole population. Screening was independently replicated three times.

Real-time RT-PCR

Total RNA was extracted using Trizol (Life Technologies) and reverse-transcribed using the Taqman miRNA Reverse Transcription Kit (Life Technologies). The Taqman MiRNA Assay Kit (Life Technologies) was used for quantitative PCR. The comparative Ct value method was used for transcript quantification. MiR-103 and miR-107 expression was normalized to RNU24 or RNU44 snoRNA.

Homologous recombination assay

U2OS DR-GFP cells (gift from Drs. Maria Jasin, and Koji Nakanishi) [281] were transfected with siRNAs or miRNA mimics and then transfected 24 hours later with pCBASce

(I-SceI expression vector) or empty vector. Two days after plasmid transfection, cells were harvested and analyzed using a FACSCalibur Analyzer to determine the percentages of GFP-positive cells.

Cell cycle analysis

Cells were pulse-labeled with BrdU (30 μM, 15 minutes), fixed and then stained for DNA content and BrdU incorporation as previously described [259]. Flow cytometry was performed to determine the cell cycle phase distribution.

Survival assay

Transfected or transduced cells were seeded into 12-well plates at 5×10^3/well (H1299 and HeLa) or 6×10^3/well (U2OS and PEO1 C4-2) and treated with cisplatin, etoposide, camptothecin, paclitaxel (Sigma) or AZD2281 (Axon Medchem) at indicated concentrations. After incubation for 5-7 days, cell survival was assessed by crystal violet staining as described [268]. Clonogenic assays were performed as described [259]. Briefly, HeLa cells were reverse-transfected with miR-Neg or miR-107 at 10 nM. Forty-eight hours after transfection, cells were seeded in 6-well plates in technical duplicates, treated the next day with cisplatin or AZD2281 for 24 hours and then allowed to recover in complete growth media for 11 days. Cells were then fixed and stained with crystal violet as described. Colonies consisting of 50 cells or more were scored and colony-forming efficiencies were expressed as a percentage of the untreated control.

Xenograft mice study

H1299 cells stably infected with lentivirus carrying pLemiR-NSC or pLemiR-107 were injected subcutaneously (1×10^6 cells in 50 μL PBS) into the flanks of 5-8 week old female mice (NOD.Cg-Prkdc⁄(scid)il2rg⁄(tm1Wjl)/SzJ, FHCRC CCEMH). Once tumors were palpable (18 days after implantation of cells), mice were randomized into 2 groups (7-8 mice each) and

treated with cisplatin (5 mg/kg/week) or PBS by intraperitoneal injection. Tumor sizes were measured every 3 days with Traceable® digital calipers (Fisher Scientific) starting the day of initial treatment. Tumor volumes were calculated using the formula: Volume = length × width^2 × 0.52. The time for each tumor to reach 10-fold their initial volume was determined using the exponential trend-line fit function of Excel (Microsoft, Inc.). All animal work was approved by the FHCRC Institutional Animal Care and Use Committee.

Statistical analysis

A Student's *t*-test was used to evaluate significance of differences of *in vitro* and *in vivo* experiments (Excel, Microsoft, Inc.). All *in vitro* experiments were expressed as mean ± SEM. A P value < 0.05 was considered significant.

CHAPTER THREE

MiR-103 and miR-107 target RAD51 and RAD51D to regulate homologous recombination and enhance chemosensitivity to DNA damaging agents

Abstract

In a set of RAD51 foci-based screens, we identified miR-103/107 in the regulation of homologous recombination and chemosensitivity to DNA damaging agents. To elucidate the molecular mechanism by which miR-103/107 regulate homologous recombination, we employed a candidate approach and found that miR-103/107 downregulate RAD51 and RAD51D expression. Furthermore, we demonstrate that miR-103/107 directly target RAD51 and RAD51D through binding sites in their respective 3'UTRs. The ectopic expression of RAD51 and RAD51D in miR-103/107-overexpressing cells largely suppressed the inhibition of IR-induced RAD51 foci formation and cellular resistance to cisplatin and AZD2281, suggesting these are the critical targets by which miR-103/107 regulate HR. We also performed microarray analyses of U2OS cells overexpressing miR-107 and identified other potential targets that may contribute to the regulation of HR and chemoresistance to DNA interstrand crosslinking agents by miR-107. We go on to show that a hit from our microarray analysis, a member of the Fanconi anemia pathway, FANCE, is regulated by miR-107 through its coding region. Our findings provides a more complete picture by which miR-103/107 regulates DNA repair and chemosensitivity.

Introduction

The paralogous microRNAs, miR-103 and miR-107, which differ at a single nucleotide, were among the first human microRNAs to be cloned [205]. In the human genome, there is one copy of miR-107 and two copies of miR-103 (-1 and -2) that are located in the penultimate introns of the pantothenate kinase genes (PANK1, PANK3 and PANK2, respectively) [200, 304]. The expression of miR-103/107 is fairly ubiquitous across many tissue types with particular enrichment in brain tissue [304]. Furthermore, miR-103/107 are relatively abundant with miR-103 being the most abundant microRNA in HEK293 cells (7% of microRNA deep-sequencing reads) [248].

MiR-103/107 are cancer-associated microRNAs and are found to be both up- and downregulated in cancer relative to normal controls. Aberrant expression of miR-103 and miR-107 are found in cancers of the stomach [305-307], pancreas [273], bladder [308] and endometrium [269] as well as in lung [274] and pancreatic cancer cell lines [272]. Consistent with roles in cancer, validated targets of miR-103/107 implicate these microRNAs in the regulation of proliferation (TIMP3 [309], granulin [310], Notch2 [311], CDK6 [272, 278], CDK2 and cyclin E [290]), cell survival (PDCD10 [312]) and metastasis (DICER [275], CDK5R1 [313], DAPK and KLF4 [270]). While miR-103/107 has not been reported to target DNA repair factors, the validated targets of DICER, TRBP2 and CLOCK are required cellular resistance to cisplatin [298, 300].

We previously identified a novel role for miR-103/107 in the regulation of homologous recombination (HR) (Chapter Two). The overexpression of miR-103/107 inhibited DNA damage-induced RAD51 foci formation, impaired HR-mediated repair of DNA double-strand breaks (DSBs), and enhanced cellular sensitivity to DSB-inducing agents like ionizing radiation,

interstrand crosslinking agents (e.g. cisplatin) and poly(ADP-ribose) polymerase (PARP) inhibitors. In this study, we identify RAD51 and RAD51D as direct targets of miR-103/107 and demonstrate their relevance to miR-103/107-mediated regulation of HR and chemosensitivity.

Results

MiR-103 and miR-107 regulate RAD51 expression

In addition to decreased DNA damage-induced RAD51 foci formation, we observed a reduction in the overall intensity of RAD51 immunostaining upon miR-103/107 overexpression (Figure 2.2B). MiR-103/107 overexpression consistently reduced RAD51 protein and mRNA expression in several cell lines (Figures 3.1A and B, 3.6A and B, 3.8B, 3.10B and C). Using the TargetScan algorithm [236], we noted that human RAD51 is a predicted target of miR-103/107 and their putative binding site in the 3'UTR of RAD51 is conserved in rats but not mice (Figure 3.1C). Consistently, we found that miR-103/107 downregulated RAD51 protein expression in RAT-1 rat-derived fibroblasts but not in mouse embryonic fibroblasts (Figure 3.1D).

In order to determine whether RAD51 is a genuine target of miR-103/107, we generated a reporter construct containing the human RAD51 3'UTR downstream of a luciferase open reading frame. While the overexpression of miR-107 did not alter the luciferase activity of the control construct, miR-107 did significantly reduce the activity of the RAD51 3'UTR-containing construct relative to miR-Neg (Figure 3.1E). Importantly, this repression is a consequence of direct interaction because point mutations introduced in the putative miR-103/107 binding site of the reporter construct relieved this repression (Figure 3.1E). This demonstrates that RAD51 is directly targeted by miR-103/107 through a single site in its 3'UTR.

In order to determine whether downregulation of RAD51 is relevant to the miR-103/107-mediated regulation of HR, we attempted to complement the defects in RAD51 foci formation and cellular chemosensitivity by ectopically expressing RAD51. In order to avoid cytotoxicity associated with high overexpression of RAD51, we cloned the RAD51 promoter (-2931 to +5) to drive ectopic expression of FLAG-RAD51 from our construct. We generated stable cell lines that ectopically express either FLAG-RAD51 (lacking its 3'UTR) or luciferase as a control. No appreciable cytotoxicity was seen in stable cell lines and FLAG-RAD51 was found to be functional because it complemented IR-induced RAD51 foci formation and chemosensitivity to cisplatin and PARP inhibition in RAD51-depleted cells (Figure 3.2A and B and data not shown). In both PEO1 C4-2 and U2OS cells transfected with miR-103 or miR-107, stable expression of FLAG-RAD51 partially complemented IR-induced RAD51 foci formation (Figure 3.3A and B and Figure 3.4A and B). Furthermore, cellular resistance to cisplatin and AZD2281 was also partially complemented in miR-103/107-transfected PEO1 C4-2 and U2OS cells (Figure 3.3C and Figure 3.4C). Interestingly, FLAG-RAD51 did not complement the chemosensitivity of H1299 cells overexpressing miR-103 or miR-107 (Figure 3.5A and B). These results collectively demonstrate that RAD51 is a relevant target of miR-103/107 in the regulation of HR and that other relevant target(s) exist.

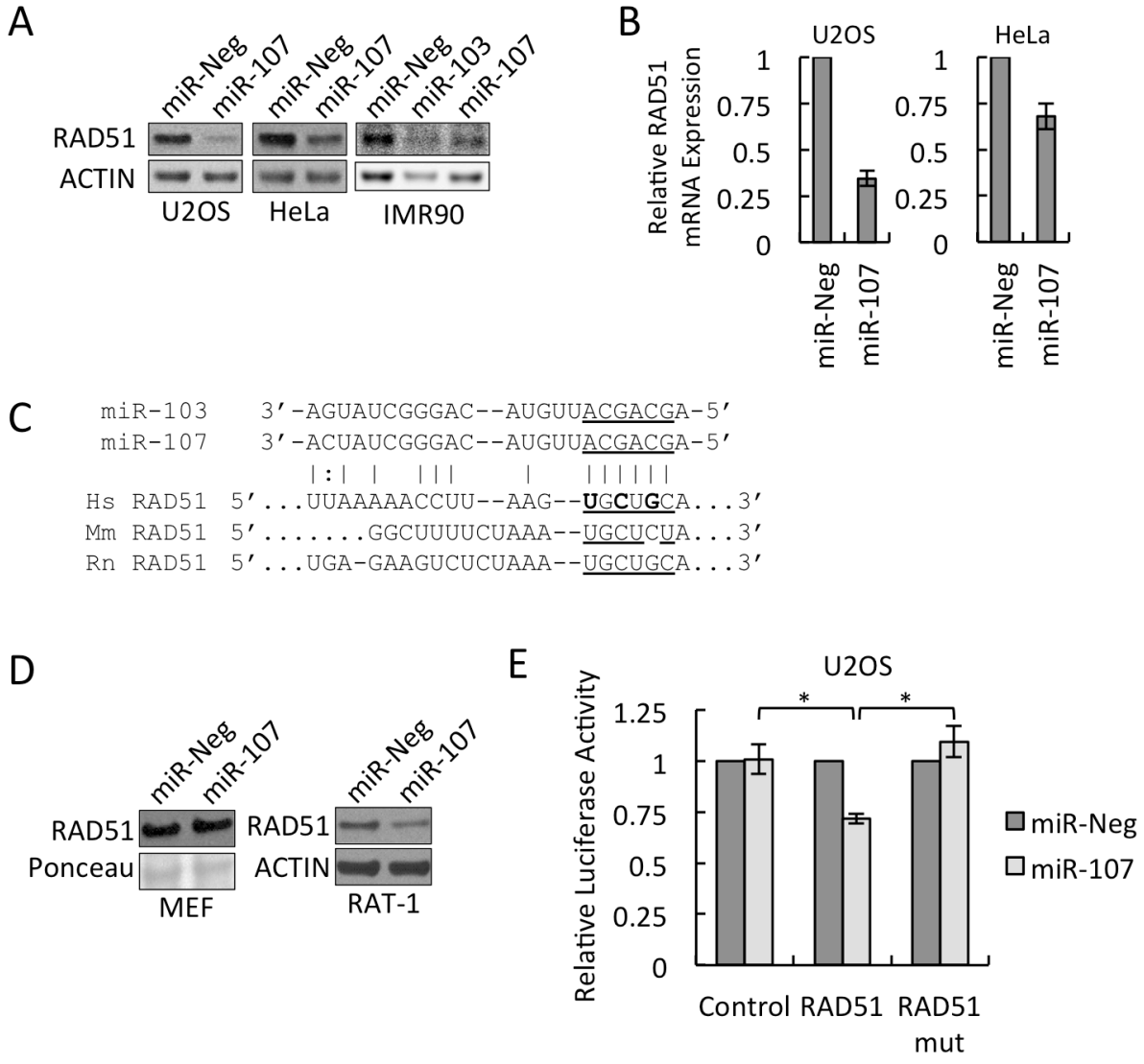

Figure 3.1. MiR-103/107 directly target RAD51.
A. HeLa, U2OS and normal lung fibroblasts (IMR90) transfected with indicated microRNAs (10 nM) were harvested 48 hours later for Western blotting. **B.** HeLa and U2OS cells transfected with indicated microRNAs (10 nM) were harvested 48 hours later for real-time PCR. **C.** Alignment of the putative miR-103/107 binding site in the 3'UTR of RAD51 from human (Hs), mouse (Mm) and rat (Rn). The seed sequences of miR-103 and miR-107 and their complementary sequences in the binding sites are underlined. **D.** Mouse embryonic fibroblasts and RAT-1 fibroblasts transfected with miR-Neg or miR-107 (25 nM) were harvested 48 hours later for Western blotting. Ponceau staining and actin immunoblotting are shown as loading controls. **E.** U2OS cells co-transfected with indicated microRNAs (0.5 nM) and luciferase constructs (*x*-axis) were assayed for luciferase activity 48 hours later (n=8, +/-SEM) (Student's t-test: **P* < 0.005). Positions of point mutations made to generate the RAD51 mutant construct are highlighted in bold in (**C**).

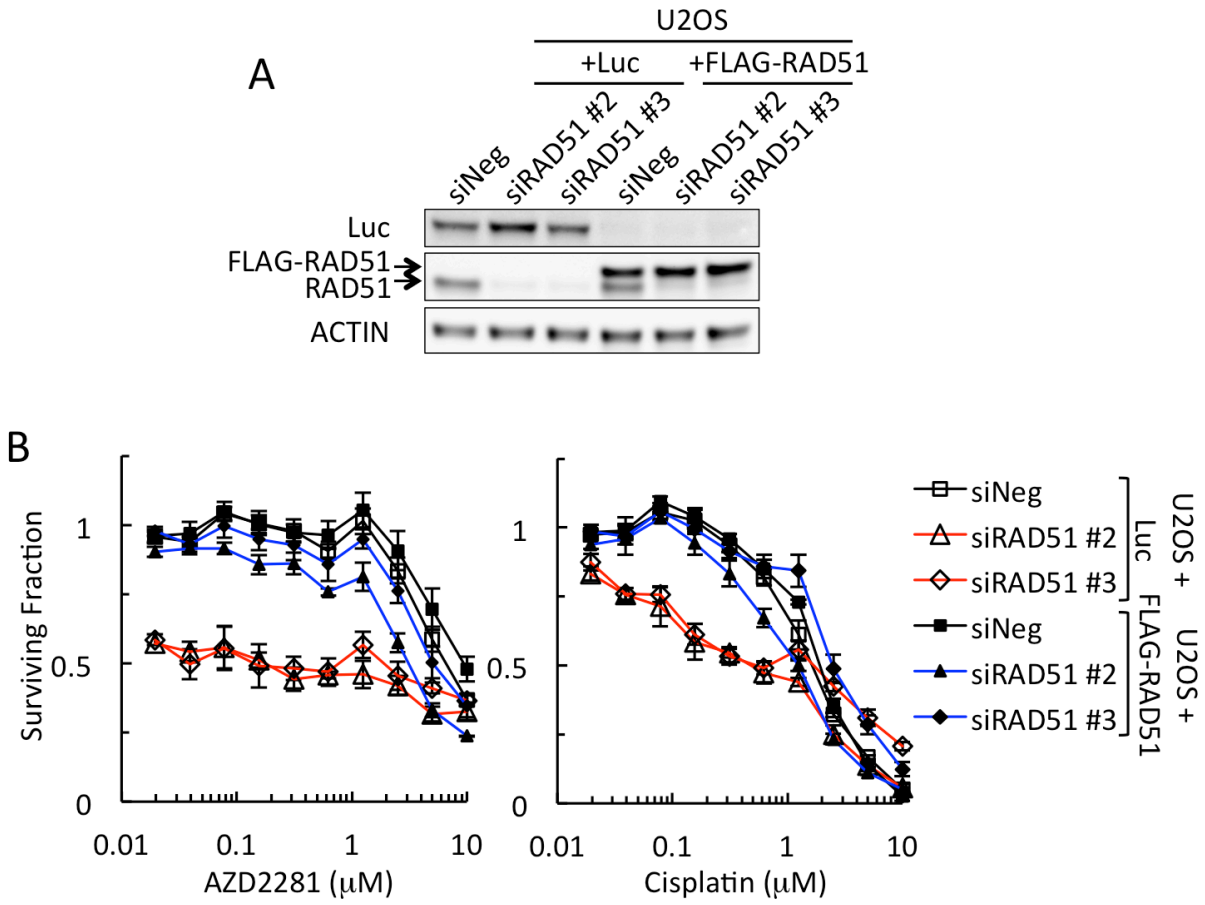

Figure 3.2. FLAG-RAD51 complements chemosensitivity of RAD51-depleted cells.
A. U2OS cells stably expressing FLAG-RAD51 or a luciferase (Luc) control were transfected with indicated siRNAs and harvested 48 hours later for Western blotting. **B.** U2OS cells stably expressing FLAG-RAD51 or Luc and transfected with indicated siRNAs were reseeded 48 hours after transfection to assay for survival in response to AZD2281 and cisplatin. Cell survival was assayed by crystal violet staining and expressed as a fraction of the untreated control (n=3, +/-SEM).

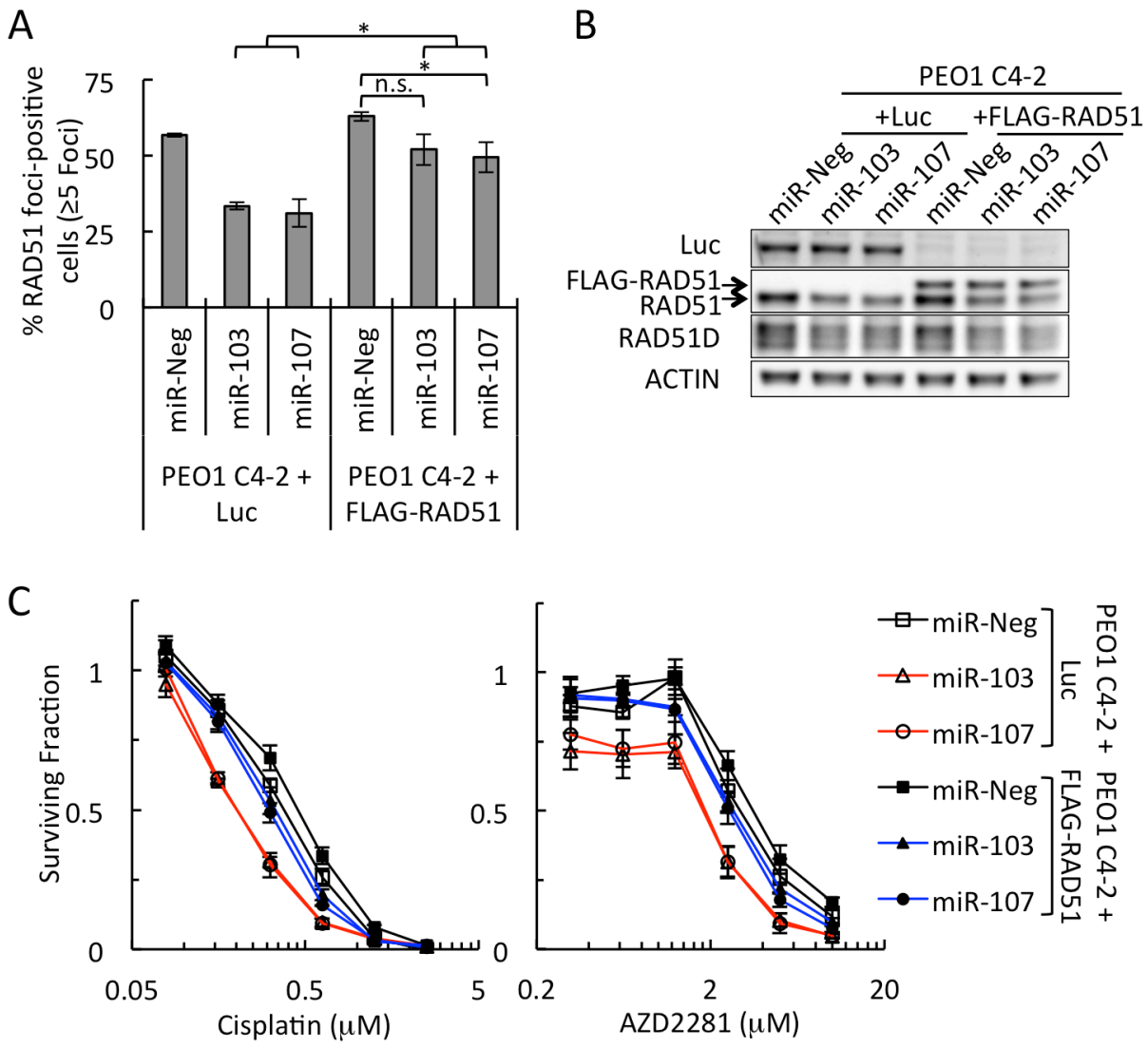

Figure 3.3. RAD51 is a critical target of miR-103/107-mediated chemosensitivity in PEO1 C4-2 cells.
A. PEO1 C4-2 cells stably expressing FLAG-RAD51 or luciferase (Luc) control were transfected with indicated microRNAs (10 nM), irradiated (10 Gy) 48 hours after transfection, fixed 6 hours after irradiation and immunostained for RAD51. RAD51 foci-positive cells are cells that contained at least 5 RAD51 nuclear foci (n=3, +/-SEM) (Student's t-test: *$P < 0.05$). **B.** Representative Western blotting of extracts from cells transfected as in (**A**). **C.** PEO1 C4-2 cells stably expressing FLAG-RAD51 or Luc were transfected with indicated microRNAs (10 nM) and reseeded 48 hours after transfection to assay for survival in response to cisplatin and AZD2281. Cell survival was assayed by crystal violet staining and expressed as a fraction of the untreated control (n=3, +/-SEM).

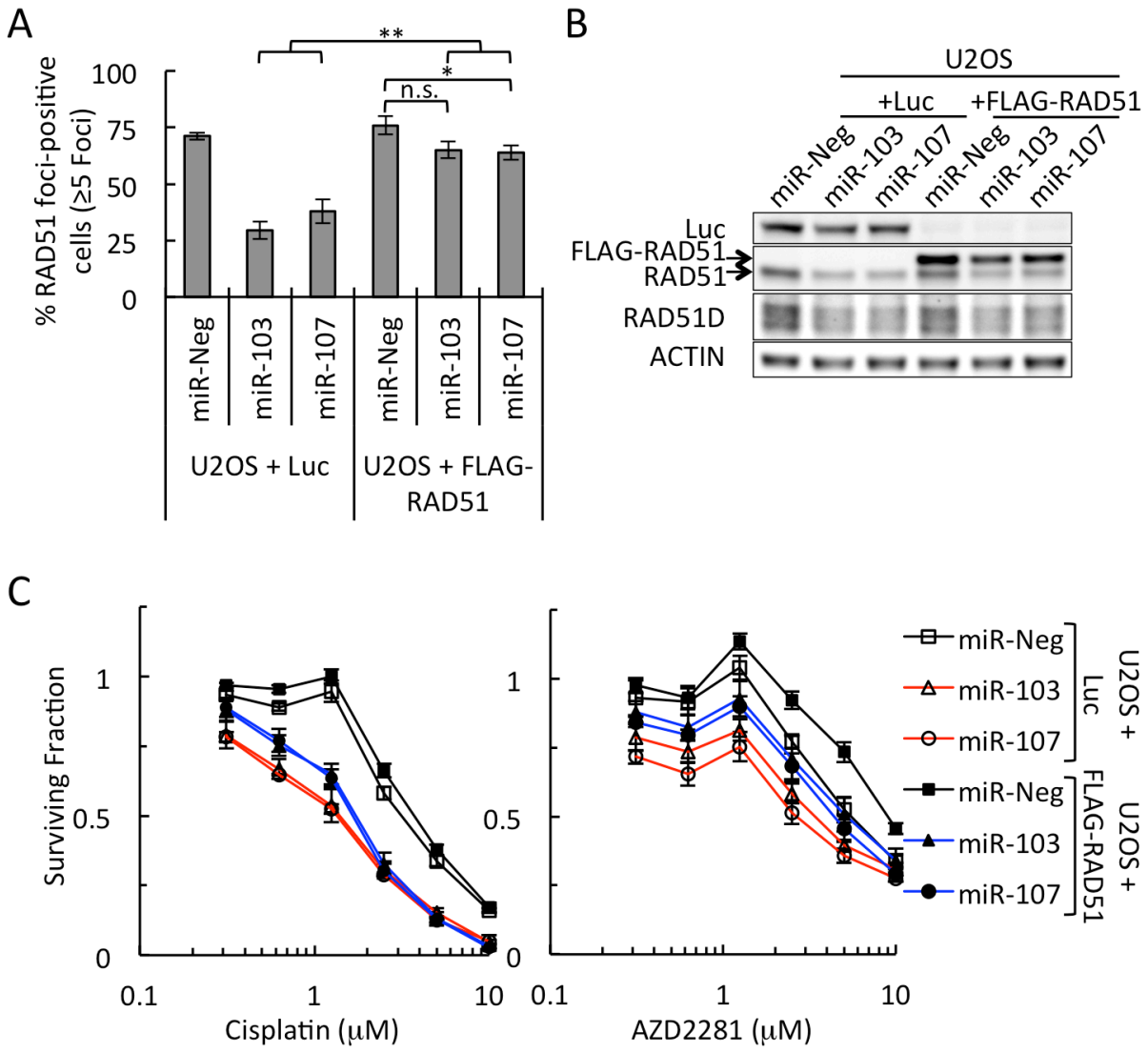

Figure 3.4. RAD51 is a relevant target of miR-103/107-mediated chemosensitivity in U2OS cells. **A.** U2OS cells stably expressing FLAG-RAD51 or luciferase (Luc) control were transfected with indicated microRNAs (10 nM), irradiated (10 Gy) 48 hours after transfection, fixed 6 hours after irradiation and immunostained for RAD51. RAD51 foci-positive cells are cells that contained at least 5 RAD51 nuclear foci (n=3, +/-SEM) (Student's t-test: **P* < 0.05, ***P* < 0.01). **B.** Representative Western blotting of extracts from cells transfected as in (**A**). **C.** U2OS cells stably expressing FLAG-RAD51 or Luc were transfected with indicated microRNAs (10 nM) and reseeded 48 hours after transfection to assay for survival in response to cisplatin and AZD2281. Cell survival was assayed by crystal violet staining and expressed as a fraction of the untreated control (n=4, +/-SEM).

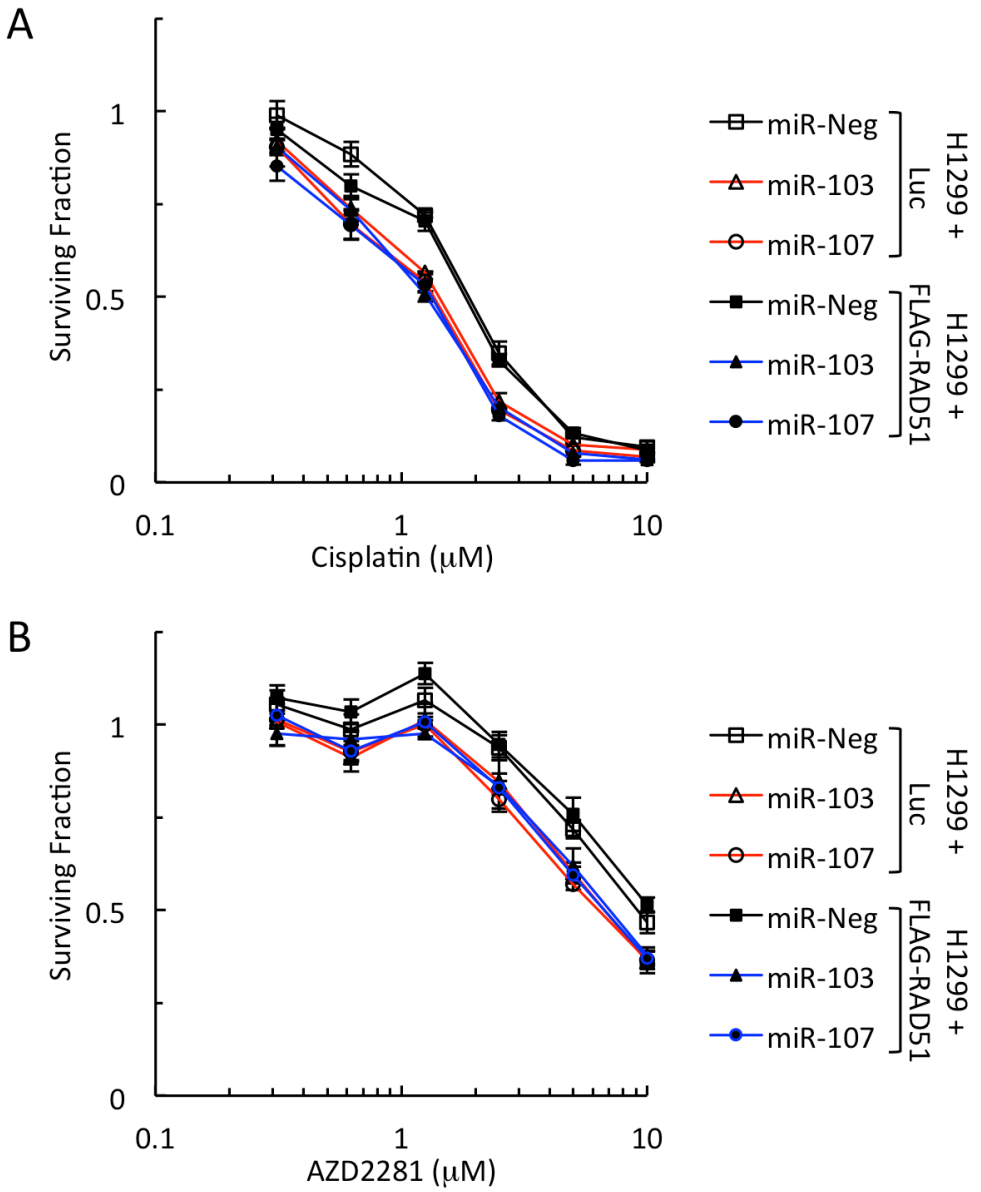

Figure 3.5. RAD51 is not a relevant target of miR-103/107-mediated chemosensitivity in H1299 cells.
A-B. H1299 cells stably expressing FLAG-RAD51 or Luc were transfected with indicated microRNAs (10 nM) and reseeded 48 hours after transfection to assay for survival in response to cisplatin (**A**) and AZD2281 (**B**). Cell survival was assayed by crystal violet staining and expressed as a fraction of the untreated control (n=3, +/-SEM).

MiR-103 and miR-107 regulate RAD51D expression

We analyzed the protein expression of several known factors that regulate RAD51 foci formation including ATR, CHK1, and BRCA1 and found no significant or consistent repression by miR-103/107 in several cell lines (Figure 3.6A). The downregulation of a known target, Dicer [275], was used to control for miR-103/107 transfection (Figure 3.6A). We also blotted for mediators of RAD51 loading such as BRCA2, PALB2 and the RAD51 paralogs (Figure 3.6A and B). We saw consistent downregulation of RAD51B, RAD51D, XRCC2 and XRCC3 when miR-103 or miR-107 are overexpressed (Figure 3.6B). We noted that RAD51D is a predicted target of miR-103/107 by TargetScan [236] with a single site in its 3'UTR (Figure 3.6C). Consistent with this, miR-103/107 overexpression also significantly downregulates RAD51D mRNA levels in several cell lines (Figure 3.6D and Figure 3.10B and C). Using luciferase reporter constructs containing the RAD51D wildtype or mutant 3'UTR, we determined that miR-103/107 directly interacts with the 3'UTR of RAD51D (Figure 3.6E). The mechanisms by which RAD51B, XRCC2 and XRCC3 are downregulated by miR-103/107 overexpression are unclear (see Discussion).

We then investigated whether RAD51D is relevant to miR-103/107-mediated regulation of HR. The stable overexpression of ectopic RAD51D partially rescued IR-induced RAD51 foci formation in miR-107 transfected PEO1 C4-2 cells, though to a lesser extent than ectopic RAD51 expression (Figure 3.7A and B). Chemoresistance to cisplatin and AZD2281 were also partially complemented (Figure 3.7C). Interestingly, the co-expression of ectopic RAD51 and RAD51D largely reversed miR-107-mediated inhibition of RAD51 foci formation and chemoresistance to cisplatin and AZD2281 (Figure 3.7D). Our results indicate that RAD51 and

RAD51D are the major targets through which miR-103/107 regulate RAD51 foci formation and chemoresistance.

Next, we inhibited endogenous miR-103/107 in two cells lines that abundantly express these microRNAs, H1299 (a non-small cell lung carcinoma cell line) and MDA-MB-231 (a breast cancer cell line) cells [275, 314, 315], and examined RAD51 and RAD51D expression. We confirmed that our antisense oligonucleotides (PI-103 and PI-107) effectively inhibit miR-103/107 (Figure 3.8A and B). Upon inhibition of miR-103/107, we observed a modest upregulation of RAD51D protein or mRNA expression in these cell lines but no appreciable upregulation of RAD51 expression (Figure 3.8B-D). This suggests that endogenous miR-103/107 have some role in regulating RAD51D expression in these cell lines, but no major role in regulating RAD51 expression.

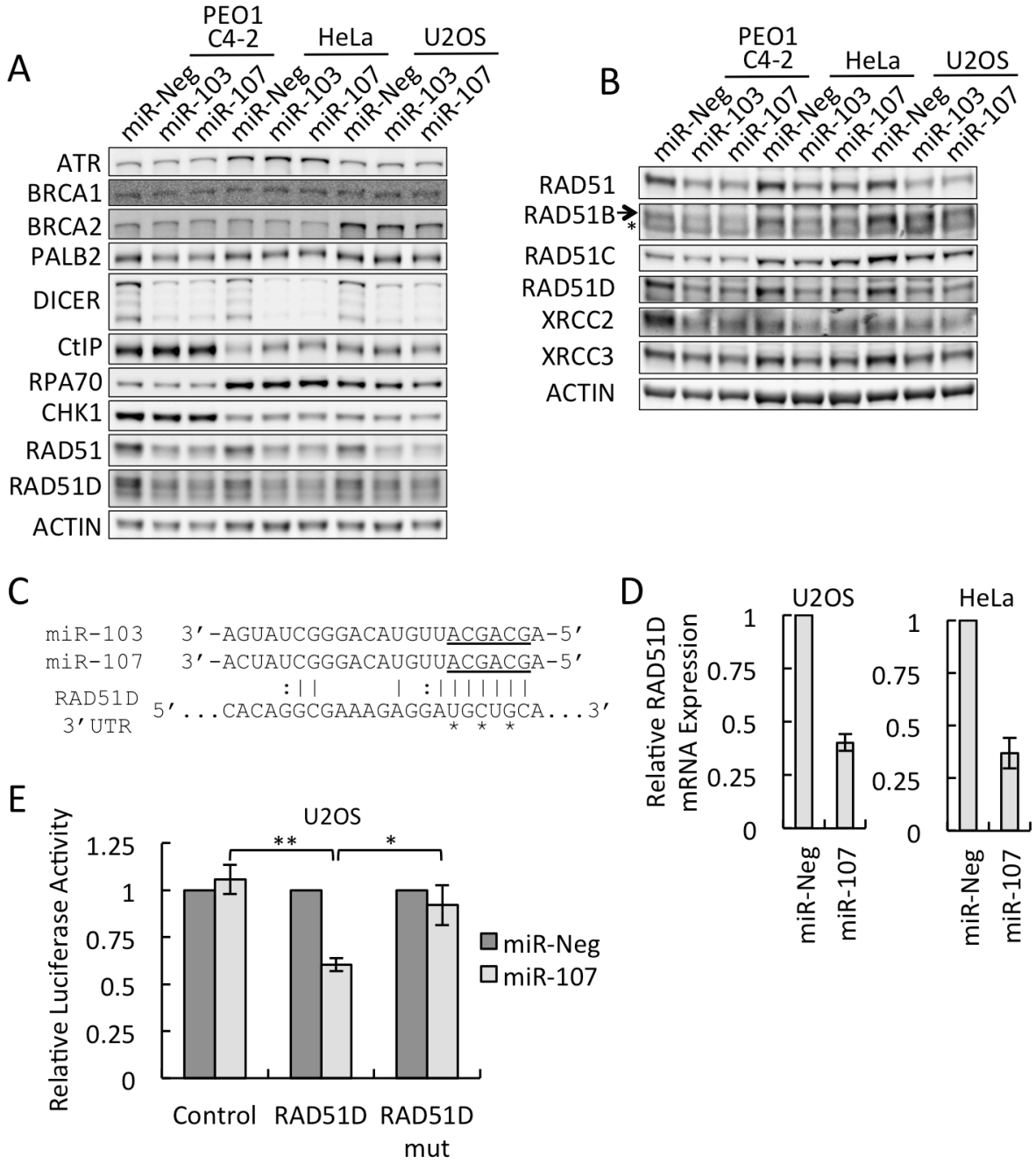

Figure 3.6. MiR-103/107 directly target RAD51D.
A-B. HeLa, U2OS and PEO1 C4-2 cells transfected with indicated microRNAs (10 nM) were harvested 48 hours later for Western blotting. Arrow indicates RAD51B and (*) indicates a non-specific band. **C.** Putative miR-103/107 binding site in the 3'UTR of RAD51D. Asterisks denote positions of substitutions made to generate mutant 3'UTR constructs in (**E**). The seed sequences of miR-103/107 are underlined. **D.** HeLa and U2OS cells transfected with indicated microRNAs (10 nM) were harvested 48 hours later for real-time PCR (n=3, +/-SEM). **E.** U2OS cells co-transfected with indicated microRNAs (0.5 nM) and luciferase constructs (*x*-axis) were assayed for luciferase activity 48 hours later (n=9, +/-SEM) (Student's t-test: **P* < 0.05, ***P* < 0.005).

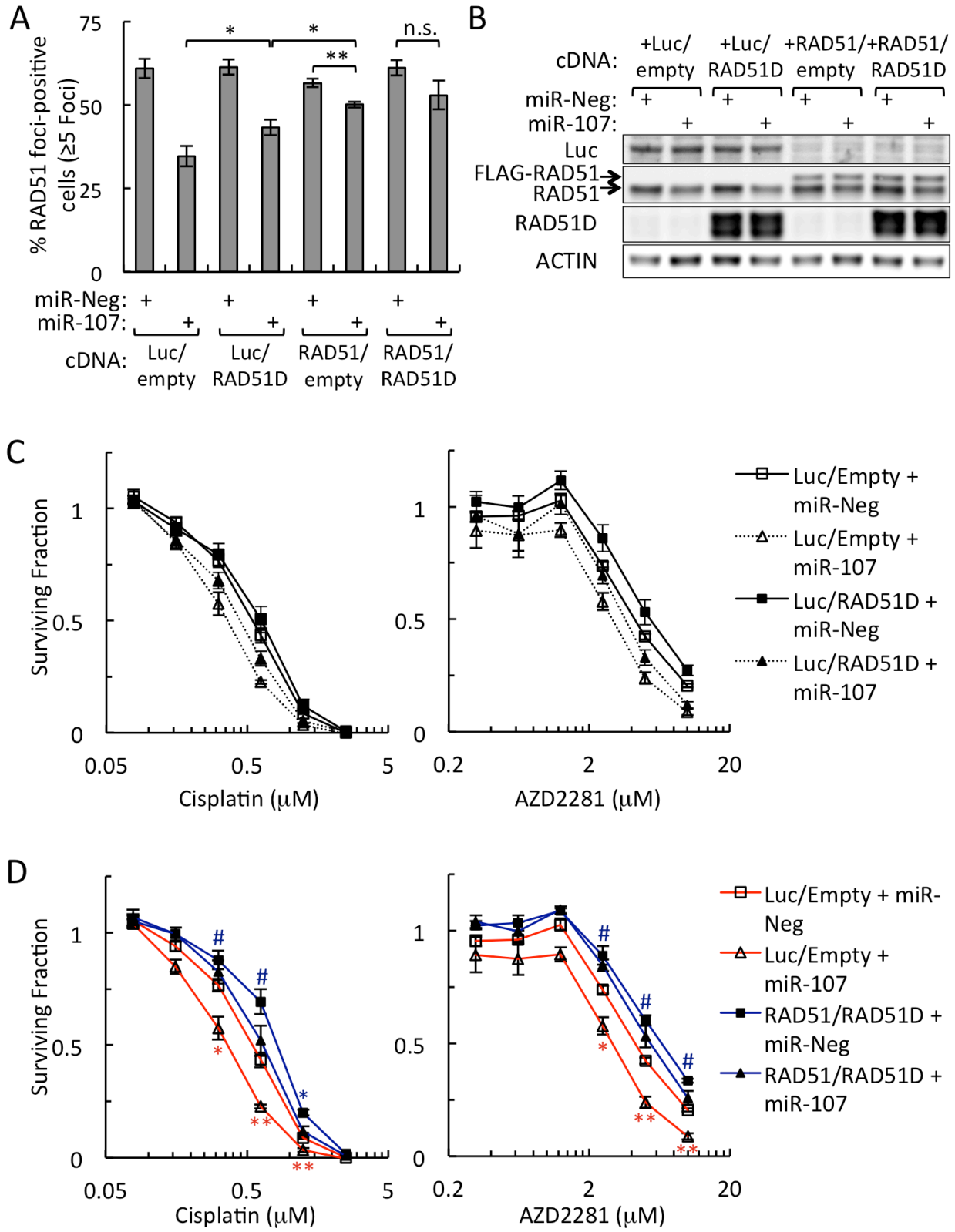
A
% RAD51 foci-positive cells (≥5 Foci)
75
50
25
0
*
*
**
n.s.
miR-Neg:
miR-107:
cDNA:
Luc/ empty
Luc/ RAD51D
RAD51/ empty
RAD51/ RAD51D
B
cDNA:
+Luc/ empty
+Luc/ RAD51D
+RAD51/ empty
+RAD51/ RAD51D
miR-Neg:
miR-107:
Luc
FLAG-RAD51
RAD51
RAD51D
ACTIN
C
Surviving Fraction
1
0.5
0
0.05
0.5
5
Cisplatin (μM)
0.2
2
20
AZD2281 (μM)
Luc/Empty + miR-Neg
Luc/Empty + miR-107
Luc/RAD51D + miR-Neg
Luc/RAD51D + miR-107
D
Surviving Fraction
Cisplatin (μM)
AZD2281 (μM)
Luc/Empty + miR-Neg
Luc/Empty + miR-107
RAD51/RAD51D + miR-Neg
RAD51/RAD51D + miR-107

Figure 3.7. RAD51 and RAD51D are both relevant targets of miR-103/107-mediated regulation of chemosensitivity.
A. PEO1 C4-2 cells stably expressing the indicated cDNAs were transfected with miR-Neg or miR-107 (10 nM), irradiated (10 Gy) 48 hours later, fixed 6 hours post-IR, and immunostained with anti-RAD51. Nuclei were counterstained with DAPI. RAD51 foci-positive cells contain at least 5 nuclear foci (n=3-4, +/- SEM) (Student's t-test: **P* < 0.05, ***P* < 0.01). **B-D.** Indicated PEO1 C4-2 stable cell lines transfected with miR-Neg or miR-107 (10 nM) were (**B**) harvested 48 hours later for Western blotting and (**C-D**) reseeded 48 hours later to assess survival in response to cisplatin and AZD2281. Cell survival is expressed as a fraction of the untreated control (n=3-4, +/-SEM) (Student's t-test: **P* < 0.05, ***P* < 0.005, #not significant).

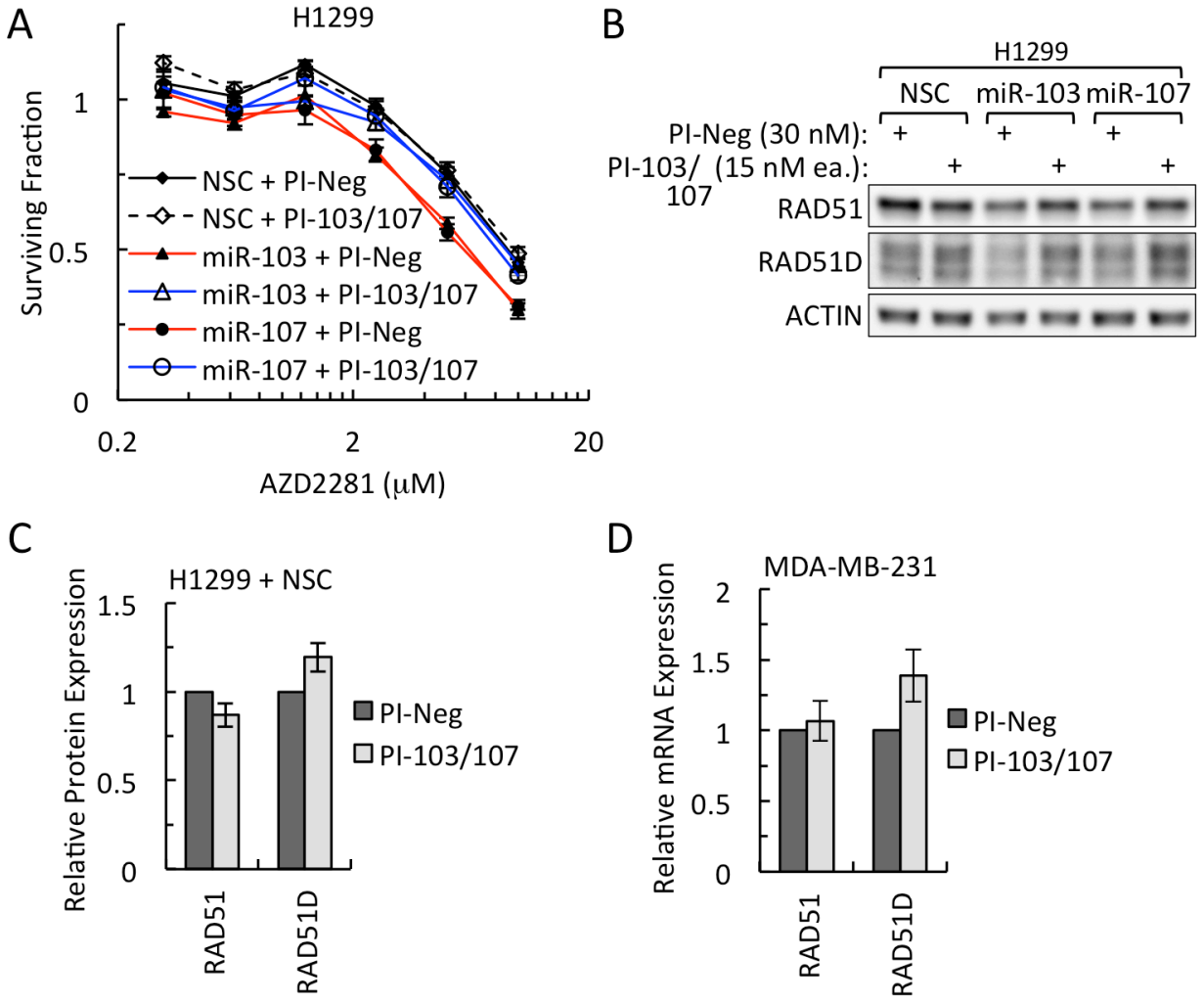

Figure 3.8. Endogenous miR-103/107 regulate RAD51D expression.
A-B. H1299 cells stably expressing NSC, miR-103 or miR-107 were transfected with microRNA inhibitors (PI-Neg at 30 nM or a combination of PI-103 and PI-107 at 15 nM each) and reseeded to assay for survival in response to AZD2281 (**A**) or harvested for Western blotting (**B**) 48 hour later. Cell survival was assayed by crystal violet staining and expressed as a fraction of the untreated control (n=3-4, +/-SEM). **C.** Quantitation of target expression in H1299 cells stably expressing NSC and transfected with indicated microRNA inhibitors, as in (**B**). RAD51 and RAD51D protein levels were normalized to actin and then expressed relative to PI-Neg-transfected cells (n=3, +/-SD). **D.** MDA-MB-231 cells transfected with microRNA inhibitors (PI-Neg at 50 nM or a combination of PI-103 and PI-107 at 25 nM each) were harvested 48 hours later for real-time PCR (n=3, +/-SEM).

MiR-103 and miR-107 regulate several factors involved in HR and chemosensitivity

In order to identify other targets of miR-103/107 that are relevant to HR and cisplatin chemosensitivity, we performed cDNA microarray analysis on U2OS cells transfected with miR-107 mimic or the negative control. We used $P < 0.01$ as the cutoff for differentially expressed transcripts. Using this cutoff for significance, we identified 1993 transcripts that were significantly regulated by miR-107 overexpression. All hits had a $|\log_2 \text{fold-change}| > 0.4$, with 962 and 1031 transcripts that were up- or down-regulated, respectively.

The array identified 14 of 31 validated targets of miR-103 and miR-107, including Dicer [275], TARBP2 [296], RAD51 and RAD51D (Table 3.1). Additionally, several putative, non-validated miR-107 targets identified by microarray analyses of Ago-immunoprecipitated RNA [316, 317] were also found to be significantly downregulated by miR-107 (Table 3.1). Of the 1031 downregulated transcripts identified in the microarray, 299 are putative 103/107 targets as predicted by TargetScan [236]. Interestingly, 97 of the significantly upregulated hits are also predicted miR-103/107 targets, including CDK6 (Table 3.1).

Using our list of HR factors required for RAD51 foci formation (Table 1.1) and HR-annotated genes (AmiGO [318]), we identified several factors that were downregulated by miR-107 overexpression in U2OS cells (Table 3.2). Some of these are predicted by TargetScan [236] to be targets of miR-103/107 (sites in the 3'UTR), while the majority had putative miR-103/107 binding sites in their coding regions. Both CtIP and FANCG did not contain putative binding sites anywhere in their respective mRNA sequences suggesting their regulation by miR-107 is indirect.

Table 3.1. MiR-107 downregulates several validated and non-validated miR-103/107 targets in U2OS (cDNA microarray).
Summary of validated and non-validated targets of miR-103/107 that were significantly downregulated by miR-107 relative to miR-Neg-transfected in U2OS cells. The log_2 fold-change ("F-C") presented is the mean of three independent experiments. Validated targets of miR-103/107 that were not significantly downregulated are also listed.

Validated Targets	F-C (Log_2)	Ref.	Non-validated Targets	F-C (Log_2)	Ref.	Validated Targets (Not Significant in Array)	Ref.
RAD51	-0.445		C22ORF13	-1.344	[316]	CREB1	[290]
RAD51D	-0.516		BOLA3	-0.832	[316]	ID2	[288]
CDK2	-0.630	[290]	NINJ1	-1.323	[316]	PRKCE (PKCε)	[319]
DICER1	-0.975	[275]	RPLP0	-0.456	[316]	NFI-A	[289]
TARBP2	-0.981	[296]	LDOC1	-0.428	[316]	CLOCK	[299]
EIF2C1	-0.858	[320]	INSIG1	-0.509	[317]	BACE1	[321]
CDK5R1	-0.765	[313]				ARNT	[279]
CCNE1	-1.497	[290]				CAV1	[322]
AIP	-1.101	[323]				NOTCH2	[311]
GRN	-1.043	[310]				NF1	[324]
CFL1	-0.523	[325]				TIMP3	[309]
FOXJ2	-0.908	[326]				CYP2C8	[327]
PDCD10	-0.696	[312]				DAPK1	[270]
CDK6	0.421	[278]				KLF4	[270]
						CACNA1C	[328]
						ADAM10	[329]

Table 3.2. MiR-107 downregulates several HR factors in U2OS (cDNA microarray).
Summary of genes that regulate HR that were significantly downregulated by miR-107 relative to miR-Neg-transfected in U2OS cells. The log_2-fold change presented is the mean of three independent experiments. The number of symbols (•) indicate the number of putative miR-103/107 binding sites as determined by the presence of a miR-103/107 seed-region complementary sequence ("UGCUGC").

Gene Name	Fold-Change (Log_2)	Predicted by TargetScan?	Putative Sites in CDS?	Putative Sites in 3'UTR?
RAD54L	-0.428		••	
RAD51	-0.445	••		
RAD51C	-0.474		•	
RAD51D	-0.516	•		
PLK1	-0.610		••••	
RBBP8 (CtIP)	-0.439			
LMNA (LAMIN A/C)	-0.405		•	•
RPA1 (RPA70)	-0.499	•		
MCM8	-0.466		••	
LIG1	-0.447		•••••	
PSMD3	-0.846	•		
FANCA	-0.408		•••••••	
FANCG	-0.414			
FANCE	-0.902		••••	
CDK2	-0.630			•
DICER1	-0.975	••••••		
TARBP2 (TRBP)	-0.981	•		

We confirmed that RPA70 and RAD51C protein expression were mildly downregulated in U2OS cells (Figure 3.6A and B), consistent with the results of the microarray. However, their downregulation was not consistently seen in other cell lines suggesting their regulation by mIR-107 is indirect and cell type-specific (Figure 3.6A and B). We did not observe any significant decrease in CtIP protein levels in any of our cell lines when miR-103/107 were overexpressed (Figure 3.6A).

Proteasome function is required for RAD51 foci formation [87]. The expression of a component of the 19S proteasome, PSMD3, was downregulated by miR-107 (Table 3.2). While we did not directly analyze PSMD3 protein or mRNA expression, we assayed for proteasome dysfunction using 293 GFPu-1 cells [330]. This 293-derived cell line stably expresses GFP fused to the CL1 degron, which results in constitutive turnover by the proteasomal degradation pathway [330]. While treatment with a proteasome inhibitor (MG132) or a siRNA targeting PSMD4 (another 19S component) stabilized GFPu expression as determined by increased fluorescence, miR-103 or miR-107 mimic transfection did not modulate the fluorescence of 293 GFPu-1 cells (Figure 3.9A-D). This indicates that the miR-103/107 does not significantly downregulate proteasome function.

The expression of several Fanconi anemia genes was downregulated by miR-103/107 in U2OS cells (Table 3.2). Among these, we found FANCE to also be significantly downregulated by microarray analysis in miR-107-overexpressing HeLa cells (data not shown). We confirmed that miR-103/107 can downregulate FANCE protein in HeLa cells (Figure 3.10A) and FANCE mRNA in several cell lines (Figure 3.10B and C). According to Targetscan, FANCE is not a predicted target of miR-103/107. Consistently, miR-107 did not significantly repress luciferase activity of a construct carrying the wildtype 3'UTR of FANCE (Figure 3.10D). We then

searched the rest of the FANCE mRNA and found four putative sites of FANCE in its coding region (Table 3.2). To test whether miR-103/107 target FANCE through its coding region, we generated a luciferase construct carrying the FANCE coding region. Surprisingly, we found that miR-107 can repress the activity of this construct (Figure 3.10D).

Lastly, we data-mined several published siRNA or shRNA-based screens that identified putative regulators of cisplatin resistance (knockdown enhanced sensitivity to cisplatin) [331-336]. From these other studies, we found that miR-107 regulates several of the hits from those screens (Table 3.3). Among those, CDK5R1 is a validated target of miR-103/107 [313] while the rest are predicted targets of miR-103/107 or have putative binding sites outside of the 3'UTR.

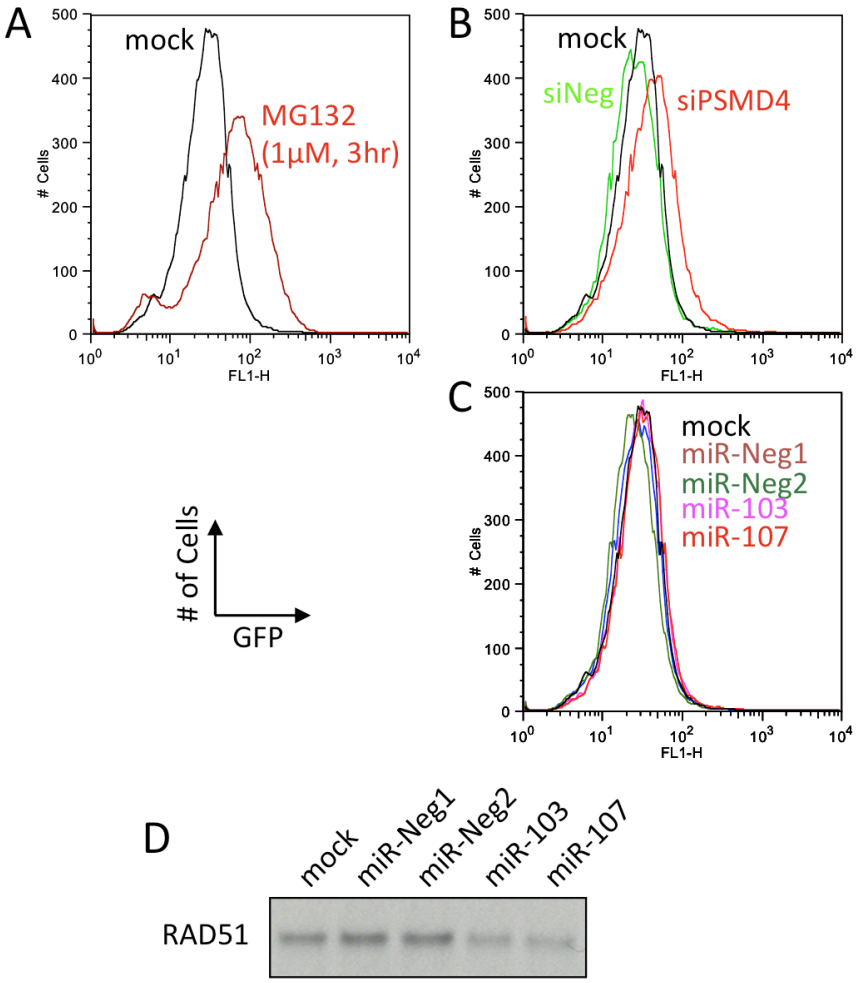

Figure 3.9. MiR-103/107 do not regulate proteasome function.
A. 293 GFPu-1 cells treated with MG132 (1 μM) for 3 hours were harvested for flow cytometry. **B-D.** 293 GFPu-1 transfected with indicated siRNAs (**B**) or microRNA mimics (**C**) were harvested 48 hours later for flow cytometry or Western blotting (**D**).

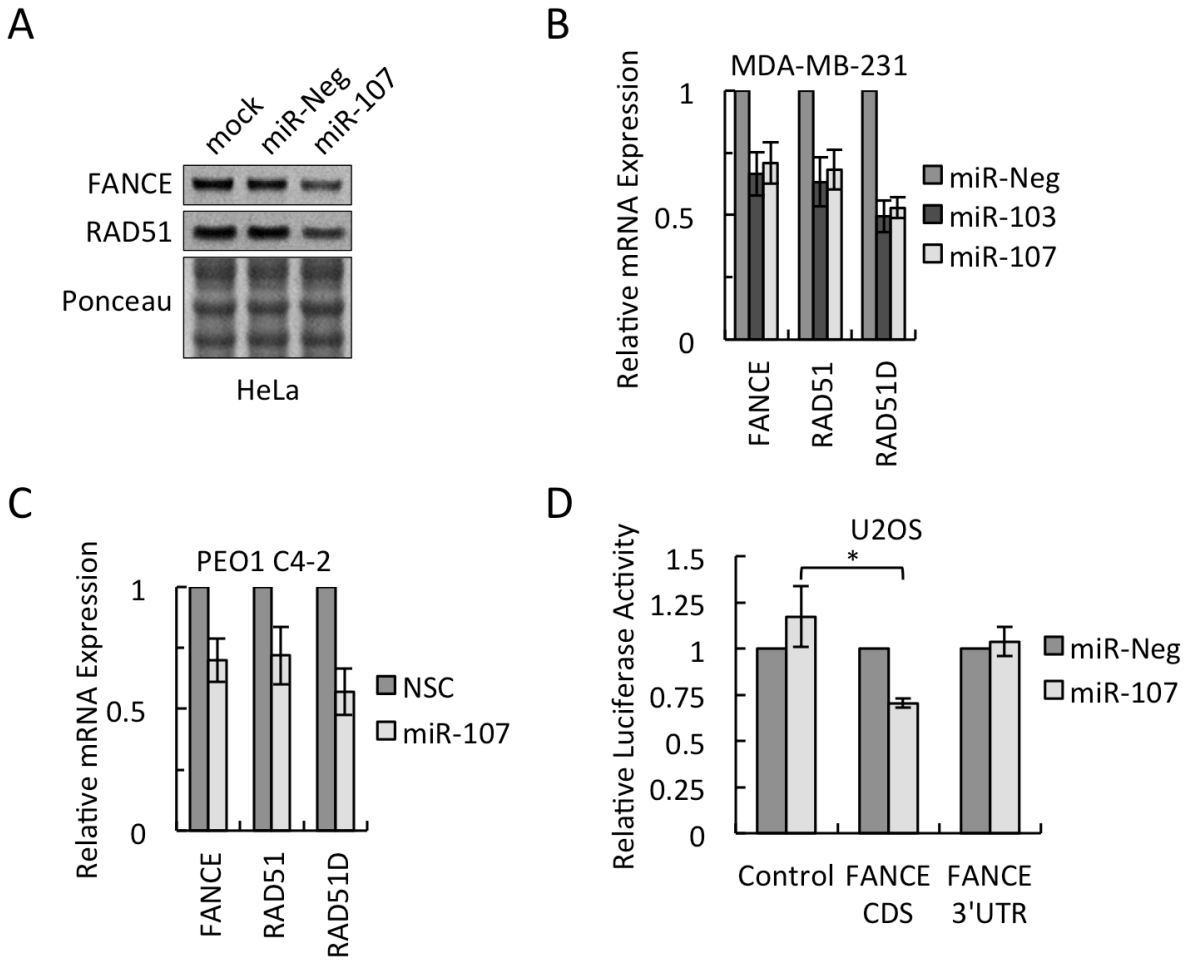

Figure 3.10. MiR-103/107 regulate FANCE expression.
A. HeLa cells mock-transfected or transfected with miR-Neg or miR-107 (10 nM) were harvested 48 hours later for Western blotting. **B.** MDA-MB-231 cells transfected with indicated miRNAs (10 nM) were harvested 48 hours after transfection for real-time PCR (n=3, +/-SEM). **C.** PEO1 C4-2 cells stably expressing NSC or miR-107 were harvested for real-time PCR (n=3, +/-SEM). **D.** U2OS cells were co-transfected with indicated miRNAs (0.5 nM) and luciferase constructs (empty vector, FANCE coding region (CDS), or FANCE 3'UTR) and assayed for luciferase activities 48 hours later (n=3-4, +/-SEM) (Student's t-test: **P* < 0.05).

Table 3.3. MiR-107 downregulates several factors implicated in cisplatin resistance in U2OS (cDNA microarray).

Summary of cisplatin resistance regulators that were significantly downregulated by miR-107 relative to miR-Neg-transfected in U2OS cells. The log_2-fold change presented is the mean of three independent experiments. The number of symbols (•) indicates the number of putative miR-103/107 binding sites as determined by the presence of a miR-103/107 seed-region complementary sequence ("UGCUGC").

Gene Name	Fold-Change (Log_2)	Predicted by TargetScan?	Putative Sites in 5'UTR?	Putative Sites in CDS?	Putative Sites in 3'UTR?	Ref.
CDK5R1	-0.765	••				[336]
RPS6KA4	-0.576			••••		[336]
UBE2A	-0.437	•				[332]
GSK3B	-0.475		•	•		[331]
MAP4K2	-0.786			•••••••		[331]
MAPKAPK2	-0.500				•••	[331]
NRBP1	-1.480	••				[331]
PRKCD	-0.459			••	•	[335]
WEE1	-0.899			•••	••	[335]
RAC2	-0.905	••				[333]
ZDHHC9	-0.873	••				[333]
EBP	-0.509			••		[333]
FLOT2	-0.712	•				[333]
CD151	-0.707	•				[333]
UBE2L3	-1.362	•				[333]
CCL2	-0.582			•		[334]
TESK1	-0.503			••		[334]

Discussion

In this and our previous work, we have now characterized several microRNAs (miR-103, miR-107 and miR-96) that post-transcriptionally regulate RAD51 expression. RAD51 has long been suspected of being a tumor suppressor in cancer [154]. It plays an essential role in HR and the deregulation of several modulators of RAD51 function such as BRCA1, BRCA2 and the RAD51 paralogs are found in sporadic and familial breast and ovarian cancers. Additionally, RAD51 gene is situated in a region of frequent LOH in cancer [337] and its downregulation of RAD51 protein and mRNA expression has been reported in some cancers [156]. However, known cancer-associated alleles of RAD51 are extremely rare [157], consistent with the intolerability of genetic defect in RAD51 [57]. Alternatives to RAD51 dysfunction may therefore exist. One potential mechanism is the regulation of its expression by cancer-associated microRNAs such as miR-103, miR-107 and miR-96. Additionally, several other microRNAs that were hits from our screen (e.g. miR-221/222, miR-124a/506, miR-494 and others) are also predicted to target RAD51 and may collectively contribute to the overall regulation of HR (Table 2.1).

In our complementation experiments, we found that chemosensitivity of H1299 cells was not suppressed by the ectopic expression of RAD51. We noted that among the cells used in our studies, the expression of RAD51 was highest in H1299 (relative to actin) (Figure 4.2A). Therefore, we propose that despite the downregulation of RAD51 by miR-103/107 in H1299, enough RAD51 protein remains to support HR and cellular resistance to DNA damaging agents. As RAD51 is a critical target for miR-103/107-mediated chemosensitivity, its relative abundance in H1299 cells may explain why overall chemosensitivity to cisplatin and AZD2881 is relatively mild when miR-107 is overexpressed (Figure 2.8D and Figure 2.10A). Nevertheless, miR-

103/107 were still able to enhance chemosensitivity indicating the existence of target(s) other than RAD51 that regulate chemoresistance. Lastly, our findings in H1299 demonstrated to us that one basis for cell type-dependent differences in microRNA-mediated phenotypes is whether target downregulation surpasses a critical threshold to elicit the phenotype, which in part depends on the expression level of the target.

In addition to RAD51, we found that miR-103/107 can also target RAD51D, which we demonstrated to be relevant for the inhibition of RAD51 foci formation and chemosensitivity to cisplatin and PARP inhibition (Figure 3.7A and C). While we found that ectopically expressing RAD51 and RAD51D largely reversed miR-103/107-mediated impairment of RAD51 foci formation and cellular sensitivity to AZD2281 (Figure 3.7D), we cannot exclude the possibility that other targets may be involved. When analyzing the expression of RAD51 paralogs in miR-103/107 overexpressing cells, we noted that RAD51B, XRCC2 and XRCC3 were consistently downregulated in several cell lines (Figure 3.6B). The mechanism of RAD51B downregulation is unclear. It is not a predicted target according to TargetScan [236] but does contain putative miR-103/107 binding sites in its coding region. Additionally, it exists in a quaternary complex with RAD51C, RAD51D and XRCC2 and interdependent protein stabilities among the members have been reported. For example, interdependent stability between XRCC2 and RAD51D likely explains the downregulation of XRCC2 (data not shown) [183]. The mechanism of miR-103/107-mediated downregulation of RAD51B thus requires further investigation. Additionally, the mechanism by which miR-103/107 regulates XRCC3 is also unknown. While XRCC3 is a predicted target of miR-103/107, our luciferase assays indicate that the 3'UTR does not contain sites for these microRNAs (data not shown). The role of XRCC3 in RAD51 foci formation is currently unclear [183, 338], but it also functions in the late stages of HR as well as in

checkpoint signaling [55, 170]. Therefore, it is possible that its repression by miR-103/107 also contributes to some of the phenotypes observed.

We identified other several potential targets of miR-103/107 involved in HR or chemosensitivity by microarray analysis (Table 3.2). The downregulation of some of these hits, such as CHEK1, CtIP and RPA70, may be specific to U2OS cells as their downregulation was not seen in other cell lines (Figure 3.6A). In order to formulate a generalized model of miR-103/107-mediated regulation of HR and chemosensitivity, candidates that are downregulated in a cell type-independent manner would be prioritized.

One such candidate is FANCE (Table 3.1). We validated the downregulation of FANCE by miR-103/107 in several cell lines (Figure 3.10A-C). FANCE is one of sixteen genes (including the RAD51 mediators BRCA2/FANCD1, PALB2/FANCN and RAD51C/FANCO) that confer an inherited hematological disorder called Fanconi anemia (FA) when mutations are inherited biallelically [339, 340]. The cellular hallmark of FA-BRCA deficient cells is sensitivity to DNA interstrand cross-linking agents and FA cells also exhibit defects in HR [341]. MiR-23a and miR-1245 have been reported to target two other FA pathway members, FANCG and FANCD1/BRCA2, respectively [257, 342]. Interestingly, we found that miR-103/107 regulate FANCE through its coding region (Figure 3.10D). We were not able to identify the exact binding site(s) for miR-103/107 and so cannot formally conclude that the mechanism of regulation is direct interaction.

We also broadened our list of possible miR-103/107 targets to include hits from several screens that identified novel regulators of cisplatin chemoresistance. Specifically, we identified 17 possible candidates whose downregulation in miR-107 overexpressing cells may play a role in miR-103/107-mediated chemosensitivity to cisplatin (Table 3.3) [331-336]. Among these, 8

are predicted targets of miR-103/107 by TargetScan [236] with one of them, CDK5R1, having been validated [313]. The rest of the candidates have putative bindings sites for miR-103/107 mainly in their respective coding regions but the mechanism of their downregulation may also be indirect (Table 3.3).

In summary, we identified RAD51 and RAD51D as the major targets of miR-103/107 for the regulation of DNA damage-induced RAD51 foci formation and chemosensitivity to DNA damaging agents. We also identified several more candidates by microarray analysis, including FANCE, whose regulation by miR-103/107 may also contribute to the regulation of DNA repair. Our findings provide a more complete picture of miR-103/107-mediated regulation of DNA repair.

Material & Methods

Cell lines

U2OS, HeLa, H1299 and 293 GFPu-1 were purchased from the American Type Culture Collections. MDA-MB-231 cells were a gift of the Paulovich lab (FHCRC). Wildtype mouse embryonic fibroblasts were a gift of the Clurman lab (FHCRC). RAT-1 cells were a gift of the Fausto Lab (FHCRC). PEO1 C4-2 clones were described previously [280]. H1299 cells were cultured in RPMI-1640 supplemented with 10% FBS and 2 mM L-glutamine in a humidified 5% CO_2-containing atmosphere at 37°C. All other cell lines were grown in DMEM with 10% FBS, 2 mM L-glutamine.

Plasmids, siRNAs, microRNA mimics/inhibitors and virus production

The 3'-UTRs of human RAD51 (position 1 to 980) and RAD51D (position 2 to 1139) were cloned into the XbaI site of pGL3-Control. Putative binding sites of miR-103/107 were

mutated using the QuikChange kit (Stratagene). All constructs were verified by Sanger sequencing.

To obtain miR-103 and miR-107 expression constructs, miR-103-2 and miR-107 precursors with flanking sequences (150 bp on each end) were PCR-amplified and cloned into the XhoI/MluI sites of the pLemiR vector (Open Biosystems). Lentivirus was produced as previously described [268].

The FLAG-RAD51 expression construct was made by initially modifying pRAD51-Luc [292]. First, we cloned the RAD51 cDNA and inserted an N-terminal FLAG-epitope tag. Next, we ligated the RAD51 promoter fragment (-2931 to +5) from pRAD51-Luc and the FLAG-RAD51 cDNA into the pENTR1A no ccDB entry vector (Addgene plasmid 17398). Lastly, we recombined into the pLenti-X1-GFP-Zeo DEST vector (Addgene plasmid 19277). The luciferase control was made by ligating the RAD51 promoter fragment (-2931 to +5) from pRAD51-Luc and luciferase from pGL3-Control into the entry vector and then recombining as above. PEO1 C4-2 and U2OS cells transduced with pLenti-X1-FLAG-RAD51 or pLenti-X1-Luc lentivirus were selected with Zeocin (Life Technologies) at 0.2 mg/mL for 1 and 2 weeks, respectively.

RAD51D cDNA was cloned into the NcoI and BamHI sites of pMMP-ires-puro. Retroviruses were produced as previously described [268]. PEO1 C4-2 cells transduced with pMMP-puro (empty vector) or pMMP-puro-RAD51D retroviruses were selected with puromycin at 2 μg/mL for 3 days.

MiRNA mimics (Dharmacon) and miRNA mimic negative control (miR-Neg1 or miR-Neg2, Dharmacon), siRNAs targeting RAD51 (#2 and #3 from [115]) and PSMD4 (Jacquemont 2007) (Sigma) and negative controls (nontargeting siRNA [343] or an equimolar pool of nontargeting siRNA, siLuc [259] and siAllstars (Qiagen)) were transfected at 10 nM using

HiPerFect (Qiagen). Locked nucleic acid (LNA)-based negative (Negative Control B) or a combination of miR-103 and miR-107 power inhibitors (Exiqon) were transfected at 15-50 nM with HiPerFect.

Western blot analysis

Whole-cell extracts were prepared and resolved by polyacrylamide gel electrophoresis as described [268]. Proteins were transferred onto nitrocellulose membranes. Antibodies against ATR (N-19, Santa Cruz), BRCA1 (D-9, Santa Cruz), BRCA2 (Ab-2, Calbiochem), CHK1 (G-4, Santa Cruz), CtIP (ab20163, Abcam), DICER (ab14601, Abcam) PALB2 (gift of Xia lab, UMDNJ), RAD51 (H-92, Santa Cruz), RAD51B (D-12 and 1H3/13, Santa Cruz), RAD51C (NB100-177, Novus), RAD51D (NB100-166, Novus), XRCC2 (N-20, Santa Cruz), XRCC3 (NB100-165, Novus), RPA70 (#2267, Cell Signaling), actin (Sc-1616-R, Santa Cruz), and luciferase (G7451, Promega) were probed with horseradish peroxidase-conjugated anti-mouse, anti-rabbit (GE Biosciences) or anti-goat IgG (sc-2020, Santa Cruz). Chemiluminescence was used for detection and membranes were exposed to film or digitally scanned with an Imagequant LAS 4000 (GE Biosciences). Films were digitalized using a standard scanner and images were processed using Photoshop CS (Adobe Systems, Inc.). Protein expression was quantified from digital images using ImageQuant TL (GE Biosciences).

Real-time RT-PCR

Total RNA was extracted using Trizol (Life Technologies) and reverse-transcribed using the Taqman miRNA Reverse Transcription Kit or the Taqman cDNA Reverse Transcription Kit (Life Technologies). The Taqman MiRNA Assay Kit or Gene Expression Kit (Life Technologies) was used for quantitative PCR. The comparative Ct value method was used for transcript quantification. MiR-103 and miR-107 expression was normalized to RNU24 or

RNU44 snoRNA. FANCE, RAD51 and RAD51D expression was normalized to18S rRNA or TBP mRNA.

Luciferase assay

U2OS cells were seeded in 24-well plates (5×10^4/well) and co-transfected with microRNA mimics (0.5 nM, HiPerFect), pRL-TK (50 ng/well, Mirus TransIT-LT-1) and pGL3-Control vectors containing empty, wild-type or mutant RAD51 (or RAD51D) 3'-UTR sequences (200 ng/well, Mirus TransIT-LT-1). Two days post-transfection, cells were lysed and the luciferase activities measured using the Dual-Luciferase Assay kit (Promega). Relative luciferase activity was calculated by normalizing the ratio of Firefly/Renilla luciferase to that of miR-Neg-transfected cells.

Microarray analysis

U2OS cells were harvested 48 hours after transfection and total RNA isolated using RNeasy Mini kit (Qiagen). RNA quality was determined by Bioanalyzer and then the RNA was labelled and hybridized to Illumina Human HT12 v4 BeadChip microarrays by the Genomics Core (FHCRC).

Proteasome assay

293 GFPu-1 cells were harvested 48 hours after transfection (10 nM) and analyzed by flow cytometry. As a positive control, 293 GFPu-1 cells were treated with MG132 (1 mM) for 3 hours prior to harvesting.

Statistical analysis

The Student's or paired *t*-tests were used to evaluate significance of differences between two groups of data (Excel, Microsoft, Inc.). All results were expressed as mean ± SD or SE. A P value < 0.05 was considered significant.

CHAPTER FOUR

Towards elucidating a physiological role for miR-103/107-mediated regulation of homologous recombination

Abstract

MicroRNA 103 and 107 directly target RAD51 and RAD51D to regulate homologous recombination and chemoresistance to DNA damaging agents. We explored several physiological contexts in which endogenous miR-103/107 levels are dynamically regulated and examined whether these changes had functional consequences for RAD51 and RAD51D expression. In particular, we investigated the reported upregulation of miR-103/107 in response to DNA damage and hypoxia and the regulation of miR-103 by the MET oncogene. While we did not detect changes in miR-103/107 expression in response to hypoxia or downstream of MET depletion, we did confirm that miR-107 is upregulated in response to DNA damage induced by topoisomerase II inhibitors. Furthermore, induction of DNA damage resulted in reduced RAD51D levels, but the mechanism appeared to be independent of miR-107 upregulation. Lastly, we looked for possible inverse relationships between miR-103/107 and RAD51/RAD51D expression levels in breast and ovarian tissue panels that would suggest endogenous interactions. While we did not detect any significant inverse correlation, we did detect positive correlation between miR-103 and miR-107 and between RAD51 and RAD51D in both tissue panels. Our studies help to elucidate potential physiological roles for miR-103/107 in the regulation of DNA repair.

Introduction

We previously identified miR-103/107 as novel regulators of HR (Chapter Two). Overexpression of miR-103/107 inhibited DNA damage-induced RAD51 foci formation, the efficiency of homology-directed repair, and chemoresistance to DNA damaging agents. We identified two targets of miR-103/107, RAD51 and RAD51D, and found them to be critical for the promotion of these phenotypes (Chapter Three). Furthermore, by inhibiting miR-103/107 with antisense oligonucleotides, we demonstrated that endogenous miR-103/107 may have some role in the regulation of RAD51D but not RAD51. We were interested in identifying other cellular contexts in which miR-103/107 regulate the expression of RAD51 and RAD51D in order to establish physiological roles for miR-103/107-mediated regulation of HR. In this study, we examined DNA damage- and hypoxia-induced upregulation of miR-103/107 [270, 276-279], MET-mediated regulation of miR-103 [344], and correlations between miR-103/107 and RAD51/RAD51D expression levels in panels of breast and ovarian tissue samples.

MiR-103/107 expression has been reported to dynamically change in response to various cellular stresses. In particular, miR-103/107 are upregulated in response to DNA damage [276-279]. This upregulation requires two p53-dependent mechanisms: transcriptional activation of the miR-107 host gene, PANK1 [276, 279], and enhanced post-transcriptional processing of miR-103/107 pri-microRNAs by the Microprocessor complex [278]. The upregulation of miR-103/107 has been proposed to inhibit proliferation, potentially by targeting CDK6, and allow for repair of damaged DNA [276, 278]. Other targets involved in cell cycle regulation, like CDK2 and cyclin E1 [290], may also be relevant to this response. We were interested in determining the importance of DNA damage-induced miR-103/107 upregulation in targeting RAD51 and RAD51D.

Hypoxic conditions have also been reported to induce miR-103/107 expression [270]. The upregulation of miR-103/107 in low oxygen conditions targets and downregulates DAPK and KLF4 to enhance cell migration *in vitro* and promote tumor invasiveness of colorectal carcinomas *in vivo* [270]. Interestingly, hypoxia has been reported to inhibit HR through the transcriptional repression of RAD51 by occupancy of p130/E2F4 repressive complexes at its promoter [151]. Consistently, RAD51 is downregulated in the hypoxic cores of some solid tumors [151]. We were interested in determining whether miR-103/107 constitute another mechanism of RAD51 downregulation in hypoxia.

The MET receptor tyrosine kinase is an oncogene that negatively regulates miR-103 expression [344]. The suppression of miR-103 promotes proliferation by de-repressing a miR-103/107 target, PKCε. The targeting of MET by small molecule inhibitors can sensitize cells to DNA damaging agents [345]. Furthermore, the downregulation of RAD51 in MET inhibitor-treated cells [345] suggests that MET may promote HR in addition to proliferation. As miR-103 can potentially regulate both processes, we were interested in determining whether the regulation of HR by MET is mediated by the modulation of miR-103 levels.

Significant inverse correlation between the expression of microRNAs and their targets suggest that regulatory interactions between microRNAs and targets occur endogenously. For example, inverse correlation between miR-103/107 and DICER has been reported in a series of breast cancer cell lines [275]. As levels of miR-103 and/or miR-107 are differentially expressed in subsets of both breast and ovarian cancers [275, 346, 347], we were interested in taking this approach in these tissue types to demonstrate a role for endogenous miR-103/107 in the regulation of RAD51 and Rad51D.

Results

MiR-107 is induced in response to doxorubicin

MiR-103 and miR-107 are upregulated in response to the topoisomerase II inhibitor, doxorubicin, in HCT116 cells [276-278]. We sought to determine whether this induction could regulate the expression of RAD51 and RAD51D. In agreement with previous studies, we found a 2-fold upregulation of miR-107 when HCT116 cells were treated with two concentrations of doxorubicin (Figure 4.1A). MiR-107 was also induced in response to another topoisomerase II inhibitor, etoposide (Figure 4.1B). We then analyzed the protein expression of RAD51 and RAD51D and found a concomitant reduction of RAD51D after treatment with the higher dose of doxorubicin (Figure 4.1C). The expression of RAD51 did not significantly change at either dose of doxorubicin relative to the untreated control (Figure 4.1C and D).

In order to determine whether the induction of miR-107 contributed to the downregulation of RAD51D protein expression, we inhibited endogenous miR-103/107 activity with a "sponge" construct [348]. This construct expresses fully complementary miR-103 and miR-107 binding sites in tandem and is designed to compete with endogenous miR-103/107 targets for binding to the microRNAs-of-interest. Additionally, interaction with perfect binding sites *in vivo* results in the destabilization of the targeted microRNAs [349]. Consistently, stable expression of a miR-103/107 sponge construct in HCT116 cells reduced endogenous miR-103/107 levels by 2-fold relative to cells expressing the empty vector control (Figure 4.1A). Furthermore, the miR-103/107 sponge construct largely blunted doxorubicin-induced miR-107 upregulation (Figure 4.1A). Despite inhibited miR-107 expression, RAD51D was similarly downregulated in response to doxorubicin as empty vector controls (Figure 4.1C and D). These

results indicate that doxorubicin-responsive downregulation of RAD51D occurs independently of miR-103/107.

To determine whether endogenous miR-103/107 plays any role in the cellular response to doxorubicin, we assayed the survival of HCT116 cells expressing the miR-103/107 sponge construct. We found that the inhibition of miR-103/107 did not modulate doxorubicin-mediated killing relative to the empty vector control (Figure 4.1E). These results collectively indicate that endogenous miR-103/107 or its DNA damage-induced upregulation does not play a significant role in the regulation of HR-relevant targets in this experimental condition.

MiR-103 and miR-107 induction in response to hypoxia

Both miR-103 and miR-107 are reportedly upregulated in hypoxic conditions in HCT116 cells, which then downregulate the targets DAPK and KLF4 [270]. We sought to determine whether hypoxia-induced miR-103/107 expression can modulate the expression of RAD51 and RAD51D. We exposed PEO1 C4-2, H1299 and HCT116 cells to hypoxic conditions (1% O_2) for 24 hours and determined miR-103/107 expression relative to normoxic controls (20% O_2). The upregulation of HIF-1α protein levels was used as a positive control for hypoxia (Figure 4.2A) [279]. Unexpectedly, we found that miR-103/107 expression did not change in response to hypoxia in any of the cell lines (Figure 4.2B). In contrast, protein levels of RAD51 were consistently downregulated in hypoxia as expected (Figure 4.2A) [151]. Surprisingly, RAD51D expression was upregulated in hypoxia (Figure 4.2A). These results suggest that miR-103/107 does not play a significant role in the regulation of RAD51 and RAD51D in response to hypoxia in this experimental condition.

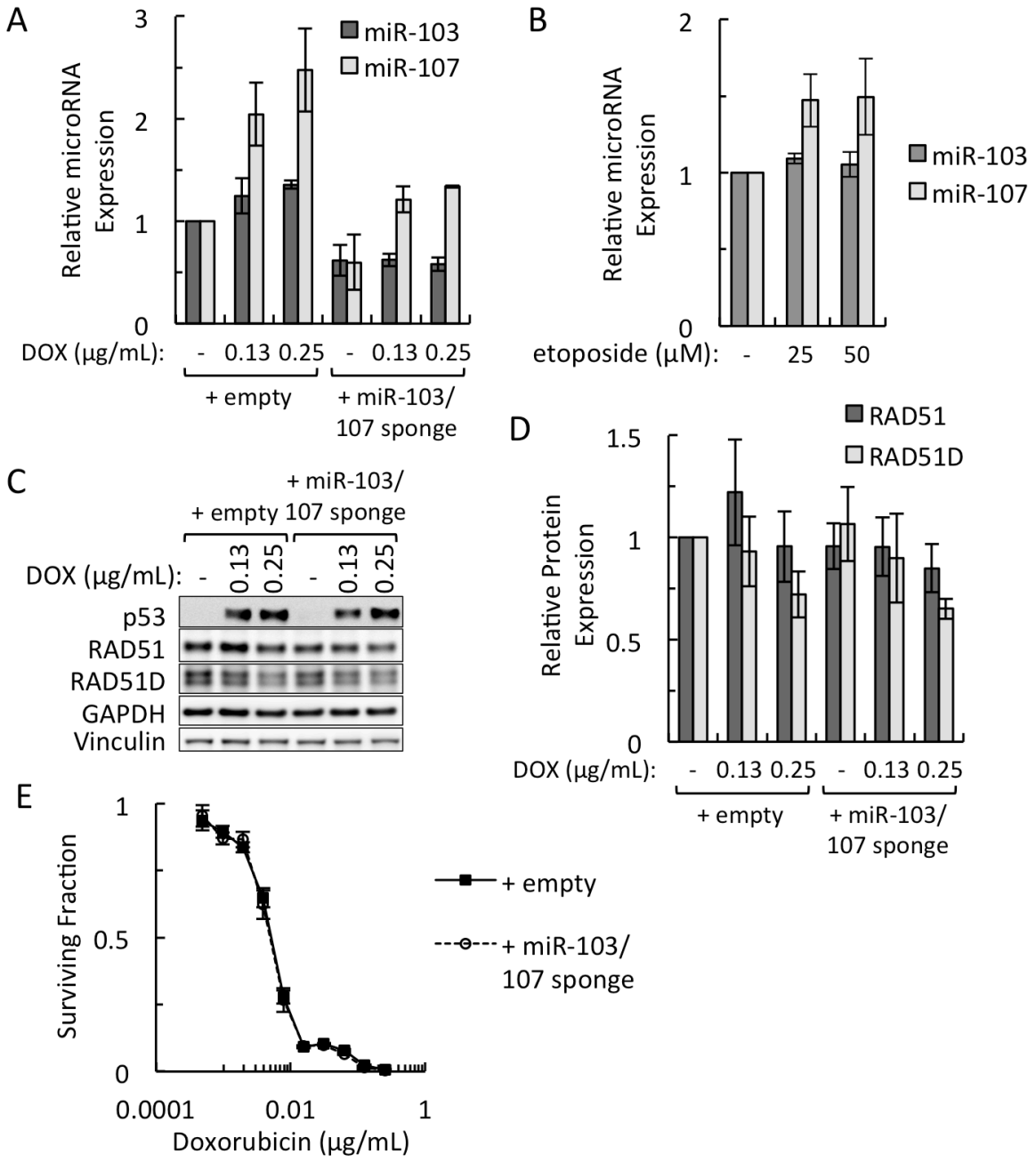

Figure 4.1. DNA damage-induced miR-103/107 expression.
A. HCT116 cells stably expressing a miR-103/107-sponge or an empty vector were treated with doxorubicin at indicated concentrations and harvested for real-time PCR 24 hours later (n=3, +/-SEM). **B.** HCT116 cells were treated with etoposide or DMSO (vehicle) and harvested for real-time PCR 24 hours later (n=3, +/-SEM). **C-D.** HCT116 cells stably expressing a miR-103/107-sponge or an empty vector were treated with doxorubicin at indicated concentrations and harvested for Western blotting 24 hours later (**C**). The **q**uantitation shown in (**D**) is the average of GAPDH and vinculin-normalized RAD51 and RAD51D protein expression (n=3, +/-SEM). E. HCT116 cells stably expressing a miR-103/107-sponge or an empty vector were assayed for cell survival in response to doxorubicin (n=3, +/-SEM).

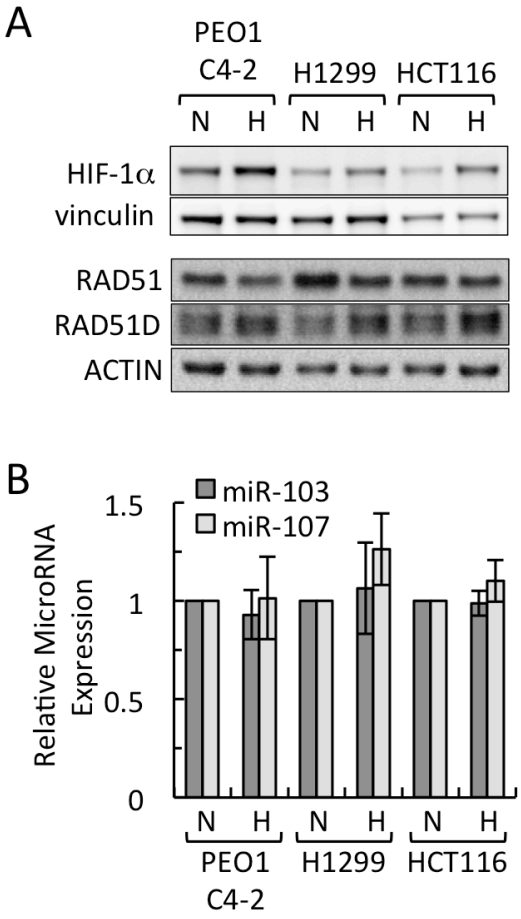

Figure 4.2. Hypoxia-induced miR-103/107 expression.
A-B. PEO1 C4-2, H1299 and HCT116 cells cultured in 20% O_2 (N) or 1% O_2 (H) for 24 hours were harvested for Western blotting (**A**) and real-time PCR (**B**) (n=3, +/-SEM). HIF-1α induction serves a control for hypoxia.

MiR-103 regulation by the MET oncogene

The MET oncogene regulates PKCε expression in lung carcinomas in part through the repression of miR-103 expression [344]. When MET is depleted, miR-103 expression is de-repressed [344]. We sought to determine whether MET potentially modulates RAD51 and RAD51D expression through the regulation of miR-103. We depleted MET protein levels in CaLu-1 lung carcinoma cells with varying concentrations of siRNAs and determined miR-103/107 expression (Figure 4.3A). Unexpectedly, contrary to the previous report [344], MET depletion mildly reduced the expression of miR-103/107 relative to the three negative controls used (Figure 4.3B). We did observe the downregulation of RAD51 expression when MET was depleted (Figure 4.3A).

MiR-103 and miR-107 are positively correlated in breast and ovarian tissues

Deregulation of miR-103/107 expression has been reported in breast and ovarian cancer [275, 346, 347]. We sought to determine whether miR-103/107 and their targets, RAD51 and RAD51D, were differentially expressed in cancer and whether their expression levels were inversely correlated in these cancers. The expression of miR-103, miR-107, RAD51 and RAD51D was determined for ovarian (15 normal ovarian epithelia and 31 tumors) and breast (4 normal and 39 tumor) tissue samples by real-time PCR. We found that miR-103/107 expression was significantly reduced in ovarian tumor samples relative to normal tissue controls (Figure 4.4A). No statistically significant difference in RAD51 or RAD51D expression was observed between normal ovarian and ovarian tumor tissues (Figure 4.4A). Furthermore, there were no significant differences observed between breast tissue samples and the normal breast tissue controls for either microRNA or target mRNA expression (data not shown).

Additionally, we analyzed pair-wise correlations (Pearson) between miR-103, miR-107, RAD51 and RAD51D expression for both tissue types. Interestingly, significant positive correlation between miR-103 and miR-107 expression and between RAD51 and RAD51D expression was detected in both ovarian (Figure 4.4B) and breast tissues (Figure 4.4C). However, we did not observe any significant correlation between the expression of miR-103 or miR-107 with either RAD51 or RAD51D in ovarian (Figure 4.5A and B) and breast tissues (Figure 4.5C and D).

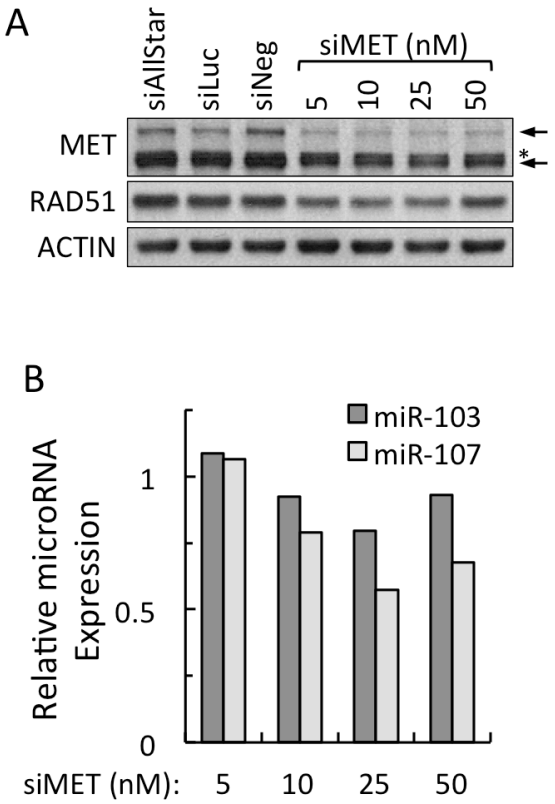

Figure 4.3. MET-mediated regulation of miR-103/107 expression.
A-B. CaLu-1 cells transfected with the indicated concentrations of siMET or three negative controls (50 nM each) were harvested 24 hours later for Western blotting (**A**) and real-time PCR (**B**). MiR-103/107 expression is the average of normalizations to each of the three negative controls. Arrows indicate MET protein and the asterisk (*) indicates a non-specific band.

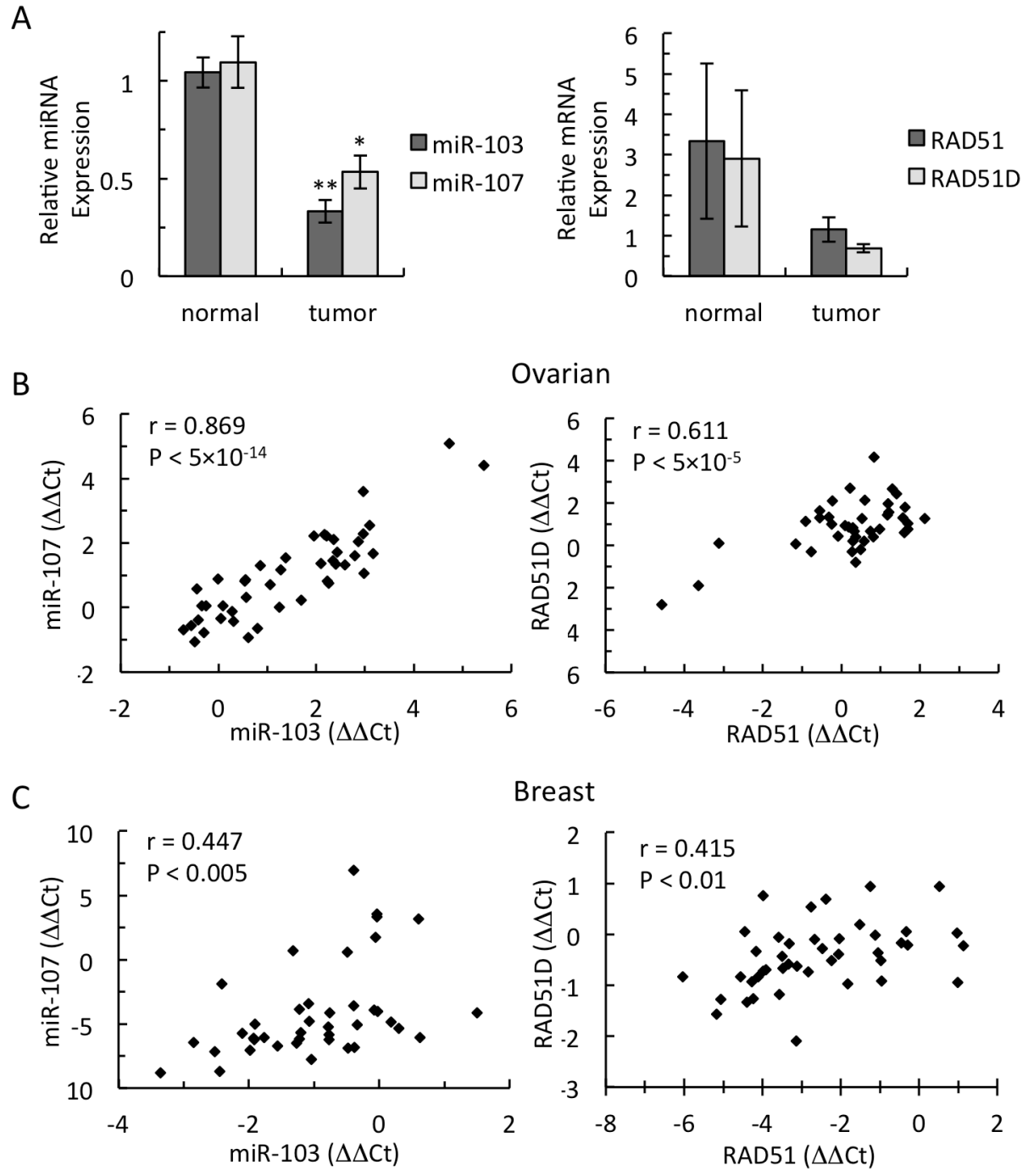

Figure 4.4. Positive correlation between miR-103 and 107 expression and between RAD51 and RAD51D expression in breast and ovarian tissues.
A. The expression of miR-103, miR-107, RAD51 and RAD51D was quantitated from ovarian tissue samples (total RNA from 15 normal and 31 tumor) by real-time PCR. Error bars represent SEM. (Student's t-test: *P < 0.001, **P < 5×10^{-9}). **B-C.** Expression plots (ΔΔCt) of miR-103/107 and RAD51/RAD51D in ovarian (15 normal and 31 tumor) (**B**) and breast tissue samples (4 normal and 39 tumor) (**C**). The Pearson correlation coefficient, r, and significance of correlation are presented for each comparison.

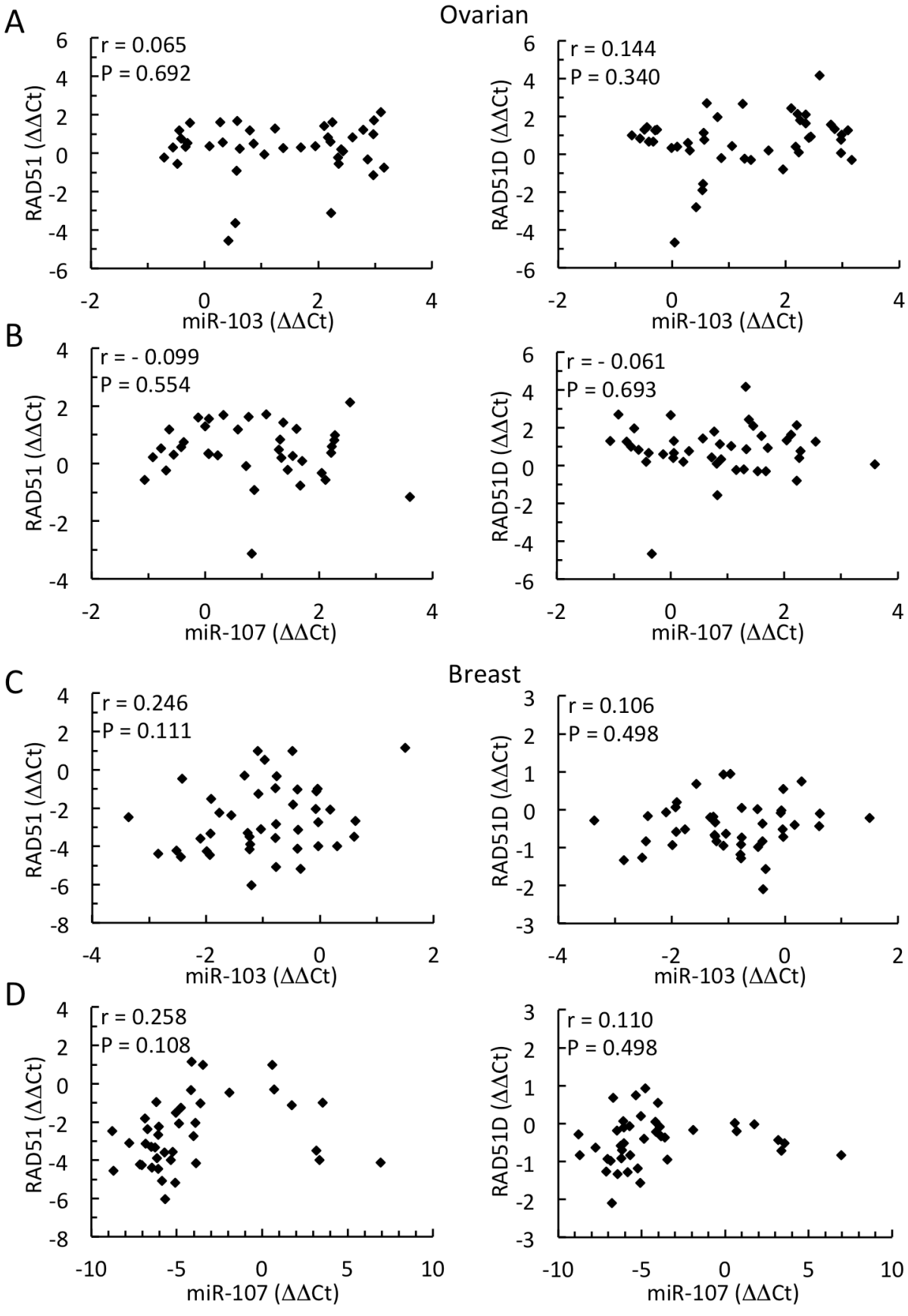
A
Ovarian
r = 0.065
P = 0.692
RAD51 (ΔΔCt)
miR-103 (ΔΔCt)
r = 0.144
P = 0.340
RAD51D (ΔΔCt)
miR-103 (ΔΔCt)
B
r = - 0.099
P = 0.554
RAD51 (ΔΔCt)
miR-107 (ΔΔCt)
r = - 0.061
P = 0.693
RAD51D (ΔΔCt)
miR-107 (ΔΔCt)
C
Breast
r = 0.246
P = 0.111
RAD51 (ΔΔCt)
miR-103 (ΔΔCt)
r = 0.106
P = 0.498
RAD51D (ΔΔCt)
miR-103 (ΔΔCt)
D
r = 0.258
P = 0.108
RAD51 (ΔΔCt)
miR-107 (ΔΔCt)
r = 0.110
P = 0.498
RAD51D (ΔΔCt)
miR-107 (ΔΔCt)

Figure 4.5. MiR-103/107 and RAD51 or RAD51D expression are not correlated in breast and ovarian tissues.

A-D. Expression plots (ΔΔCt) of miR-103/107 and RAD51 or RAD51D in ovarian (15 normal and 31 tumor) (**A** and **B**) and breast tissue samples (4 normal and 39 tumor) (**C** and **D**). The Pearson correlation coefficient, r, and significance of correlation are presented for each comparison.

Discussion

In our previous studies, we established that miR-103/107 directly target and downregulate RAD51 and RAD51D expression (Chapter Three). The overexpression of miR-103/107 also had functional consequences for HR and cellular resistance to DNA damaging agents (Chapter Two). However, the physiological role for these microRNAs in the regulation of DNA repair is not well characterized. We previously found that endogenous miR-103/107 has a role in the regulation of RAD51D but not RAD51in microRNA inhibitor experiments (Figure 3.8C and D). In this study, we investigated whether several cellular stresses that induce miR-103/107 expression led to changes in RAD51 and RAD51D expression. In particular, we examined DNA damage-induced and hypoxia-induced miR-107 upregulation and the negative regulation of miR-103 by the MET oncogene. Additionally, we examined whether miR-103/107 and RAD51 and RAD51D expression are correlated in panels of breast and ovarian tissues.

We found that DNA damage generated by topoisomerase inhibitors (doxorubicin or etoposide) resulted in a 2-fold upregulation of miR-107, consistent with previous reports [276-279]. While RAD51 protein expression remained largely unchanged despite p53 activation, a 2-fold downregulation of RAD51D protein expression was observed in damaged cells. However, the inhibition of miR-103/107 with a sponge construct did not restore RAD51D expression suggesting that the downregulation of RAD51D in response to DNA damage relies on a different mechanism. Consistent with this, miR-103/107 inhibition also did not alter cell survival in response to doxorubicin. Our results suggest that in the context of DNA damage, changes in miR-107 (and/or miR-103) expression alone do not play a major role in the regulation of the DNA repair-relevant targets, RAD51 and RAD51D.

Our findings raise the question of why miR-107 is upregulated in response to DNA damage. In our previous studies, we found that a relatively high level of miR-107 overexpression (~30-fold in HeLa cells) results in a modest downregulation of both target expression (data not shown) and chemoresistance (Figure 2.8F). It is unclear whether the 2-fold induction of miR-107 observed in response to DNA damage would have any functional consequence on HR. The induction of miR-107 expression in response to DNA damage is partly transcriptional due to p53 binding the promoter of the host gene, PANK1, thereby upregulating the expression of both PANK1 and miR-107 [276, 279]. This occurs despite the presence of a putative promoter within the intron that miR-107 resides in, which can drive miR-107 expression independent of PANK1 [350]. This suggests that PANK1 itself may be a p53 effector. A role for PANK1 in the DNA damage response has not been reported but one of the other pantothenate kinase homologs, PANK2, was identified in a screen for kinases that regulate cisplatin resistance (though it was not further validated) [331]. Therefore, it is a possibility that p53 upregulates PANK1 as part of the DNA damage response while miR-107 upregulation may be incidental. In order to address whether there is actually a role for DNA damage-induced miR-107 expression, expression profiling of miR-103/107-inhibited or null cells following DNA damage would be needed to be done to identify the relevant targets.

Previous studies have established a functional link between hypoxia and HR [151]. Hypoxic conditions results in the transcriptional downregulation of factors such as RAD51 and BRCA1 thereby inhibiting HR-mediated repair [151]. Consistent with these *in vitro* studies, downregulation of RAD51 expression is found in the core of solid tumors, where respiration is lower due to poor vascularization [151]. This mechanism of HR inhibition has been suggested to promote genomic instability and the progression of hypoxic tumors [151]. MiR-103/107 have

been reported to be hypoxia-inducible microRNAs [270]. We examined whether miR-103/107 upregulation in low oxygen can also play a role in the post-transcriptional regulation of RAD51 and RAD51D and impact HR. However, we were not able to reproduce the hypoxia-inducible expression of miR-103/107. The reasons for the inconsistency are unclear and may involve differences in experimental conditions. For example, while some experiments by Chen and colleagues [270] used a 24-hour period of 1% O_2 to induce hypoxia, other experiments used a 48-hour treatment. We did not test miR-103/107 expression after this longer hypoxic treatment. Nevertheless, reduction in RAD51 protein expression was seen with the 24-hour treatment without any detectable change in miR-103/107 expression. These findings suggest that miR-103/107 plays little to no part in the regulation of RAD51 in hypoxia. The use of microRNA sponge/inhibitors or a miR-103/107-null cell line would be needed to further investigate these possibilities. We also observed the upregulation of RAD51D in hypoxic conditions, but the mechanism for this is unclear. Whether the upregulation of RAD51D is downstream of hypoxic signaling or compensates for reduced RAD51 expression also requires further investigation.

The MET oncogene is a receptor tyrosine kinase that has been linked to cellular resistance to DNA damaging agents [345]. Small molecule inhibitors of MET radio- and chemo-sensitize cells and reduces RAD51 expression suggesting the possible mechanism of sensitivity to DNA damaging agents is a downregulation of HR [345]. We wanted to explore whether the negative regulation of miR-103 expression by MET contributes to the modulation of HR. Consistent with previous reports [345], we observed a decrease in RAD51 expression when MET was depleted. However, miR-103/107 expression did not change or was even decreased in MET-depleted cells. The reasons for this inconsistency are unclear and may involve differences in experimental conditions. It is possible that our level of depletion was not as efficient as in [344],

where a pool of 3 shRNAs was used to silence MET expression. Alternatively, off-target effects of our particular siRNA against MET may have affected miR-103/107 expression, thereby confounding our study.

Lastly, we looked for indirect evidence of miR-103/107-mediated regulation of RAD51 and RAD51D by examining whether miR-103/107 expression correlates with its HR-relevant targets in panels of breast and ovarian tissue samples. Inverse correlation between miR-103/107 and the expression of other targets such as Dicer have been reported [275]. In our panels of breast and ovarian tissue samples, we were not able to detect any correlation between the mRNA levels of RAD51 and RAD51D and miR-103/107. Interestingly, we did find a positive correlation between miR-103 and miR-107 expression. This suggests that miR-103/107 are potentially co-regulated. MiR-107 and both copies of miR-103 are situated in the penultimate introns of the pantothenate kinase homologs, PANK1-3 [200, 304]. These kinases catalyze the rate-limiting step of acetyl coA biogenesis and are ubiquitously expressed with different subcellular localizations [351]. Due to the potential co-expression of their host genes, positive correlation between miR-103 and miR-107 may not be surprising. Another possibility, though not mutually exclusive, is that miR-103 can also regulate miR-107 expression or vice versa. Consistent with this possibility, we have observed that ectopic expression of mir-103 upregulates miR-107 expression (Figure 2.8A). The mechanism of this regulation between these paralagous microRNAs or its significance is unclear.

We also saw positive correlation between the expression of RAD51 and RAD51D in both the breast and ovarian tissue panels. As RAD51D is a critical mediator of RAD51 loading at resected ends, the co-regulation of RAD51 and RAD51D expression is not surprising. The RAD51D promoter has not been well characterized and little is known about the transcription

factors that regulate it. It is therefore unclear whether common transcription factors regulate the expression of these two miR-103/107 targets of whether they are both downstream of separate transcriptional programs initiated during cell cycle entry.

In summary, we searched for instances of miR-103/107-mediated regulation of RAD51 and RAD51D in several physiological contexts but were unable to identify a clear and convincing example. We found that DNA damage-induced downregulation of RAD51D likely occurs independent of miR-107 upregulation. We were unable to reproduce published reports of hypoxia-induced miR-103/107 upregulation or the negative regulation of miR-103 expression by the MET oncogene. Lastly, we were not able to detect significant inverse correlation between miR-103/107 and RAD51/RAD51D in two tissue-specific panels. Thus, a physiological role for miR-103/107-mediated regulation of HR remains to be identified.

Material & Methods

Cell lines

HeLa, H1299 and CaLu-1 were purchased from the American Type Culture Collections. PEO1 C4-2 clones were described previously [280]. HCT116 cells were a gift of the Clurman lab (FHCRC). H1299 cells were cultured in RPMI-1640 supplemented with 10% FBS and 2 mM L-glutamine in a humidified 5% CO_2-containing atmosphere at 37°C. All other cell lines were grown in DMEM with 10% FBS, 2 mM L-glutamine. For hypoxia experiments, cells were seeded in 1 mL of media per well of 6-well plates and placed in a hypoxic incubator (Bielas lab, FHCRC) flushed with 1% O_2, 5% CO_2 and 94% N_2 for 24 hours.

Tissue samples

Breast tissue samples were a gift of the Porter lab (FHCRC) and included 4 normal and 39 tumor samples. Total RNA was extracted using the RNeasy Mini kit (Qiagen). Total RNAs from 46 ovarian tissue samples were a gift of the Swisher lab (FHCRC) and included 15 normal and 31 tumor samples.

Plasmids, siRNAs and virus production

To obtain miR-103/107 sponge constructs, the following oligos were annealed and ligated into the XhoI and MluI sites of the pLemiR vector (Open Biosystems): forward: 5'-TCGAGTCATAGCCCTGTACAATGCTGCTGGCCTCATAGCCCTGTACAATGCTGCTGGCCTCATAGCCCTGTACAATGCTGCTGGCCTCATAGCCCTGTACAATGCTGCTGGCCTGATAGCCCTGTACAATGCTGCTGGCCTGATAGCCCTGTACAATGCTGCTGGCCTGATAGCCCTGTACAATGCTGCTA-3' and reverse: 5'-CGCGTAGCAGCATTGTACAGGGCTATCAGGCCAGCAGCATTGTACAGGGCTATCAGGCCAGCAGCATTGTACAGGGCTATCAGGCCAGCAGCATTGTACAGGGCTATGAGGCCAGCAGCATTGTACAGGGCTATGAGGCCAGCAGCATTGTACAGGGCTATGAGGCCAGCAGCATTGTACAGGGCTATGAC-3'. Lentivirus was produced as previously described [268] and transduced HCT116 cells were selected in 12.5 μg/mL of puromycin (Life Technologies).

An siRNA targeting MET (target sequence 5'-AACCAATGGATCGATCTGCCA-3') (Sigma) was transfected at 5-50 nM using HiPerFect (Qiagen). A non-targeting siRNA [303], siLuc [259] and siAllstars (Qiagen) were used as negative controls.

Western blot analysis

Whole-cell extracts were prepared and resolved by polyacrylamide gel electrophoresis as described [268]. Proteins were transferred onto nitrocellulose membranes. Antibodies against

HIF-1α (#3716, Cell Signaling), MET (#3127S, Cell Signaling), p53 (DO-1, Santa Cruz), RAD51 (H-92, Santa Cruz), RAD51D (NB100-166, Novus), actin (Sc-1616-R, Santa Cruz), GAPDH (GT239, GeneTex) and vinculin (V9131, Sigma-Aldrich) were probed with horseradish peroxidase-conjugated anti-mouse or anti-rabbit IgG (GE Biosciences). Chemiluminescence was used for detection and membranes were exposed to film or digitally scanned with an Imagequant LAS 4000 (GE Biosciences). Films were digitalized using a standard scanner and images were processed using Photoshop CS (Adobe Systems, Inc.). Protein expression was quantified from digital images using ImageQuant TL (GE Biosciences).

Real-time RT-PCR

Total RNA was extracted using Trizol (Life Technologies) and reverse-transcribed using the Taqman microRNA Reverse Transcription Kit or the Taqman cDNA Reverse Transcription Kit (Life Technologies). The Taqman microRNA Assay Kit or Gene Expression Kit (Life Technologies) was used for quantitative PCR. The comparative Ct value (ΔΔCt) method was used for transcript quantification. MiR-103 and miR-107 expression was normalized to RNU24 or RNU44 snoRNAs. RAD51 and RAD51D expression was normalized to18S rRNA. For the breast and ovarian correlation studies, the expression (ΔΔCt) of miR-103/107, RAD51 and RAD51D for all samples were normalized to the average ΔCt values of the respective normal tissue controls.

Survival assay

Transduced HCT116 cells were seeded into 12-well plates at 5×10^3/well and treated with doxorubicin (Sigma) at indicated concentrations. After incubation for 5-6 days, monolayers were fixed, stained with crystal violet and resolubilized as previously described [268]. Cell survival is expressed as a fraction of the untreated control.

Statistical analysis

Pearson correlation and associated P values were calculated in Excel (Microsoft, Inc.). The Student's *t*-test was used to evaluate significance of differences between two groups of data (Microsoft Excel). A *P* value less that 0.05 was considered significant.

CHAPTER FIVE

Conclusions and future directions

Several forms of crosstalk exist between the microRNA and DNA repair pathways. First, ATM and BRCA1, which are required for DSB repair, promote the maturation of a subset of microRNAs [261, 262]. Specifically, BRCA1 interacts with the Microprocessor complex to regulate microRNA expression [261] while ATM phosphorylates KHSRP to modulate microRNA expression in response to DNA damage [262]. Secondly, components of the microRNA biogenesis machinery promote the efficiency of both ATM-mediated DNA damage response signaling and HR-mediated DSB repair [264, 265]. Lastly, several microRNAs have been found to target components of various DNA repair pathways. A subset of these regulates HR factors, including miR-24 [249], miR-146a/b-5p [256] and miR-182 [260], which target BRCA1, and miR-1245, which targets BRCA2 [257]. However, these microRNAs likely represent only a fraction of the human "microRNAome" that target the HR pathway.

We were interested in screening the human microRNAome to systematically identify microRNAs that regulate HR. To this end, we devised cell-based screens using IR-induced RAD51 foci formation as an indicator of HR pathway integrity. We screened human microRNA mimic libraries in two different cell lines, HeLa and U2OS, which allowed us to identify potential cell-type specific effects. Surprisingly, only three microRNAs were commonly identified in both of our screens: miR-103, miR-107 and miR-221. I went on to demonstrate that these microRNAs are potent inhibitors of HR and that miR-103/107 enhanced cellular sensitivity to various DNA DSB-inducing agents (Figure 5.1). Consistent with the findings of our foci-based screens, miR-107 and miR-221 were both recently identified in a screen that used cellular

sensitivity to a PARP inhibitor as a readout [352]. While I focused on the characterization of miR-103/107 and miR-221, a subset of the other hits, which may not have been commonly identified due to technical differences between our two screens, may also be regulators of HR (Figure 2.1A and Table 2.1). It would therefore be of interest to further investigate several of these microRNAs, particularly those that are deregulated in cancer such as the members of the miR-15/16-family [202], the miR-124a/506 family [353], miR-383 [354], miR-137 and miR-147 [355]. In work that was not presented in this dissertation, we further characterized miR-96, which is part of the oncogenic miR-183/96/182 cluster and a hit from our U2OS screen only, in the regulation of HR and chemosensitivity to DNA damaging agents [259].

Using a candidate gene approach, I was able to identify and then demonstrate that RAD51 and RAD51D were direct targets of miR-103/107 (Figure 5.1). Moreover, I showed that their downregulation was critical for miR-103/107-mediated inhibition of RAD51 foci formation as well as chemosensitivity to cisplatin and PARP inhibition (Figure 5.1). Studies from our lab have now identified several microRNAs that regulate RAD51 expression [259]. Interestingly, several of the other hits are also predicted to target RAD51 (Figure 2.1A and Table 2.1, indicated by "#"). As disease-causing alleles of RAD51 are rare [157, 159, 161], miR-103/107, miR-96 and other microRNAs identified in our screens may contribute to RAD51 deregulation in the progression of cancer or in the development of the congenital mirror movements syndrome. It would therefore be of interest to identify and validate RAD51-targeting microRNAs.

Having identified miR-103/107 as novel regulators of HR, my findings raise the possibility that these microRNAs may contribute to (1) genomic instability and chemosensitivity in cancer or to (2) the regulation of HR in physiological contexts. To address the former possibility, I inhibited endogenous miR-103/107 by antisense oligonucleotides in H1299 and

MDA-MB-231 cells, which are cancer cell lines that abundantly express these microRNAs [275, 314, 315]. Antagonizing endogenous miR-103/107 resulted in only a mild effect on the expression of RAD51D (~20% upregulation) and no significant effect on RAD51 (Figure 3.8B-D). Not surprisingly, chemoresistance was not increased in these miR-103/107-inhibited cells (Figure 3.8A). While endogenous miR-103/107 may not regulate chemosensitivity in H1299, they may play a critical role in chemosensitivity in other cancer cell lines. These potentially include MiaPACA-2 and PANC-1, which are cisplatin-resistant pancreatic cancer cell lines [356]. MiR-103/107 are epigenetically silenced in these cell lines [272], which raises the possibility that miR-103/107 repression contributes to their chemoresistance to cisplatin.

We also examined several different physiological contexts in which miR-103/107 may be regulating HR, such as in hypoxia [270]. While some of our findings were inconsistent with published reports, we did observe significant upregulation of miR-107 and concomitant downregulation of RAD51D protein in response to DNA damage. However, the inhibition of miR-107 with a sponge construct did not restore RAD51D expression or modulate chemosensitivity suggesting that changes in miR-107 expression may not be relevant to the regulation of HR in this particular context. Cellular differentiation is another potential avenue of future investigation. MiR-103 and miR-107 are upregulated during retinoic acid-induced differentiation of neuroblastoma (SH-SY5Y) [288] and leukemia (NB4) [289] cell lines, respectively. The exit of these cells from the cell cycle may be coupled to the restriction of the HR pathway that is partly mediated by the upregulation miR-103/107 and their subsequent targeting of RAD51 and RAD51D. This would parallel the role described for miR-24 in the targeting H2AX during the differentiation of hematopoietic cell lines [255].

Lastly, our finding that miR-103/107 enhances chemosensitivity to DNA damaging agents raises the possibility that these microRNAs may have clinical utility as (1) therapeutic agents for the chemosensitization of tumors or as (2) prognostic indicators of chemosensitive tumors. I addressed the first possibility with a xenograft model of tumor growth. We elected to use H1299 cells because stable overexpression of miR-107 sensitized H1299 cells to cisplatin *in vitro* and these cells are highly tumorigenic. Consistent with our findings *in vitro*, the overexpression of miR-107 conferred mild cisplatin chemosensitivity to H1299 tumors *in vivo*, although our results did not reach statistical significance. Further optimization of our experimental system is therefore required, particularly with regards to the cell line used and the method of delivery [301]. Nevertheless, our *in vitro* and *in vivo* experiments collectively suggest that tumors that highly express RAD51 may be less responsive to the combination of miR-107 overexpression and cisplatin treatment. Another aspect to consider is whether miR-103/107 delivery would inhibit proliferation of tumors cells, such as in head and neck squamous cell carcinoma [301] and colon carcinoma [279], as the generation of DSBs by cisplatin and PARP inhibition relies on S phase entry [266, 357]. In this regard, the combination of miR-103/107 delivery and cisplatin treatment may be more effective in tumors that overexpress proliferation-relevant targets of miR-103/107, such as cyclin E, CDK6 or PKCε oncogenes.

In summary, we identified the paralogous miR-103 and miR-107 as novel players in the regulation of HR and chemoresistance to DNA damaging agents. MiR-103, miR-107 and other hits from our screen help to provide a more complete picture of the regulatory crosstalk that exists between microRNA and DNA repair pathways to maintain genomic stability. Furthermore, these microRNAs may potentially be useful as prognostic indicators of chemotherapy response or as therapeutic agents for the chemosensitization of tumors.

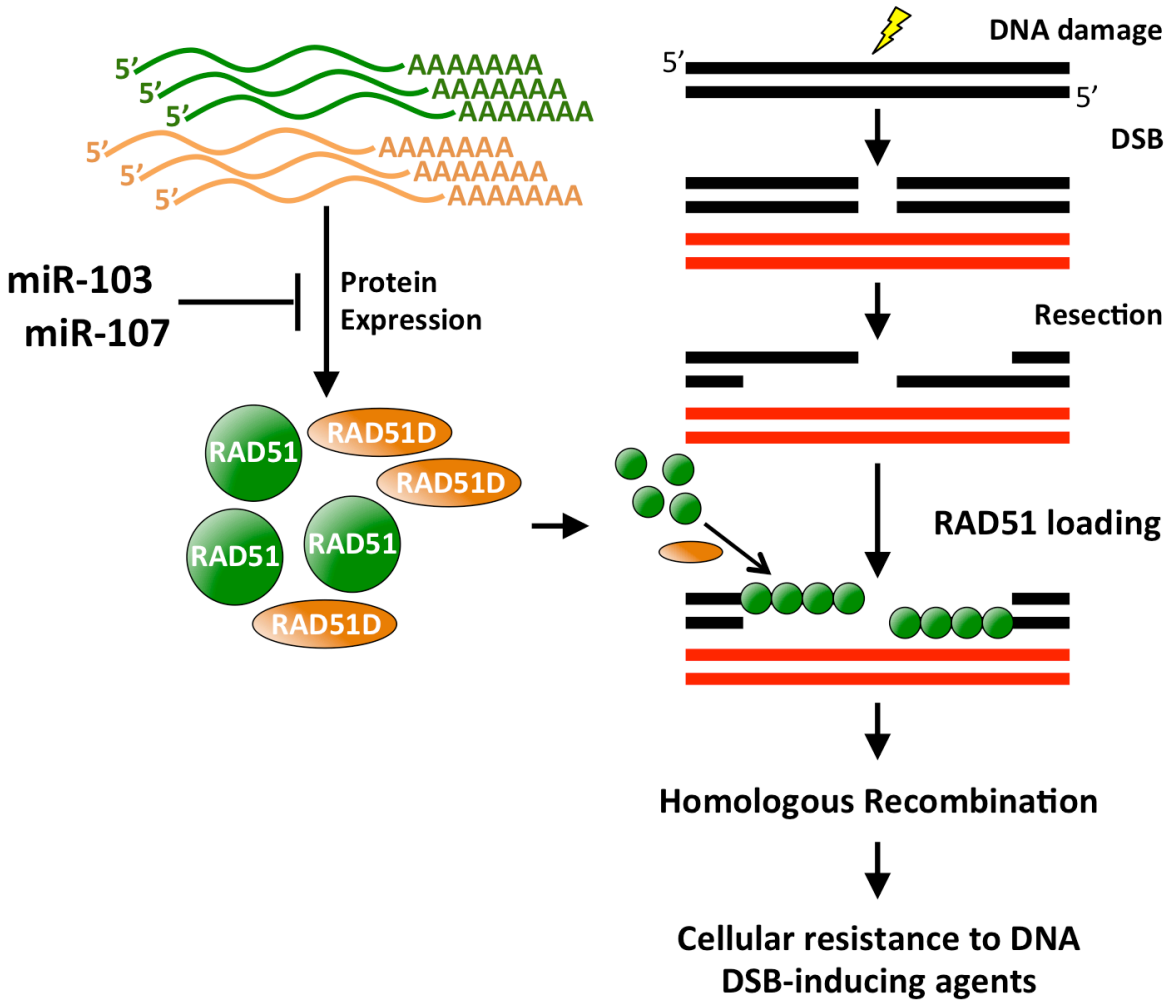

Figure 5.1. A model of miR-103/107-mediated regulation of homologous recombination.
A model showing that miR-103/107 post-transcriptionally downregulate the expression of RAD51 and RAD51D to inhibit the loading of RAD51 at double-strand breaks (DSBs), which reduces the efficiency of DSB repair by homologous recombination and confers cellular sensitivity to DNA DSB-inducing agents.

REFERENCES

1. Friedberg, E.C. and E.C. Friedberg, *DNA repair and mutagenesis*. 2nd ed. 2006, Washington, D.C.: ASM Press. xxix, 1118 p.

2. Lindahl, T. and D.E. Barnes, *Repair of endogenous DNA damage.* Cold Spring Harb Symp Quant Biol, 2000. **65**: p. 127-33.

3. Curtin, N.J., *DNA repair dysregulation from cancer driver to therapeutic target.* Nat Rev Cancer, 2012. **12**(12): p. 801-17.

4. Huang, L.C., K.C. Clarkin, and G.M. Wahl, *Sensitivity and selectivity of the DNA damage sensor responsible for activating p53-dependent G1 arrest.* Proc Natl Acad Sci U S A, 1996. **93**(10): p. 4827-32.

5. Bennett, C.B., et al., *Lethality induced by a single site-specific double-strand break in a dispensable yeast plasmid.* Proc Natl Acad Sci U S A, 1993. **90**(12): p. 5613-7.

6. Lieber, M.R., *The mechanism of double-strand DNA break repair by the nonhomologous DNA end-joining pathway.* Annu Rev Biochem, 2010. **79**: p. 181-211.

7. San Filippo, J., P. Sung, and H. Klein, *Mechanism of eukaryotic homologous recombination.* Annu Rev Biochem, 2008. **77**: p. 229-57.

8. Loveday, C., et al., *Germline mutations in RAD51D confer susceptibility to ovarian cancer.* Nat Genet, 2011. **43**(9): p. 879-82.

9. Meindl, A., et al., *Germline mutations in breast and ovarian cancer pedigrees establish RAD51C as a human cancer susceptibility gene.* Nat Genet, 2010. **42**(5): p. 410-4.

10. Park, D.J., et al., *Rare mutations in XRCC2 increase the risk of breast cancer.* Am J Hum Genet, 2012. **90**(4): p. 734-9.

11. Rahman, N., et al., *PALB2, which encodes a BRCA2-interacting protein, is a breast cancer susceptibility gene.* Nat Genet, 2007. **39**(2): p. 165-7.

12. Szostak, J.W., et al., *The double-strand-break repair model for recombination.* Cell, 1983. **33**(1): p. 25-35.

13. Nassif, N., et al., *Efficient copying of nonhomologous sequences from ectopic sites via P-element-induced gap repair.* Mol Cell Biol, 1994. **14**(3): p. 1613-25.

14. Bakkenist, C.J. and M.B. Kastan, *DNA damage activates ATM through intermolecular autophosphorylation and dimer dissociation.* Nature, 2003. **421**(6922): p. 499-506.

15. Uziel, T., et al., *Requirement of the MRN complex for ATM activation by DNA damage.* EMBO J, 2003. **22**(20): p. 5612-21.

16. Matsuoka, S., et al., *ATM and ATR substrate analysis reveals extensive protein networks responsive to DNA damage.* Science, 2007. **316**(5828): p. 1160-6.

17. Stucki, M., et al., *MDC1 directly binds phosphorylated histone H2AX to regulate cellular responses to DNA double-strand breaks.* Cell, 2005. **123**(7): p. 1213-26.

18. Lou, Z., et al., *MDC1 maintains genomic stability by participating in the amplification of ATM-dependent DNA damage signals.* Mol Cell, 2006. **21**(2): p. 187-200.

19. Kolas, N.K., et al., *Orchestration of the DNA-damage response by the RNF8 ubiquitin ligase.* Science, 2007. **318**(5856): p. 1637-40.

20. Huen, M.S., et al., *RNF8 transduces the DNA-damage signal via histone ubiquitylation and checkpoint protein assembly.* Cell, 2007. **131**(5): p. 901-14.

21. Mailand, N., et al., *RNF8 ubiquitylates histones at DNA double-strand breaks and promotes assembly of repair proteins.* Cell, 2007. **131**(5): p. 887-900.

22. Wang, B. and S.J. Elledge, *Ubc13/Rnf8 ubiquitin ligases control foci formation of the Rap80/Abraxas/Brca1/Brcc36 complex in response to DNA damage.* Proc Natl Acad Sci U S A, 2007. **104**(52): p. 20759-63.

23. Doil, C., et al., *RNF168 binds and amplifies ubiquitin conjugates on damaged chromosomes to allow accumulation of repair proteins.* Cell, 2009. **136**(3): p. 435-46.

24. Stewart, G.S., et al., *The RIDDLE syndrome protein mediates a ubiquitin-dependent signaling cascade at sites of DNA damage.* Cell, 2009. **136**(3): p. 420-34.

25. Zhang, F., et al., *MDC1 and RNF8 function in a pathway that directs BRCA1-dependent localization of PALB2 required for homologous recombination.* J Cell Sci, 2012. **125**(Pt 24): p. 6049-57.

26. Sartori, A.A., et al., *Human CtIP promotes DNA end resection.* Nature, 2007. **450**(7169): p. 509-14.

27. Huertas, P. and S.P. Jackson, *Human CtIP mediates cell cycle control of DNA end resection and double strand break repair.* J Biol Chem, 2009. **284**(14): p. 9558-65.

28. Peterson, S.E., et al., *Activation of DSB processing requires phosphorylation of CtIP by ATR.* Mol Cell, 2013. **49**(4): p. 657-67.

29. Wang, H., et al., *The interaction of CtIP and Nbs1 connects CDK and ATM to regulate HR-mediated double-strand break repair.* PLoS Genet, 2013. **9**(2): p. e1003277.

30. Escribano-Diaz, C., et al., *A Cell Cycle-Dependent Regulatory Circuit Composed of 53BP1-RIF1 and BRCA1-CtIP Controls DNA Repair Pathway Choice.* Mol Cell, 2013.

31. Symington, L.S. and J. Gautier, *Double-strand break end resection and repair pathway choice.* Annu Rev Genet, 2011. **45**: p. 247-71.

32. Eid, W., et al., *DNA end resection by CtIP and exonuclease 1 prevents genomic instability.* EMBO Rep, 2010. **11**(12): p. 962-8.

33. Gravel, S., et al., *DNA helicases Sgs1 and BLM promote DNA double-strand break resection.* Genes Dev, 2008. **22**(20): p. 2767-72.

34. Nimonkar, A.V., et al., *BLM-DNA2-RPA-MRN and EXO1-BLM-RPA-MRN constitute two DNA end resection machineries for human DNA break repair.* Genes Dev, 2011. **25**(4): p. 350-62.

35. Raderschall, E., E.I. Golub, and T. Haaf, *Nuclear foci of mammalian recombination proteins are located at single-stranded DNA regions formed after DNA damage.* Proc Natl Acad Sci U S A, 1999. **96**(5): p. 1921-6.

36. Golub, E.I., et al., *Interaction of human rad51 recombination protein with single-stranded DNA binding protein, RPA.* Nucleic Acids Res, 1998. **26**(23): p. 5388-93.

37. Baumann, P. and S.C. West, *The human Rad51 protein: polarity of strand transfer and stimulation by hRP-A.* EMBO J, 1997. **16**(17): p. 5198-206.

38. Sugiyama, T., E.M. Zaitseva, and S.C. Kowalczykowski, *A single-stranded DNA-binding protein is needed for efficient presynaptic complex formation by the Saccharomyces cerevisiae Rad51 protein.* J Biol Chem, 1997. **272**(12): p. 7940-5.

39. Fanning, E., V. Klimovich, and A.R. Nager, *A dynamic model for replication protein A (RPA) function in DNA processing pathways.* Nucleic Acids Res, 2006. **34**(15): p. 4126-37.

40. Zou, L. and S.J. Elledge, *Sensing DNA damage through ATRIP recognition of RPA-ssDNA complexes.* Science, 2003. **300**(5625): p. 1542-8.

41. Cimprich, K.A. and D. Cortez, *ATR: an essential regulator of genome integrity.* Nat Rev Mol Cell Biol, 2008. **9**(8): p. 616-27.

42. Sorensen, C.S., et al., *The cell-cycle checkpoint kinase Chk1 is required for mammalian homologous recombination repair.* Nat Cell Biol, 2005. **7**(2): p. 195-201.

43. Sigurdsson, S., et al., *Mediator function of the human Rad51B-Rad51C complex in Rad51/RPA-catalyzed DNA strand exchange.* Genes Dev, 2001. **15**(24): p. 3308-18.

44. Eggler, A.L., R.B. Inman, and M.M. Cox, *The Rad51-dependent pairing of long DNA substrates is stabilized by replication protein A.* J Biol Chem, 2002. **277**(42): p. 39280-8.

45. Heyer, W.D., et al., *Rad54: the Swiss Army knife of homologous recombination?* Nucleic Acids Res, 2006. **34**(15): p. 4115-25.

46. McIlwraith, M.J., et al., *Human DNA polymerase eta promotes DNA synthesis from strand invasion intermediates of homologous recombination.* Mol Cell, 2005. **20**(5): p. 783-92.

47. Li, X., et al., *PCNA is required for initiation of recombination-associated DNA synthesis by DNA polymerase delta.* Mol Cell, 2009. **36**(4): p. 704-13.

48. Ip, S.C., et al., *Identification of Holliday junction resolvases from humans and yeast.* Nature, 2008. **456**(7220): p. 357-61.

49. Fekairi, S., et al., *Human SLX4 is a Holliday junction resolvase subunit that binds multiple DNA repair/recombination endonucleases.* Cell, 2009. **138**(1): p. 78-89.

50. Heyer, W.D., K.T. Ehmsen, and J. Liu, *Regulation of homologous recombination in eukaryotes.* Annu Rev Genet, 2010. **44**: p. 113-39.

51. Shinohara, A., H. Ogawa, and T. Ogawa, *Rad51 protein involved in repair and recombination in S. cerevisiae is a RecA-like protein.* Cell, 1992. **69**(3): p. 457-70.

52. Bezzubova, O., et al., *A chicken RAD51 homologue is expressed at high levels in lymphoid and reproductive organs.* Nucleic Acids Res, 1993. **21**(7): p. 1577-80.

53. Shinohara, A., et al., *Cloning of human, mouse and fission yeast recombination genes homologous to RAD51 and recA.* Nat Genet, 1993. **4**(3): p. 239-43.

54. Sandler, S.J., et al., *recA-like genes from three archaean species with putative protein products similar to Rad51 and Dmc1 proteins of the yeast Saccharomyces cerevisiae.* Nucleic Acids Res, 1996. **24**(11): p. 2125-32.

55. Thacker, J., *The RAD51 gene family, genetic instability and cancer.* Cancer Lett, 2005. **219**(2): p. 125-35.

56. Tsuzuki, T., et al., *Targeted disruption of the Rad51 gene leads to lethality in embryonic mice.* Proc Natl Acad Sci U S A, 1996. **93**(13): p. 6236-40.

57. Lim, D.S. and P. Hasty, *A mutation in mouse rad51 results in an early embryonic lethal that is suppressed by a mutation in p53.* Mol Cell Biol, 1996. **16**(12): p. 7133-43.

58. Sonoda, E., et al., *Rad51-deficient vertebrate cells accumulate chromosomal breaks prior to cell death.* EMBO J, 1998. **17**(2): p. 598-608.

59. Pellegrini, L., et al., *Insights into DNA recombination from the structure of a RAD51-BRCA2 complex.* Nature, 2002. **420**(6913): p. 287-93.

60. Aihara, H., et al., *The N-terminal domain of the human Rad51 protein binds DNA: structure and a DNA binding surface as revealed by NMR.* J Mol Biol, 1999. **290**(2): p. 495-504.

61. Matsuo, Y., et al., *Roles of the human Rad51 L1 and L2 loops in DNA binding.* FEBS J, 2006. **273**(14): p. 3148-59.

62. Benson, F.E., A. Stasiak, and S.C. West, *Purification and characterization of the human Rad51 protein, an analogue of E. coli RecA.* EMBO J, 1994. **13**(23): p. 5764-71.

63. Baumann, P., F.E. Benson, and S.C. West, *Human Rad51 protein promotes ATP-dependent homologous pairing and strand transfer reactions in vitro.* Cell, 1996. **87**(4): p. 757-66.

64. Mazin, A.V., et al., *Tailed duplex DNA is the preferred substrate for Rad51 protein-mediated homologous pairing.* EMBO J, 2000. **19**(5): p. 1148-56.

65. Gupta, R.C., et al., *Polarity of DNA strand exchange promoted by recombination proteins of the RecA family.* Proc Natl Acad Sci U S A, 1998. **95**(17): p. 9843-8.

66. Chi, P., et al., *Roles of ATP binding and ATP hydrolysis in human Rad51 recombinase function.* DNA Repair (Amst), 2006. **5**(3): p. 381-91.

67. Kim, T.M., et al., *RAD51 mutants cause replication defects and chromosomal instability.* Mol Cell Biol, 2012. **32**(18): p. 3663-80.

68. Stark, J.M., et al., *ATP hydrolysis by mammalian RAD51 has a key role during homology-directed DNA repair.* J Biol Chem, 2002. **277**(23): p. 20185-94.

69. Sung, P., et al., *Rad51 recombinase and recombination mediators.* J Biol Chem, 2003. **278**(44): p. 42729-32.

70. Chen, Z., H. Yang, and N.P. Pavletich, *Mechanism of homologous recombination from the RecA-ssDNA/dsDNA structures.* Nature, 2008. **453**(7194): p. 489-4.

71. Reymer, A., et al., *Structure of human Rad51 protein filament from molecular modeling and site-specific linear dichroism spectroscopy.* Proc Natl Acad Sci U S A, 2009. **106**(32): p. 13248-53.

72. Gupta, R.C., et al., *Rapid exchange of A:T base pairs is essential for recognition of DNA homology by human Rad51 recombination protein.* Mol Cell, 1999. **4**(5): p. 705-14.

73. Forget, A.L. and S.C. Kowalczykowski, *Single-molecule imaging of DNA pairing by RecA reveals a three-dimensional homology search.* Nature, 2012. **482**(7385): p. 423-7.

74. Haaf, T., et al., *Nuclear foci of mammalian Rad51 recombination protein in somatic cells after DNA damage and its localization in synaptonemal complexes.* Proc Natl Acad Sci U S A, 1995. **92**(6): p. 2298-302.

75. Takata, M., et al., *The Rad51 paralog Rad51B promotes homologous recombinational repair.* Mol Cell Biol, 2000. **20**(17): p. 6476-82.

76. Takata, M., et al., *Chromosome instability and defective recombinational repair in knockout mutants of the five Rad51 paralogs.* Mol Cell Biol, 2001. **21**(8): p. 2858-66.

77. O'Regan, P., et al., *XRCC2 is a nuclear RAD51-like protein required for damage-dependent RAD51 focus formation without the need for ATP binding.* J Biol Chem, 2001. **276**(25): p. 22148-53.

78. Bishop, D.K., et al., *Xrcc3 is required for assembly of Rad51 complexes in vivo.* J Biol Chem, 1998. **273**(34): p. 21482-8.

79. Yuan, S.S., et al., *BRCA2 is required for ionizing radiation-induced assembly of Rad51 complex in vivo.* Cancer Res, 1999. **59**(15): p. 3547-51.

80. Sy, S.M., M.S. Huen, and J. Chen, *PALB2 is an integral component of the BRCA complex required for homologous recombination repair.* Proc Natl Acad Sci U S A, 2009. **106**(17): p. 7155-60.

81. Feng, Z., et al., *Rad52 inactivation is synthetically lethal with BRCA2 deficiency.* Proc Natl Acad Sci U S A, 2011. **108**(2): p. 686-91.

82. Bhattacharyya, A., et al., *The breast cancer susceptibility gene BRCA1 is required for subnuclear assembly of Rad51 and survival following treatment with the DNA cross-linking agent cisplatin.* J Biol Chem, 2000. **275**(31): p. 23899-903.

83. Huang, J., et al., *RAD18 transmits DNA damage signalling to elicit homologous recombination repair.* Nat Cell Biol, 2009. **11**(5): p. 592-603.

84. Yu, Y.M., et al., *A PP1-binding motif present in BRCA1 plays a role in its DNA repair function.* Int J Biol Sci, 2008. **4**(6): p. 352-61.

85. Yue, J., et al., *The cytoskeleton protein filamin-A is required for an efficient recombinational DNA double strand break repair.* Cancer Res, 2009. **69**(20): p. 7978-85.

86. Liang, Y., et al., *BRIT1/MCPH1 is essential for mitotic and meiotic recombination DNA repair and maintaining genomic stability in mice.* PLoS Genet, 2010. **6**(1): p. e1000826.

87. Jacquemont, C. and T. Taniguchi, *Proteasome function is required for DNA damage response and fanconi anemia pathway activation.* Cancer Res, 2007. **67**(15): p. 7395-405.

88. Lu, H., et al., *The BRCA2-interacting protein BCCIP functions in RAD51 and BRCA2 focus formation and homologous recombinational repair.* Mol Cell Biol, 2005. **25**(5): p. 1949-57.

89. Brough, R., et al., *APRIN is a cell cycle specific BRCA2-interacting protein required for genome integrity and a predictor of outcome after chemotherapy in breast cancer.* EMBO J, 2012. **31**(5): p. 1160-76.

90. Hayakawa, T., et al., *MRG15 binds directly to PALB2 and stimulates homology-directed repair of chromosomal breaks.* J Cell Sci, 2010. **123**(Pt 7): p. 1124-30.

91. Tan, T.L., et al., *Mouse Rad54 affects DNA conformation and DNA-damage-induced Rad51 foci formation.* Curr Biol, 1999. **9**(6): p. 325-8.

92. Park, J., et al., *The MCM8-MCM9 complex promotes RAD51 recruitment at DNA damage sites to facilitate homologous recombination.* Mol Cell Biol, 2013. **33**(8): p. 1632-44.

93. Yuan, J. and J. Chen, *The role of the human SWI5-MEI5 complex in homologous recombination repair.* J Biol Chem, 2011. **286**(11): p. 9888-93.

94. Takizawa, Y., et al., *GEMIN2 promotes accumulation of RAD51 at double-strand breaks in homologous recombination.* Nucleic Acids Res, 2010. **38**(15): p. 5059-74.

95. Zhang, J., et al., *MDC1 interacts with Rad51 and facilitates homologous recombination.* Nat Struct Mol Biol, 2005. **12**(10): p. 902-9.

96. Jirawatnotai, S., et al., *A function for cyclin D1 in DNA repair uncovered by protein interactome analyses in human cancers.* Nature, 2011. **474**(7350): p. 230-4.

97. Takaku, M., et al., *Recombination activator function of the novel RAD51- and RAD51B-binding protein, human EVL.* J Biol Chem, 2009. **284**(21): p. 14326-36.

98. Liu, T., et al., *hSWS1.SWSAP1 is an evolutionarily conserved complex required for efficient homologous recombination repair.* J Biol Chem, 2011. **286**(48): p. 41758-66.

99. Vadnais, C., et al., *CUX1 transcription factor is required for optimal ATM/ATR-mediated responses to DNA damage.* Nucleic Acids Res, 2012. **40**(10): p. 4483-95.

100. Singh, M., et al., *Lamin A/C depletion enhances DNA damage-induced stalled replication fork arrest.* Mol Cell Biol, 2013. **33**(6): p. 1210-22.

101. Chen, J., et al., *E2F1 promotes the recruitment of DNA repair factors to sites of DNA double-strand breaks.* Cell Cycle, 2011. **10**(8): p. 1287-94.

102. Dedes, K.J., et al., *PTEN deficiency in endometrioid endometrial adenocarcinomas predicts sensitivity to PARP inhibitors.* Sci Transl Med, 2010. **2**(53): p. 53ra75.

103. Zhang, N., et al., *FoxM1 inhibition sensitizes resistant glioblastoma cells to temozolomide by downregulating the expression of DNA-repair gene Rad51.* Clin Cancer Res, 2012. **18**(21): p. 5961-71.

104. Ogiwara, H. and T. Kohno, *CBP and p300 histone acetyltransferases contribute to homologous recombination by transcriptionally activating the BRCA1 and RAD51 genes.* PLoS One, 2012. **7**(12): p. e52810.

105. Tian, L., et al., *Essential roles of Jab1 in cell survival, spontaneous DNA damage and DNA repair.* Oncogene, 2010. **29**(46): p. 6125-37.

106. Boichuk, S., et al., *Functional connection between Rad51 and PML in homology-directed repair.* PLoS One, 2011. **6**(10): p. e25814.

107. Dungey, F.A., K.W. Caldecott, and A.J. Chalmers, *Enhanced radiosensitization of human glioma cells by combining inhibition of poly(ADP-ribose) polymerase with inhibition of heat shock protein 90.* Mol Cancer Ther, 2009. **8**(8): p. 2243-54.

108. Kanamoto, T., et al., *Functional proteomics of transforming growth factor-beta1-stimulated Mv1Lu epithelial cells: Rad51 as a target of TGFbeta1-dependent regulation of DNA repair.* EMBO J, 2002. **21**(5): p. 1219-30.

109. Bornstein, S., et al., *Smad4 loss in mice causes spontaneous head and neck cancer with increased genomic instability and inflammation.* J Clin Invest, 2009. **119**(11): p. 3408-19.

110. Adamson, B., et al., *A genome-wide homologous recombination screen identifies the RNA-binding protein RBMX as a component of the DNA-damage response.* Nat Cell Biol, 2012. **14**(3): p. 318-28.

111. Tomimatsu, N., et al., *Exo1 plays a major role in DNA end resection in humans and influences double-strand break repair and damage signaling decisions.* DNA Repair (Amst), 2012. **11**(4): p. 441-8.

112. Peng, G., et al., *Human nuclease/helicase DNA2 alleviates replication stress by promoting DNA end resection.* Cancer Res, 2012. **72**(11): p. 2802-13.

113. Yuan, S.S., H.L. Chang, and E.Y. Lee, *Ionizing radiation-induced Rad51 nuclear focus formation is cell cycle-regulated and defective in both ATM(-/-) and c-Abl(-/-) cells.* Mutat Res, 2003. **525**(1-2): p. 85-92.

114. Kocher, S., et al., *Radiation-induced double-strand breaks require ATM but not Artemis for homologous recombination during S-phase.* Nucleic Acids Res, 2012. **40**(17): p. 8336-47.

115. Yata, K., et al., *Plk1 and CK2 act in concert to regulate Rad51 during DNA double strand break repair.* Mol Cell, 2012. **45**(3): p. 371-83.

116. Johnson, N., et al., *Compromised CDK1 activity sensitizes BRCA-proficient cancers to PARP inhibition.* Nat Med, 2011. **17**(7): p. 875-82.

117. Deans, A.J., et al., *Cyclin-dependent kinase 2 functions in normal DNA repair and is a therapeutic target in BRCA1-deficient cancers.* Cancer Res, 2006. **66**(16): p. 8219-26.

118. Nakada, S., R.M. Yonamine, and K. Matsuo, *RNF8 regulates assembly of RAD51 at DNA double-strand breaks in the absence of BRCA1 and 53BP1.* Cancer Res, 2012. **72**(19): p. 4974-83.

119. Chernikova, S.B., et al., *Deficiency in Bre1 impairs homologous recombination repair and cell cycle checkpoint response to radiation damage in mammalian cells.* Radiat Res, 2010. **174**(5): p. 558-65.

120. Nakamura, K., et al., *Regulation of homologous recombination by RNF20-dependent H2B ubiquitination.* Mol Cell, 2011. **41**(5): p. 515-28.

121. Meerang, M., et al., *The ubiquitin-selective segregase VCP/p97 orchestrates the response to DNA double-strand breaks.* Nat Cell Biol, 2011. **13**(11): p. 1376-82.

122. Zhao, G.Y., et al., *A critical role for the ubiquitin-conjugating enzyme Ubc13 in initiating homologous recombination.* Mol Cell, 2007. **25**(5): p. 663-75.

123. Schoenfeld, A.R., et al., *BRCA2 is ubiquitinated in vivo and interacts with USP11, a deubiquitinating enzyme that exhibits prosurvival function in the cellular response to DNA damage.* Mol Cell Biol, 2004. **24**(17): p. 7444-55.

124. Wiltshire, T.D., et al., *Sensitivity to poly(ADP-ribose) polymerase (PARP) inhibition identifies ubiquitin-specific peptidase 11 (USP11) as a regulator of DNA double-strand break repair.* J Biol Chem, 2010. **285**(19): p. 14565-71.

125. Galanty, Y., et al., *RNF4, a SUMO-targeted ubiquitin E3 ligase, promotes DNA double-strand break repair.* Genes Dev, 2012. **26**(11): p. 1179-95.

126. Butler, L.R., et al., *The proteasomal de-ubiquitinating enzyme POH1 promotes the double-strand DNA break response.* EMBO J, 2012. **31**(19): p. 3918-34.

127. Lee, D.H., et al., *A PP4 phosphatase complex dephosphorylates RPA2 to facilitate DNA repair via homologous recombination.* Nat Struct Mol Biol, 2010. **17**(3): p. 365-72.

128. Duro, E., et al., *Identification of the MMS22L-TONSL complex that promotes homologous recombination.* Mol Cell, 2010. **40**(4): p. 632-44.

129. O'Connell, B.C., et al., *A genome-wide camptothecin sensitivity screen identifies a mammalian MMS22L-NFKBIL2 complex required for genomic stability.* Mol Cell, 2010. **40**(4): p. 645-57.

130. Sleeth, K.M., et al., *RPA mediates recombination repair during replication stress and is displaced from DNA by checkpoint signalling in human cells.* J Mol Biol, 2007. **373**(1): p. 38-47.

131. Liu, S., et al., *RING finger and WD repeat domain 3 (RFWD3) associates with replication protein A (RPA) and facilitates RPA-mediated DNA damage response.* J Biol Chem, 2011. **286**(25): p. 22314-22.

132. Collis, S.J., et al., *HCLK2 is essential for the mammalian S-phase checkpoint and impacts on Chk1 stability.* Nat Cell Biol, 2007. **9**(4): p. 391-401.

133. Skaar, J.R., et al., *INTS3 controls the hSSB1-mediated DNA damage response.* J Cell Biol, 2009. **187**(1): p. 25-32.

134. Gohler, T., et al., *PTIP/Swift is required for efficient PCNA ubiquitination in response to DNA damage.* DNA Repair (Amst), 2008. **7**(5): p. 775-87.

135. Courilleau, C., et al., *The chromatin remodeler p400 ATPase facilitates Rad51-mediated repair of DNA double-strand breaks.* J Cell Biol, 2012. **199**(7): p. 1067-81.

136. Wu, G., et al., *A novel role of the chromokinesin Kif4A in DNA damage response.* Cell Cycle, 2008. **7**(13): p. 2013-20.

137. Gospodinov, A., I. Tsaneva, and B. Anachkova, *RAD51 foci formation in response to DNA damage is modulated by TIP49.* Int J Biochem Cell Biol, 2009. **41**(4): p. 925-33.

138. Murr, R., et al., *Histone acetylation by Trrap-Tip60 modulates loading of repair proteins and repair of DNA double-strand breaks.* Nat Cell Biol, 2006. **8**(1): p. 91-9.

139. Baldeyron, C., et al., *HP1alpha recruitment to DNA damage by p150CAF-1 promotes homologous recombination repair.* J Cell Biol, 2011. **193**(1): p. 81-95.

140. Jensen, R.B., A. Carreira, and S.C. Kowalczykowski, *Purified human BRCA2 stimulates RAD51-mediated recombination.* Nature, 2010. **467**(7316): p. 678-83.

141. Carreira, A., et al., *The BRC repeats of BRCA2 modulate the DNA-binding selectivity of RAD51.* Cell, 2009. **136**(6): p. 1032-43.

142. Yang, H., et al., *BRCA2 function in DNA binding and recombination from a BRCA2-DSS1-ssDNA structure.* Science, 2002. **297**(5588): p. 1837-48.

143. Dray, E., et al., *Enhancement of RAD51 recombinase activity by the tumor suppressor PALB2.* Nat Struct Mol Biol, 2010. **17**(10): p. 1255-9.

144. Benson, F.E., P. Baumann, and S.C. West, *Synergistic actions of Rad51 and Rad52 in recombination and DNA repair.* Nature, 1998. **391**(6665): p. 401-4.

145. Rijkers, T., et al., *Targeted inactivation of mouse RAD52 reduces homologous recombination but not resistance to ionizing radiation.* Mol Cell Biol, 1998. **18**(11): p. 6423-9.

146. Fujimori, A., et al., *Rad52 partially substitutes for the Rad51 paralog XRCC3 in maintaining chromosomal integrity in vertebrate cells.* EMBO J, 2001. **20**(19): p. 5513-20.

147. Lok, B.H., et al., *RAD52 inactivation is synthetically lethal with deficiencies in BRCA1 and PALB2 in addition to BRCA2 through RAD51-mediated homologous recombination.* Oncogene, 2012.

148. Chen, F., et al., *Cell cycle-dependent protein expression of mammalian homologs of yeast DNA double-strand break repair genes Rad51 and Rad52.* Mutat Res, 1997. **384**(3): p. 205-11.

149. Hasselbach, L., et al., *Characterisation of the promoter region of the human DNA-repair gene Rad51.* Eur J Gynaecol Oncol, 2005. **26**(6): p. 589-98.

150. Arias-Lopez, C., et al., *p53 modulates homologous recombination by transcriptional regulation of the RAD51 gene.* EMBO Rep, 2006. **7**(2): p. 219-24.

151. Bindra, R.S. and P.M. Glazer, *Repression of RAD51 gene expression by E2F4/p130 complexes in hypoxia.* Oncogene, 2007. **26**(14): p. 2048-57.

152. Huang, Y., et al., *Role for caspase-mediated cleavage of Rad51 in induction of apoptosis by DNA damage.* Mol Cell Biol, 1999. **19**(4): p. 2986-97.

153. Jackson, S.P. and J. Bartek, *The DNA-damage response in human biology and disease.* Nature, 2009. **461**(7267): p. 1071-8.

154. Bertrand, P., et al., *Overexpression of mammalian Rad51 does not stimulate tumorigenesis while a dominant-negative Rad51 affects centrosome fragmentation, ploidy and stimulates tumorigenesis, in p53-defective CHO cells.* Oncogene, 2003. **22**(48): p. 7587-92.

155. Munshi, N.C., et al., *Identification of genes modulated in multiple myeloma using genetically identical twin samples.* Blood, 2004. **103**(5): p. 1799-806.

156. Yoshikawa, K., et al., *Abnormal expression of BRCA1 and BRCA1-interactive DNA-repair proteins in breast carcinomas.* Int J Cancer, 2000. **88**(1): p. 28-36.

157. Kato, M., et al., *Identification of Rad51 alteration in patients with bilateral breast cancer.* J Hum Genet, 2000. **45**(3): p. 133-7.

158. Ishida, T., et al., *Altered DNA binding by the human Rad51-R150Q mutant found in breast cancer patients.* Biol Pharm Bull, 2007. **30**(8): p. 1374-8.

159. Le Calvez-Kelm, F., et al., *RAD51 and breast cancer susceptibility: no evidence for rare variant association in the Breast Cancer Family Registry study.* PLoS One, 2012. **7**(12): p. e52374.

160. Antoniou, A.C., et al., *RAD51 135G-->C modifies breast cancer risk among BRCA2 mutation carriers: results from a combined analysis of 19 studies.* Am J Hum Genet, 2007. **81**(6): p. 1186-200.

161. Depienne, C., et al., *RAD51 haploinsufficiency causes congenital mirror movements in humans.* Am J Hum Genet, 2012. **90**(2): p. 301-7.

162. Srour, M., et al., *Mutations in DCC cause congenital mirror movements.* Science, 2010. **328**(5978): p. 592.

163. Liu, Q., et al., *The spinal muscular atrophy disease gene product, SMN, and its associated protein SIP1 are in a complex with spliceosomal snRNP proteins.* Cell, 1997. **90**(6): p. 1013-21.

164. Albala, J.S., et al., *Identification of a novel human RAD51 homolog, RAD51B.* Genomics, 1997. **46**(3): p. 476-9.

165. Cartwright, R., et al., *The XRCC2 DNA repair gene from human and mouse encodes a novel member of the recA/RAD51 family.* Nucleic Acids Res, 1998. **26**(13): p. 3084-9.

166. Dosanjh, M.K., et al., *Isolation and characterization of RAD51C, a new human member of the RAD51 family of related genes.* Nucleic Acids Res, 1998. **26**(5): p. 1179-84.

167. Pittman, D.L., L.R. Weinberg, and J.C. Schimenti, *Identification, characterization, and genetic mapping of Rad51d, a new mouse and human RAD51/RecA-related gene.* Genomics, 1998. **49**(1): p. 103-11.

168. Liu, N., et al., *XRCC2 and XRCC3, new human Rad51-family members, promote chromosome stability and protect against DNA cross-links and other damages.* Mol Cell, 1998. **1**(6): p. 783-93.

169. Miller, K.A., et al., *Domain mapping of the Rad51 paralog protein complexes.* Nucleic Acids Res, 2004. **32**(1): p. 169-78.

170. Suwaki, N., K. Klare, and M. Tarsounas, *RAD51 paralogs: roles in DNA damage signalling, recombinational repair and tumorigenesis.* Semin Cell Dev Biol, 2011. **22**(8): p. 898-905.

171. Braybrooke, J.P., et al., *The RAD51 family member, RAD51L3, is a DNA-stimulated ATPase that forms a complex with XRCC2.* J Biol Chem, 2000. **275**(37): p. 29100-6.

172. Kurumizaka, H., et al., *Homologous-pairing activity of the human DNA-repair proteins Xrcc3.Rad51C.* Proc Natl Acad Sci U S A, 2001. **98**(10): p. 5538-43.

173. Kurumizaka, H., et al., *Homologous pairing and ring and filament structure formation activities of the human Xrcc2*Rad51D complex.* J Biol Chem, 2002. **277**(16): p. 14315-20.

174. Lio, Y.C., et al., *Complex formation by the human Rad51B and Rad51C DNA repair proteins and their activities in vitro.* J Biol Chem, 2003. **278**(4): p. 2469-78.

175. Masson, J.Y., et al., *Complex formation by the human RAD51C and XRCC3 recombination repair proteins.* Proc Natl Acad Sci U S A, 2001. **98**(15): p. 8440-6.

176. Masson, J.Y., et al., *Identification and purification of two distinct complexes containing the five RAD51 paralogs.* Genes Dev, 2001. **15**(24): p. 3296-307.

177. Pittman, D.L. and J.C. Schimenti, *Midgestation lethality in mice deficient for the RecA-related gene, Rad51d/Rad51l3.* Genesis, 2000. **26**(3): p. 167-73.

178. Shu, Z., et al., *Disruption of muREC2/RAD51L1 in mice results in early embryonic lethality which can Be partially rescued in a p53(-/-) background.* Mol Cell Biol, 1999. **19**(12): p. 8686-93.

179. Kuznetsov, S.G., et al., *Loss of Rad51c leads to embryonic lethality and modulation of Trp53-dependent tumorigenesis in mice.* Cancer Res, 2009. **69**(3): p. 863-72.

180. Deans, B., et al., *Xrcc2 is required for genetic stability, embryonic neurogenesis and viability in mice.* EMBO J, 2000. **19**(24): p. 6675-85.

181. Adam, J., B. Deans, and J. Thacker, *A role for Xrcc2 in the early stages of mouse development.* DNA Repair (Amst), 2007. **6**(2): p. 224-34.

182. Smiraldo, P.G., et al., *Extensive chromosomal instability in Rad51d-deficient mouse cells.* Cancer Res, 2005. **65**(6): p. 2089-96.

183. Chun, J., E.S. Buechelmaier, and S.N. Powell, *Rad51 paralog complexes BCDX2 and CX3 act at different stages in the BRCA1-BRCA2-dependent homologous recombination pathway.* Mol Cell Biol, 2013. **33**(2): p. 387-95.

184. Yonetani, Y., et al., *Differential and collaborative actions of Rad51 paralog proteins in cellular response to DNA damage.* Nucleic Acids Res, 2005. **33**(14): p. 4544-52.

185. Gildemeister, O.S., J.M. Sage, and K.L. Knight, *Cellular redistribution of Rad51 in response to DNA damage: novel role for Rad51C.* J Biol Chem, 2009. **284**(46): p. 31945-52.

186. Badie, S., et al., *RAD51C facilitates checkpoint signaling by promoting CHK2 phosphorylation.* J Cell Biol, 2009. **185**(4): p. 587-600.

187. Forget, A.L., B.T. Bennett, and K.L. Knight, *Xrcc3 is recruited to DNA double strand breaks early and independent of Rad51.* J Cell Biochem, 2004. **93**(3): p. 429-36.

188. Rodrigue, A., et al., *Interplay between human DNA repair proteins at a unique double-strand break in vivo.* EMBO J, 2006. **25**(1): p. 222-31.

189. Yokoyama, H., et al., *Preferential binding to branched DNA strands and strand-annealing activity of the human Rad51B, Rad51C, Rad51D and Xrcc2 protein complex.* Nucleic Acids Res, 2004. **32**(8): p. 2556-65.

190. Compton, S.A., S. Ozgur, and J.D. Griffith, *Ring-shaped Rad51 paralog protein complexes bind Holliday junctions and replication forks as visualized by electron microscopy.* J Biol Chem, 2010. **285**(18): p. 13349-56.

191. Braybrooke, J.P., et al., *Functional interaction between the Bloom's syndrome helicase and the RAD51 paralog, RAD51L3 (RAD51D).* J Biol Chem, 2003. **278**(48): p. 48357-66.

192. Liu, Y., et al., *RAD51C is required for Holliday junction processing in mammalian cells.* Science, 2004. **303**(5655): p. 243-6.

193. Rodrigue, A., et al., *The RAD51 paralogs ensure cellular protection against mitotic defects and aneuploidy.* J Cell Sci, 2013. **126**(Pt 1): p. 348-59.

194. Bartel, D.P., *MicroRNAs: genomics, biogenesis, mechanism, and function.* Cell, 2004. **116**(2): p. 281-97.

195. Winter, J., et al., *Many roads to maturity: microRNA biogenesis pathways and their regulation.* Nat Cell Biol, 2009. **11**(3): p. 228-34.

196. Lee, R.C., R.L. Feinbaum, and V. Ambros, *The C. elegans heterochronic gene lin-4 encodes small RNAs with antisense complementarity to lin-14.* Cell, 1993. **75**(5): p. 843-54.

197. Wightman, B., I. Ha, and G. Ruvkun, *Posttranscriptional regulation of the heterochronic gene lin-14 by lin-4 mediates temporal pattern formation in C. elegans.* Cell, 1993. **75**(5): p. 855-62.

198. Pasquinelli, A.E., et al., *Conservation of the sequence and temporal expression of let-7 heterochronic regulatory RNA.* Nature, 2000. **408**(6808): p. 86-9.

199. Reinhart, B.J., et al., *The 21-nucleotide let-7 RNA regulates developmental timing in Caenorhabditis elegans.* Nature, 2000. **403**(6772): p. 901-6.

200. Griffiths-Jones, S., et al., *miRBase: tools for microRNA genomics.* Nucleic Acids Res, 2008. **36**(Database issue): p. D154-8.

201. Friedman, R.C., et al., *Most mammalian mRNAs are conserved targets of microRNAs.* Genome Res, 2009. **19**(1): p. 92-105.

202. Croce, C.M., *Causes and consequences of microRNA dysregulation in cancer.* Nat Rev Genet, 2009. **10**(10): p. 704-14.

203. Lund, E., et al., *Nuclear export of microRNA precursors.* Science, 2004. **303**(5654): p. 95-8.

204. Chendrimada, T.P., et al., *TRBP recruits the Dicer complex to Ago2 for microRNA processing and gene silencing.* Nature, 2005. **436**(7051): p. 740-4.

205. Mourelatos, Z., et al., *miRNPs: a novel class of ribonucleoproteins containing numerous microRNAs.* Genes Dev, 2002. **16**(6): p. 720-8.

206. Berezikov, E., et al., *Mammalian mirtron genes.* Mol Cell, 2007. **28**(2): p. 328-36.

207. Ladewig, E., et al., *Discovery of hundreds of mirtrons in mouse and human small RNA data.* Genome Res, 2012. **22**(9): p. 1634-45.

208. Cifuentes, D., et al., *A novel miRNA processing pathway independent of Dicer requires Argonaute2 catalytic activity.* Science, 2010. **328**(5986): p. 1694-8.

209. Cheloufi, S., et al., *A dicer-independent miRNA biogenesis pathway that requires Ago catalysis.* Nature, 2010. **465**(7298): p. 584-9.

210. Bartel, D.P., *MicroRNAs: target recognition and regulatory functions.* Cell, 2009. **136**(2): p. 215-33.

211. Baek, D., et al., *The impact of microRNAs on protein output.* Nature, 2008. **455**(7209): p. 64-71.

212. Selbach, M., et al., *Widespread changes in protein synthesis induced by microRNAs.* Nature, 2008. **455**(7209): p. 58-63.

213. Lim, L.P., et al., *Microarray analysis shows that some microRNAs downregulate large numbers of target mRNAs.* Nature, 2005. **433**(7027): p. 769-73.

214. Doench, J.G. and P.A. Sharp, *Specificity of microRNA target selection in translational repression.* Genes Dev, 2004. **18**(5): p. 504-11.

215. Behm-Ansmant, I., et al., *mRNA degradation by miRNAs and GW182 requires both CCR4:NOT deadenylase and DCP1:DCP2 decapping complexes.* Genes Dev, 2006. **20**(14): p. 1885-98.

216. Liu, J., et al., *A role for the P-body component GW182 in microRNA function.* Nat Cell Biol, 2005. **7**(12): p. 1261-6.

217. Eulalio, A., et al., *A C-terminal silencing domain in GW182 is essential for miRNA function.* RNA, 2009. **15**(6): p. 1067-77.

218. Eulalio, A., E. Huntzinger, and E. Izaurralde, *GW182 interaction with Argonaute is essential for miRNA-mediated translational repression and mRNA decay.* Nat Struct Mol Biol, 2008. **15**(4): p. 346-53.

219. Lazzaretti, D., I. Tournier, and E. Izaurralde, *The C-terminal domains of human TNRC6A, TNRC6B, and TNRC6C silence bound transcripts independently of Argonaute proteins.* RNA, 2009. **15**(6): p. 1059-66.

220. Braun, J.E., et al., *GW182 proteins directly recruit cytoplasmic deadenylase complexes to miRNA targets.* Mol Cell, 2011. **44**(1): p. 120-33.

221. Chekulaeva, M., et al., *miRNA repression involves GW182-mediated recruitment of CCR4-NOT through conserved W-containing motifs.* Nat Struct Mol Biol, 2011. **18**(11): p. 1218-26.

222. Chen, C.Y., et al., *Ago-TNRC6 triggers microRNA-mediated decay by promoting two deadenylation steps.* Nat Struct Mol Biol, 2009. **16**(11): p. 1160-6.

223. Fabian, M.R., et al., *miRNA-mediated deadenylation is orchestrated by GW182 through two conserved motifs that interact with CCR4-NOT.* Nat Struct Mol Biol, 2011. **18**(11): p. 1211-7.

224. Fabian, M.R., et al., *Mammalian miRNA RISC recruits CAF1 and PABP to affect PABP-dependent deadenylation.* Mol Cell, 2009. **35**(6): p. 868-80.

225. Yamashita, A., et al., *Concerted action of poly(A) nucleases and decapping enzyme in mammalian mRNA turnover.* Nat Struct Mol Biol, 2005. **12**(12): p. 1054-63.

226. Cooke, A., A. Prigge, and M. Wickens, *Translational repression by deadenylases.* J Biol Chem, 2010. **285**(37): p. 28506-13.

227. Meijer, H.A., et al., *Translational repression and eIF4A2 activity are critical for microRNA-mediated gene regulation.* Science, 2013. **340**(6128): p. 82-5.

228. Kiriakidou, M., et al., *An mRNA m7G cap binding-like motif within human Ago2 represses translation.* Cell, 2007. **129**(6): p. 1141-51.

229. Chendrimada, T.P., et al., *MicroRNA silencing through RISC recruitment of eIF6.* Nature, 2007. **447**(7146): p. 823-8.

230. Zekri, L., D. Kuzuoglu-Ozturk, and E. Izaurralde, *GW182 proteins cause PABP dissociation from silenced miRNA targets in the absence of deadenylation.* EMBO J, 2013. **32**(7): p. 1052-65.

231. Liu, J., et al., *Argonaute2 is the catalytic engine of mammalian RNAi.* Science, 2004. **305**(5689): p. 1437-41.

232. Yekta, S., I.H. Shih, and D.P. Bartel, *MicroRNA-directed cleavage of HOXB8 mRNA.* Science, 2004. **304**(5670): p. 594-6.

233. Davis, E., et al., *RNAi-mediated allelic trans-interaction at the imprinted Rtl1/Peg11 locus.* Curr Biol, 2005. **15**(8): p. 743-9.

234. John, B., et al., *Human MicroRNA targets.* PLoS Biol, 2004. **2**(11): p. e363.

235. Lall, S., et al., *A genome-wide map of conserved microRNA targets in C. elegans.* Curr Biol, 2006. **16**(5): p. 460-71.

236. Lewis, B.P., C.B. Burge, and D.P. Bartel, *Conserved seed pairing, often flanked by adenosines, indicates that thousands of human genes are microRNA targets.* Cell, 2005. **120**(1): p. 15-20.

237. Grimson, A., et al., *MicroRNA targeting specificity in mammals: determinants beyond seed pairing.* Mol Cell, 2007. **27**(1): p. 91-105.

238. Brodersen, P. and O. Voinnet, *Revisiting the principles of microRNA target recognition and mode of action.* Nat Rev Mol Cell Biol, 2009. **10**(2): p. 141-8.

239. Shin, C., et al., *Expanding the microRNA targeting code: functional sites with centered pairing.* Mol Cell, 2010. **38**(6): p. 789-802.

240. Chi, S.W., G.J. Hannon, and R.B. Darnell, *An alternative mode of microRNA target recognition.* Nat Struct Mol Biol, 2012. **19**(3): p. 321-7.

241. Helwak, A., et al., *Mapping the Human miRNA Interactome by CLASH Reveals Frequent Noncanonical Binding.* Cell, 2013. **153**(3): p. 654-65.

242. Nagaraj, N., et al., *Deep proteome and transcriptome mapping of a human cancer cell line.* Mol Syst Biol, 2011. **7**: p. 548.

243. Bazzini, A.A., M.T. Lee, and A.J. Giraldez, *Ribosome profiling shows that miR-430 reduces translation before causing mRNA decay in zebrafish.* Science, 2012. **336**(6078): p. 233-7.

244. Bethune, J., C.G. Artus-Revel, and W. Filipowicz, *Kinetic analysis reveals successive steps leading to miRNA-mediated silencing in mammalian cells.* EMBO Rep, 2012. **13**(8): p. 716-23.

245. Djuranovic, S., A. Nahvi, and R. Green, *miRNA-mediated gene silencing by translational repression followed by mRNA deadenylation and decay.* Science, 2012. **336**(6078): p. 237-40.

246. Guo, H., et al., *Mammalian microRNAs predominantly act to decrease target mRNA levels.* Nature, 2010. **466**(7308): p. 835-40.

247. Chi, S.W., et al., *Argonaute HITS-CLIP decodes microRNA-mRNA interaction maps.* Nature, 2009. **460**(7254): p. 479-86.

248. Hafner, M., et al., *Transcriptome-wide identification of RNA-binding protein and microRNA target sites by PAR-CLIP.* Cell, 2010. **141**(1): p. 129-41.

249. Lal, A., et al., *miR-24 Inhibits cell proliferation by targeting E2F2, MYC, and other cell-cycle genes via binding to "seedless" 3'UTR microRNA recognition elements.* Mol Cell, 2009. **35**(5): p. 610-25.

250. Rissland, O.S., S.J. Hong, and D.P. Bartel, *MicroRNA destabilization enables dynamic regulation of the miR-16 family in response to cell-cycle changes.* Mol Cell, 2011. **43**(6): p. 993-1004.

251. Seitz, H., *Redefining microRNA targets.* Curr Biol, 2009. **19**(10): p. 870-3.

252. Chowdhury, D., Y.E. Choi, and M.E. Brault, *Charity begins at home: non-coding RNA functions in DNA repair.* Nat Rev Mol Cell Biol, 2013. **14**(3): p. 181-9.

253. Wang, Y. and T. Taniguchi, *MicroRNAs and DNA damage response: Implications for cancer therapy.* Cell Cycle, 2013. **12**(1): p. 32-42.

254. Hu, H., et al., *ATM is down-regulated by N-Myc-regulated microRNA-421.* Proc Natl Acad Sci U S A, 2010. **107**(4): p. 1506-11.

255. Lal, A., et al., *miR-24-mediated downregulation of H2AX suppresses DNA repair in terminally differentiated blood cells.* Nat Struct Mol Biol, 2009. **16**(5): p. 492-8.

256. Garcia, A.I., et al., *Down-regulation of BRCA1 expression by miR-146a and miR-146b-5p in triple negative sporadic breast cancers.* EMBO Mol Med, 2011. **3**(5): p. 279-90.

257. Song, L., et al., *Up-regulation of miR-1245 by c-myc targets BRCA2 and impairs DNA repair.* J Mol Cell Biol, 2012. **4**(2): p. 108-17.

258. Crosby, M.E., et al., *MicroRNA regulation of DNA repair gene expression in hypoxic stress.* Cancer Res, 2009. **69**(3): p. 1221-9.

259. Wang, Y., et al., *MiR-96 downregulates REV1 and RAD51 to promote cellular sensitivity to cisplatin and PARP inhibition.* Cancer Res, 2012. **72**(16): p. 4037-46.

260. Moskwa, P., et al., *miR-182-mediated downregulation of BRCA1 impacts DNA repair and sensitivity to PARP inhibitors.* Mol Cell, 2011. **41**(2): p. 210-20.

261. Kawai, S. and A. Amano, *BRCA1 regulates microRNA biogenesis via the DROSHA microprocessor complex.* J Cell Biol, 2012. **197**(2): p. 201-8.

262. Zhang, X., et al., *The ATM kinase induces microRNA biogenesis in the DNA damage response.* Mol Cell, 2011. **41**(4): p. 371-83.

263. Trabucchi, M., et al., *The RNA-binding protein KSRP promotes the biogenesis of a subset of microRNAs.* Nature, 2009. **459**(7249): p. 1010-4.

264. Francia, S., et al., *Site-specific DICER and DROSHA RNA products control the DNA-damage response.* Nature, 2012. **488**(7410): p. 231-5.

265. Wei, W., et al., *A role for small RNAs in DNA double-strand break repair.* Cell, 2012. **149**(1): p. 101-12.

266. Farmer, H., et al., *Targeting the DNA repair defect in BRCA mutant cells as a therapeutic strategy.* Nature, 2005. **434**(7035): p. 917-21.

267. Farazi, T.A., et al., *miRNAs in human cancer.* J Pathol, 2011. **223**(2): p. 102-15.

268. Wang, Y., et al., *MicroRNA-138 modulates DNA damage response by repressing histone H2AX expression.* Mol Cancer Res, 2011. **9**(8): p. 1100-11.

269. Boren, T., et al., *MicroRNAs and their target messenger RNAs associated with endometrial carcinogenesis.* Gynecol Oncol, 2008. **110**(2): p. 206-15.

270. Chen, H.Y., et al., *miR-103/107 promote metastasis of colorectal cancer by targeting the metastasis suppressors DAPK and KLF4.* Cancer Res, 2012. **72**(14): p. 3631-41.

271. Guo, Y., et al., *Distinctive microRNA profiles relating to patient survival in esophageal squamous cell carcinoma.* Cancer Res, 2008. **68**(1): p. 26-33.

272. Lee, K.H., et al., *Epigenetic silencing of MicroRNA miR-107 regulates cyclin-dependent kinase 6 expression in pancreatic cancer.* Pancreatology, 2009. **9**(3): p. 293-301.

273. Roldo, C., et al., *MicroRNA expression abnormalities in pancreatic endocrine and acinar tumors are associated with distinctive pathologic features and clinical behavior.* J Clin Oncol, 2006. **24**(29): p. 4677-84.

274. Takahashi, Y., et al., *MiR-107 and MiR-185 can induce cell cycle arrest in human non small cell lung cancer cell lines.* PLoS One, 2009. **4**(8): p. e6677.

275. Martello, G., et al., *A MicroRNA targeting dicer for metastasis control.* Cell, 2010. **141**(7): p. 1195-207.

276. Bohlig, L., M. Friedrich, and K. Engeland, *p53 activates the PANK1/miRNA-107 gene leading to downregulation of CDK6 and p130 cell cycle proteins.* Nucleic Acids Res, 2011. **39**(2): p. 440-53.

277. Chang, T.C., et al., *Transactivation of miR-34a by p53 broadly influences gene expression and promotes apoptosis.* Mol Cell, 2007. **26**(5): p. 745-52.

278. Suzuki, H.I., et al., *Modulation of microRNA processing by p53.* Nature, 2009. **460**(7254): p. 529-33.

279. Yamakuchi, M., et al., *P53-induced microRNA-107 inhibits HIF-1 and tumor angiogenesis.* Proc Natl Acad Sci U S A, 2010. **107**(14): p. 6334-9.

280. Sakai, W., et al., *Functional restoration of BRCA2 protein by secondary BRCA2 mutations in BRCA2-mutated ovarian carcinoma.* Cancer Res, 2009. **69**(16): p. 6381-6.

281. Weinstock, D.M., et al., *Assaying double-strand break repair pathway choice in mammalian cells using a targeted endonuclease or the RAG recombinase.* Methods Enzymol, 2006. **409**: p. 524-40.

282. Pierce, A.J., et al., *XRCC3 promotes homology-directed repair of DNA damage in mammalian cells.* Genes Dev, 1999. **13**(20): p. 2633-8.

283. Evers, B., T. Helleday, and J. Jonkers, *Targeting homologous recombination repair defects in cancer.* Trends Pharmacol Sci, 2010. **31**(8): p. 372-80.

284. Garofalo, M., et al., *miR-221&222 regulate TRAIL resistance and enhance tumorigenicity through PTEN and TIMP3 downregulation.* Cancer Cell, 2009. **16**(6): p. 498-509.

285. Chun-Zhi, Z., et al., *MicroRNA-221 and microRNA-222 regulate gastric carcinoma cell proliferation and radioresistance by targeting PTEN.* BMC Cancer, 2010. **10**: p. 367.

286. Zhao, G., et al., *MicroRNA-221 induces cell survival and cisplatin resistance through PI3K/Akt pathway in human osteosarcoma.* PLoS One, 2013. **8**(1): p. e53906.

287. Forbes, S.A., et al., *COSMIC: mining complete cancer genomes in the Catalogue of Somatic Mutations in Cancer.* Nucleic Acids Res, 2011. **39**(Database issue): p. D945-50.

288. Annibali, D., et al., *A new module in neural differentiation control: two microRNAs upregulated by retinoic acid, miR-9 and -103, target the differentiation inhibitor ID2.* PLoS One, 2012. **7**(7): p. e40269.

289. Garzon, R., et al., *MicroRNA gene expression during retinoic acid-induced differentiation of human acute promyelocytic leukemia.* Oncogene, 2007. **26**(28): p. 4148-57.

290. Liao, Y. and B. Lonnerdal, *Global microRNA characterization reveals that miR-103 is involved in IGF-1 stimulated mouse intestinal cell proliferation.* PLoS One, 2010. **5**(9): p. e12976.

291. Richardson, C., *RAD51, genomic stability, and tumorigenesis.* Cancer Lett, 2005. **218**(2): p. 127-39.

292. Hine, C.M., A. Seluanov, and V. Gorbunova, *Use of the Rad51 promoter for targeted anti-cancer therapy.* Proc Natl Acad Sci U S A, 2008. **105**(52): p. 20810-5.

293. Rajagopalan, S., et al., *Mapping the physical and functional interactions between the tumor suppressors p53 and BRCA2.* Proc Natl Acad Sci U S A, 2010. **107**(19): p. 8587-92.

294. Romanova, L.Y., et al., *The interaction of p53 with replication protein A mediates suppression of homologous recombination.* Oncogene, 2004. **23**(56): p. 9025-33.

295. Sturzbecher, H.W., et al., *p53 is linked directly to homologous recombination processes via RAD51/RecA protein interaction.* EMBO J, 1996. **15**(8): p. 1992-2002.

296. Shu, J., et al., *Genomewide microRNA down-regulation as a negative feedback mechanism in the early phases of liver regeneration.* Hepatology, 2011. **54**(2): p. 609-19.

297. Bu, Y., et al., *Knockdown of Dicer in MCF-7 human breast carcinoma cells results in G1 arrest and increased sensitivity to cisplatin.* Oncol Rep, 2009. **21**(1): p. 13-7.

298. Pouliot, L.M., et al., *Contributions of microRNA dysregulation to cisplatin resistance in adenocarcinoma cells.* Exp Cell Res, 2013. **319**(4): p. 566-74.

299. Nagalla, S., et al., *Platelet microRNA-mRNA coexpression profiles correlate with platelet reactivity.* Blood, 2011. **117**(19): p. 5189-97.

300. Igarashi, T., et al., *Clock and ATF4 transcription system regulates drug resistance in human cancer cell lines.* Oncogene, 2007. **26**(33): p. 4749-60.

301. Piao, L., et al., *Lipid-based nanoparticle delivery of Pre-miR-107 inhibits the tumorigenicity of head and neck squamous cell carcinoma.* Mol Ther, 2012. **20**(6): p. 1261-9.

302. le Sage, C., et al., *Regulation of the p27(Kip1) tumor suppressor by miR-221 and miR-222 promotes cancer cell proliferation.* EMBO J, 2007. **26**(15): p. 3699-708.

303. Sakai, W., et al., *Secondary mutations as a mechanism of cisplatin resistance in BRCA2-mutated cancers.* Nature, 2008. **451**(7182): p. 1116-20.

304. Finnerty, J.R., et al., *The miR-15/107 group of microRNA genes: evolutionary biology, cellular functions, and roles in human diseases.* J Mol Biol, 2010. **402**(3): p. 491-509.

305. Li, X., et al., *miRNA-223 promotes gastric cancer invasion and metastasis by targeting tumor suppressor EPB41L3.* Mol Cancer Res, 2011. **9**(7): p. 824-33.

306. Tchernitsa, O., et al., *Systematic evaluation of the miRNA-ome and its downstream effects on mRNA expression identifies gastric cancer progression.* J Pathol, 2010. **222**(3): p. 310-9.

307. Volinia, S., et al., *A microRNA expression signature of human solid tumors defines cancer gene targets.* Proc Natl Acad Sci U S A, 2006. **103**(7): p. 2257-61.

308. Gottardo, F., et al., *Micro-RNA profiling in kidney and bladder cancers.* Urol Oncol, 2007. **25**(5): p. 387-92.

309. Yu, D., et al., *microRNA-103 regulates the growth and invasion of endometrial cancer cells through the downregulation of tissue inhibitor of metalloproteinase 3.* Oncol Lett, 2012. **3**(6): p. 1221-1226.

310. Wang, W.X., et al., *miR-107 regulates granulin/progranulin with implications for traumatic brain injury and neurodegenerative disease.* Am J Pathol, 2010. **177**(1): p. 334-45.

311. Chen, L., et al., *MicroRNA-107 inhibits glioma cell migration and invasion by modulating Notch2 expression.* J Neurooncol, 2013. **112**(1): p. 59-66.

312. Kim, H.W., et al., *Concomitant activation of miR-107/PDCD10 and Hypoxamir-210/Casp8ap2 and their role in cytoprotection during ischemic preconditioning of stem cells.* Antioxid Redox Signal, 2012. **17**(8): p. 1053-65.

313. Moncini, S., et al., *The role of miR-103 and miR-107 in regulation of CDK5R1 expression and in cellular migration.* PLoS One, 2011. **6**(5): p. e20038.

314. Chen, P.S., et al., *miR-107 promotes tumor progression by targeting the let-7 microRNA in mice and humans.* J Clin Invest, 2011. **121**(9): p. 3442-55.

315. Selcuklu, S.D., M.C. Yakicier, and A.E. Erson, *An investigation of microRNAs mapping to breast cancer related genomic gain and loss regions.* Cancer Genet Cytogenet, 2009. **189**(1): p. 15-23.

316. Nelson, P.T., et al., *Specific sequence determinants of miR-15/107 microRNA gene group targets.* Nucleic Acids Res, 2011. **39**(18): p. 8163-72.

317. Wang, W.X., et al., *Individual microRNAs (miRNAs) display distinct mRNA targeting "rules".* RNA Biol, 2010. **7**(3): p. 373-80.

318. Carbon, S., et al., *AmiGO: online access to ontology and annotation data.* Bioinformatics, 2009. **25**(2): p. 288-9.

319. Datta, J., et al., *microRNA-107 functions as a candidate tumor-suppressor gene in head and neck squamous cell carcinoma by downregulation of protein kinase Cvarepsilon.* Oncogene, 2012. **31**(36): p. 4045-53.

320. Chen, Z., et al., *Hypoxia-responsive miRNAs target argonaute 1 to promote angiogenesis.* J Clin Invest, 2013. **123**(3): p. 1057-67.

321. Wang, W.X., et al., *The expression of microRNA miR-107 decreases early in Alzheimer's disease and may accelerate disease progression through regulation of beta-site amyloid precursor protein-cleaving enzyme 1.* J Neurosci, 2008. **28**(5): p. 1213-23.

322. Trajkovski, M., et al., *MicroRNAs 103 and 107 regulate insulin sensitivity.* Nature, 2011. **474**(7353): p. 649-53.

323. Trivellin, G., et al., *MicroRNA miR-107 is overexpressed in pituitary adenomas and inhibits the expression of aryl hydrocarbon receptor-interacting protein in vitro.* Am J Physiol Endocrinol Metab, 2012. **303**(6): p. E708-19.

324. Paschou, M. and E. Doxakis, *Neurofibromin 1 is a miRNA target in neurons.* PLoS One, 2012. **7**(10): p. e46773.

325. Yao, J., et al., *MicroRNA-related cofilin abnormality in Alzheimer's disease.* PLoS One, 2010. **5**(12): p. e15546.

326. Yang, G.H., et al., *MicroRNAs are involved in erythroid differentiation control.* J Cell Biochem, 2009. **107**(3): p. 548-56.

327. Zhang, S.Y., et al., *Human CYP2C8 is post-transcriptionally regulated by microRNAs 103 and 107 in human liver.* Mol Pharmacol, 2012. **82**(3): p. 529-40.

328. Favereaux, A., et al., *Bidirectional integrative regulation of Cav1.2 calcium channel by microRNA miR-103: role in pain.* EMBO J, 2011. **30**(18): p. 3830-41.

329. Augustin, R., et al., *Computational identification and experimental validation of microRNAs binding to the Alzheimer-related gene ADAM10.* BMC Med Genet, 2012. **13**: p. 35.

330. Bence, N.F., R.M. Sampat, and R.R. Kopito, *Impairment of the ubiquitin-proteasome system by protein aggregation.* Science, 2001. **292**(5521): p. 1552-5.

331. Arora, S., et al., *RNAi screening of the kinome identifies modulators of cisplatin response in ovarian cancer cells.* Gynecol Oncol, 2010. **118**(3): p. 220-7.

332. Bartz, S.R., et al., *Small interfering RNA screens reveal enhanced cisplatin cytotoxicity in tumor cells having both BRCA network and TP53 disruptions.* Mol Cell Biol, 2006. **26**(24): p. 9377-86.

333. Galluzzi, L., et al., *Prognostic impact of vitamin B6 metabolism in lung cancer.* Cell Rep, 2012. **2**(2): p. 257-69.

334. Peterson, D., et al., *A chemosensitization screen identifies TP53RK, a kinase that restrains apoptosis after mitotic stress.* Cancer Res, 2010. **70**(15): p. 6325-35.

335. Salm, F., et al., *RNA interference screening identifies a novel role for autocrine fibroblast growth factor signaling in neuroblastoma chemoresistance.* Oncogene, 2012.

336. Swanton, C., et al., *Regulators of mitotic arrest and ceramide metabolism are determinants of sensitivity to paclitaxel and other chemotherapeutic drugs.* Cancer Cell, 2007. **11**(6): p. 498-512.

337. Nowacka-Zawisza, M., et al., *Loss of heterozygosity in the RAD51 and BRCA2 regions in breast cancer.* Cancer Detect Prev, 2008. **32**(2): p. 144-8.

338. Somyajit, K., et al., *ATM- and ATR-mediated phosphorylation of XRCC3 regulates DNA double-strand break-induced checkpoint activation and repair.* Mol Cell Biol, 2013.

339. Bogliolo, M., et al., *Mutations in ERCC4, Encoding the DNA-Repair Endonuclease XPF, Cause Fanconi Anemia.* Am J Hum Genet, 2013. **92**(5): p. 800-6.

340. Kee, Y. and A.D. D'Andrea, *Molecular pathogenesis and clinical management of Fanconi anemia.* J Clin Invest, 2012. **122**(11): p. 3799-806.

341. Nakanishi, K., et al., *Human Fanconi anemia monoubiquitination pathway promotes homologous DNA repair.* Proc Natl Acad Sci U S A, 2005. **102**(4): p. 1110-5.

342. Tsai, Y.S., et al., *Areca nut induces miR-23a and inhibits repair of DNA double-strand breaks by targeting FANCG.* Toxicol Sci, 2011. **123**(2): p. 480-90.

343. Sakai, W., et al., *Secondary mutations as a mechanism of cisplatin resistance in BRCA2-mutated cancers.* Nature, 2008. **451**(7182): p. 1116-1120.

344. Garofalo, M., et al., *EGFR and MET receptor tyrosine kinase-altered microRNA expression induces tumorigenesis and gefitinib resistance in lung cancers.* Nat Med, 2012. **18**(1): p. 74-82.

345. Welsh, J.W., et al., *The c-Met receptor tyrosine kinase inhibitor MP470 radiosensitizes glioblastoma cells.* Radiat Oncol, 2009. **4**: p. 69.

346. Dahiya, N. and P.J. Morin, *MicroRNAs in ovarian carcinomas.* Endocr Relat Cancer, 2010. **17**(1): p. F77-89.

347. Wu, Q., et al., *Analysis of serum genome-wide microRNAs for breast cancer detection.* Clin Chim Acta, 2012. **413**(13-14): p. 1058-65.

348. Ebert, M.S., J.R. Neilson, and P.A. Sharp, *MicroRNA sponges: competitive inhibitors of small RNAs in mammalian cells.* Nat Methods, 2007. **4**(9): p. 721-6.

349. Ameres, S.L., et al., *Target RNA-directed trimming and tailing of small silencing RNAs.* Science, 2010. **328**(5985): p. 1534-9.

350. Monteys, A.M., et al., *Structure and activity of putative intronic miRNA promoters.* RNA, 2010. **16**(3): p. 495-505.

351. Alfonso-Pecchio, A., et al., *Compartmentalization of mammalian pantothenate kinases.* PLoS One, 2012. **7**(11): p. e49509.

352. Neijenhuis, S., et al., *Identification of miRNA modulators to PARP inhibitor response.* DNA Repair (Amst), 2013.

353. Furuta, M., et al., *miR-124 and miR-203 are epigenetically silenced tumor-suppressive microRNAs in hepatocellular carcinoma.* Carcinogenesis, 2010. **31**(5): p. 766-76.

354. He, Z., et al., *Downregulation of miR-383 promotes glioma cell invasion by targeting insulin-like growth factor 1 receptor.* Med Oncol, 2013. **30**(2): p. 557.

355. Wong, T.S., et al., *Mature miR-184 as Potential Oncogenic microRNA of Squamous Cell Carcinoma of Tongue.* Clin Cancer Res, 2008. **14**(9): p. 2588-92.

356. Arumugam, T., et al., *Epithelial to mesenchymal transition contributes to drug resistance in pancreatic cancer.* Cancer Res, 2009. **69**(14): p. 5820-8.

357. Long, D.T., et al., *Mechanism of RAD51-dependent DNA interstrand cross-link repair.* Science, 2011. **333**(6038): p. 84-7.

CURRICULUM VITAE

Jen-Wei Huang

EDUCATION

PhD, Molecular and Cellular Biology, University of Washington, Seattle, WA. *September 2006 – June 2013.*

BA, Biology, Pomona College, Claremont, CA.
September 1999 - May 2003.

RESEARCH EXPERIENCE

Graduate Research Assistant
Howard Hughes Medical Institute, Divisions of Human Biology and Public Health Sciences, Fred Hutchinson Cancer Research Center.
September 2007 – June 2013.
Advisor: Toshiyasu Taniguchi, MD, PhD

- Dissertation Title: MicroRNA-103 and 107 Target RAD51 and RAD51D to Regulate Homologous Recombination and Enhance Cellular Sensitivity to DNA Damaging Agents.

Research Technician I
Department of Biochemistry, Weill Medical College of Cornell University, New York, NY.
November 2003 - August 2006.
Supervisor: Y. Amy Lam, PhD

- Project title: Separation of the energy requirements for substrate unfolding versus translocation in proteolysis by the 26S proteasome.

PUBLICATIONS

Huang, J.W., Wang, Y., Calses, P., Villegas, E., Mitchell, P.S., Tewari, M., Kemp, C.J. & Taniguchi, T. 2013. MicroRNA-103 and 107 target RAD51 and RAD51D to enhance chemosensitivity to cisplatin and PARP inhibitors. *Submitted.*

Wang, Y., **Huang, J. W.**, Calses, P., Kemp, C. J. & Taniguchi, T. 2012. MiR-96 downregulates REV1 and RAD51 to promote cellular sensitivity to cisplatin and PARP inhibition. *Cancer Research.* 72(16): 4037-46.

Wang, Y., **Huang, J.W.**, Mitchell, P., Tewari, M. & Taniguchi, T. 2011. MiR-138 regulates H2AX and the DNA damage response. *Molecular Cancer Research.* 9(8): 1100-11.

Lam, Y.A., **Huang, J.W.** & Showole, O. 2005. The synthesis and proteasomal degradation of a model substrate Ub5DHFR. *Methods in Enzymology*, 398: 379-390.

TEACHING EXPERIENCE	**Graduate Teaching Assistant** – Cellular and Molecular Biology (Bioc442). Department of Biochemistry, University of Washington, Seattle, WA. *Spring 2008.* **Instructors:** David Kimelman, PhD & Richard Palmiter, PhD **Graduate Teaching Assistant** – Animal and Plant Physiology (Biol220). Department of Biology, University of Washington, Seattle, WA. *Winter 2008.* **Instructors:** Steve Trudell, PhD, Mary Pat Wenderoth, PhD & Leslie Zeman, DVM
PROFESSIONAL MEETINGS & PRESENTATIONS	**Cold Spring Harbor Laboratory Meeting – Regulatory and non-coding RNAs.** Poster presentation. Cold Spring Harbor Laboratory, Cold Spring Harbor, NY. *August 28 – September 1, 2012.* **Howard Hughes Medical Institute Science Meeting.** Poster presentation. Janelia Farm Research Campus, Ashburn, VA. *June 5-8, 2011.* **Keystone Symposia on Molecular Biology – Genomic Instability and DNA Repair (B4).** Oral and poster presentation. Keystone, CO. *January 30 – February 4, 2011.* **22nd Annual Fanconi Anemia Research Fund Scientific Symposium.** Oral presentation. Minneapolis, MN. *October 21-24, 2010.* **101st Annual Meeting of the American Association of Cancer Research.** Oral presentation. Washington, DC. *April 17-21, 2010.* **21st Annual Fanconi Anemia Research Fund Scientific Symposium.** Oral presentation. Baltimore, MD. *October 1-4, 2009.* **20th Annual Fanconi Anemia Research Fund Scientific Symposium.** Poster presentation. Eugene, OR. *October 4-7, 2008.*
FELLOWSHIPS & AWARDS	**Cellular & Molecular Biology Training Grant** (NIGMS PHS NRSA 2TSA GM007270), University of Washington. *July 2008 – June 2011.* **AACR-Bristol Myers Squib-Oncology Division Scholar-in-Training Travel Award.** *April 2010.* **Distinction in Senior Exercise,** Pomona College. *Spring 2003.* **Pomona College Scholar,** Pomona College. *Fall 2002.*